Angewandte Chemie
Eine Zeitschrift der Gesellschaft Deutscher Chemiker

Supporting Information

A Click Cage: Organelle-Specific Uncaging of Lipid Messengers

*Nicolai Wagner, Milena Stephan, Doris Höglinger, and André Nadler**

anie_201807497_sm_miscellaneous_information.pdf

Table of contents

(A)

compound	absorption max. (nm)	extinction coefficient ($L*mol^{-1}*cm^{-1}$)	quantum yield
Coumarin 1	375	25777.13	0.73
6	380	31191.58	0.58
11	380	18655.53	0.36
12	380	45061.38	0.78
13	380	28424.01	0.41
14	380	29739.20	0.53
17	380	32001.32	0.86
18	380	19663.84	0.56
19	380	22868.25	0.55
20	380	32661.49	0.74
21	380	33124.64	0.72
23	380	35239.26	0.53
22	380	30466.42	0.39

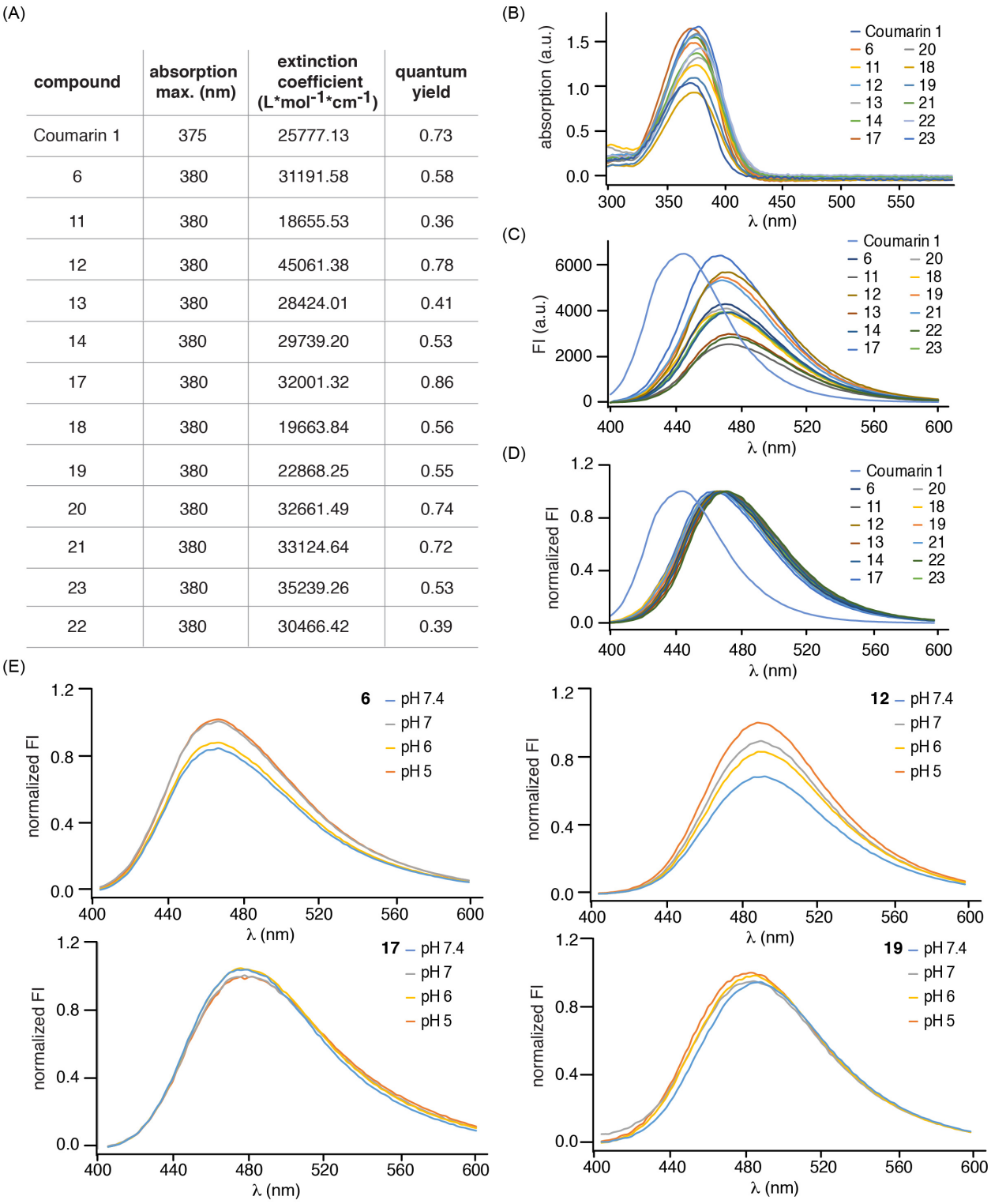

Figure S1. (A) Absorption maxima, extinction coefficients and quantum yields of all synthesized coumarin compounds. (B) UV-Vis absorption spectra of all synthesized coumarin compounds. (C) Fluorescence spectra of all synthesized coumarin compounds. (D) Fluorescence spectra were normalized to maximal fluorescent intensities of all synthesized coumarin containing compounds.

(E) pH dependency of coumarin fluorescence. Fluorescence spectra of compounds **6**, **12**, **17** and **19** were measured in PBS buffer with pH 7.4, 7, 6 and 5. Spectra are normalized to the emission observed at the physiological pH 7.4. Changes of fluorescence intensity with changing pH appear to be minor in the physiological pH range.

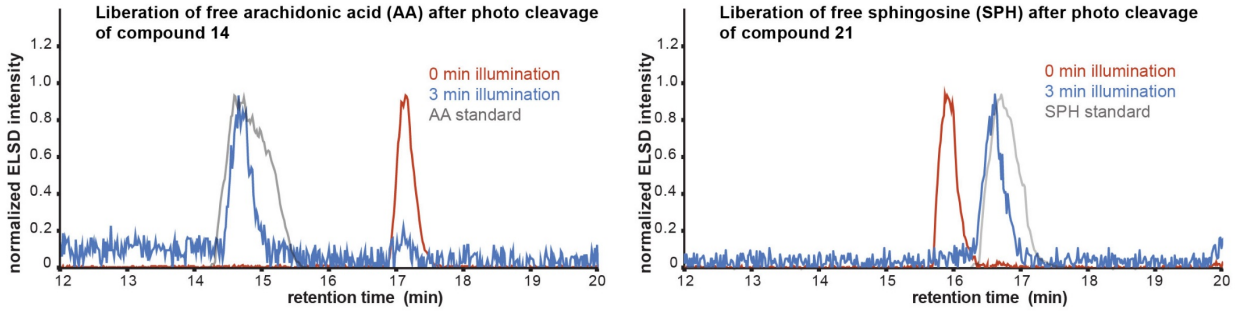

Figure S2. Normalized HPLC elution profiles of compound **14** and compound **21** without UV illumination (red) and after 3 min illumination (blue). Elution profiles of the respective standards (sphingosine (**15**) or arachidonate (**5**)) are shown in grey. UV cleavage and HPLC analysis were carried out with diluted samples to minimize substance loss.

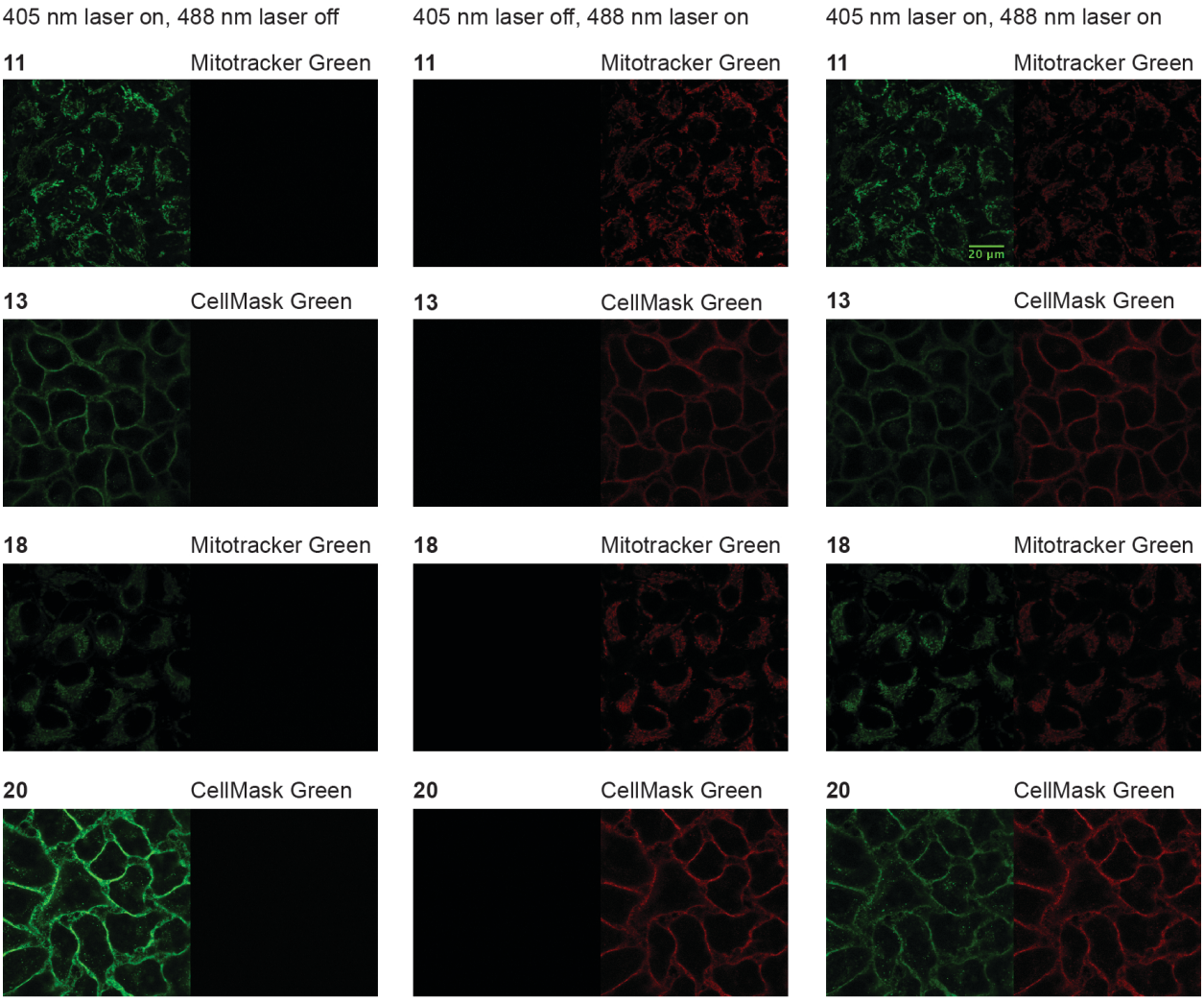

Figure S3. Bleed-through controls for representative caged lipids. Compounds were loaded as described below (section “Loading procedures of caged compounds and organelle markers”). Left panels: Cells loaded with the caged lipid and the respective organelle marker were illuminated solely with the 405 nm laser while sampling both coumarin (blue, between 425-475 nm) and organelle tracker fluorescence (green, between 500-550 nm). Note that signal is detected only in the blue channel and no bleed-through occurs. Middle panels: The same cells were subsequently illuminated solely with the 488 nm laser while sampling both coumarin (blue, between 425-475 nm) and organelle tracker fluorescence (green, between 500-550 nm). Note that signal is only in the green channel. Right panels: The same cells were subsequently illuminated with both lasers while sampling both coumarin (blue, between 425-475 nm) and organelle tracker fluorescence (green, between 500-550 nm). Note that signal is now detected in both channels. All images were acquired using the same magnification, the scale bar indicates 20 µm. Identical settings were used for each caged lipid / organelle marker pair. Fluorescence intensities tended to be slightly lower in the last set of measurements due to photobleaching.

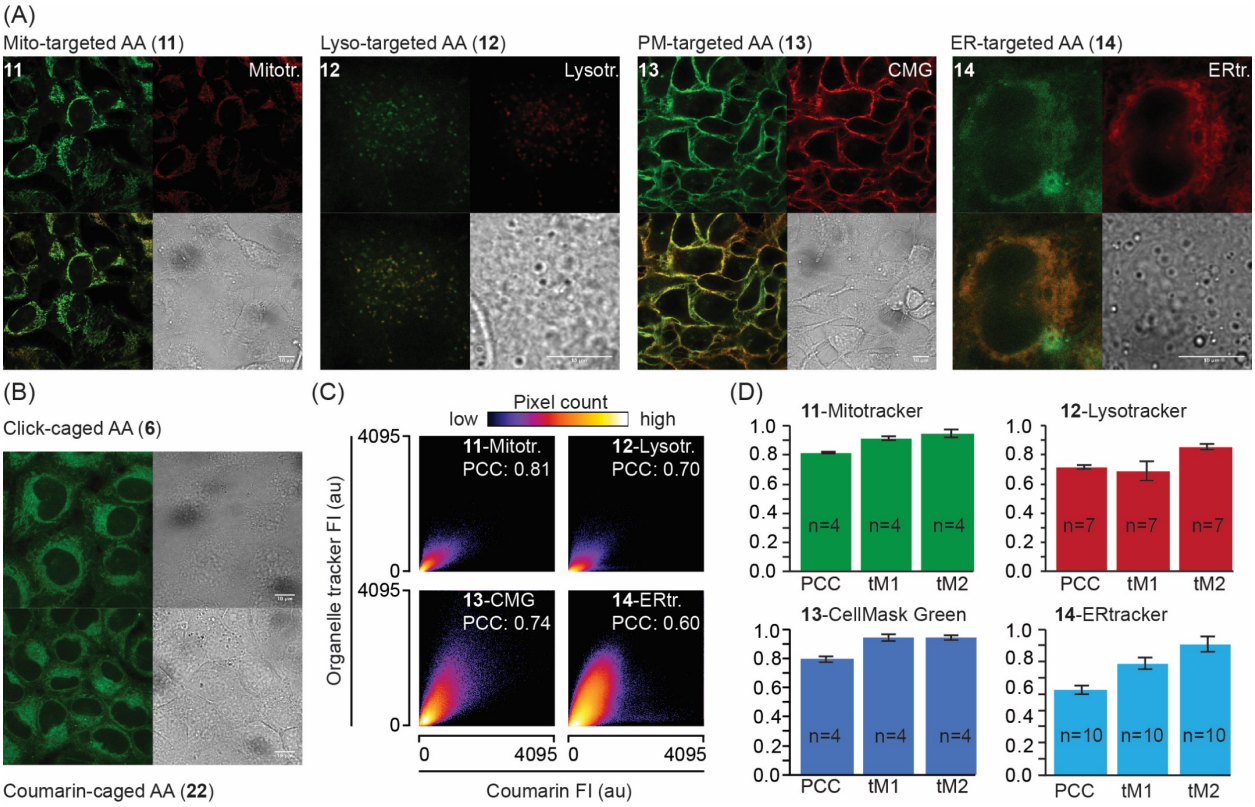

Figure S4. (A) Cellular localization of organelle-targeted caged arachidonic acid derivatives. Upper left panels depict the localization of the respective arachidonic acid probes (**11**-**14**, left to right for mitochondria- (**11**), lysosome- (**12**), plasma membrane- (**13**) and ER- (**14**) targeted localization, while upper right panels show the respective organelle markers (left to right: mitotracker green, lysotracker green, cell mask green, ER tracker). Lower left panels show overlays of probe and organelle marker fluorescence while lower right panels depict the corresponding bright-field images. (B) Cellular localization of click-caged arachidonic acid (**6**) and untargeted diethylamino coumarin caged arachidonic acid (**22**). Scale bars indicate 10 µm in all images. (C), (D) Quantification of colocalization between caged compounds and organelle markers. 2D histograms of representative images showing correlation between pixel intensities in both channels. Source images for 2D histograms are displayed in Figure S5. Bar graphs show Pearson correlation coefficients (PCC) of non-thresholded images and Manders correlation coefficients above the autothreshold for both channels, in every case derived from a minimum of four images. Only images that could be thresholded using a standardized automated routine were included for the determination of Manders overlap coefficients to avoid human bias. Error bars indicate standard deviation.

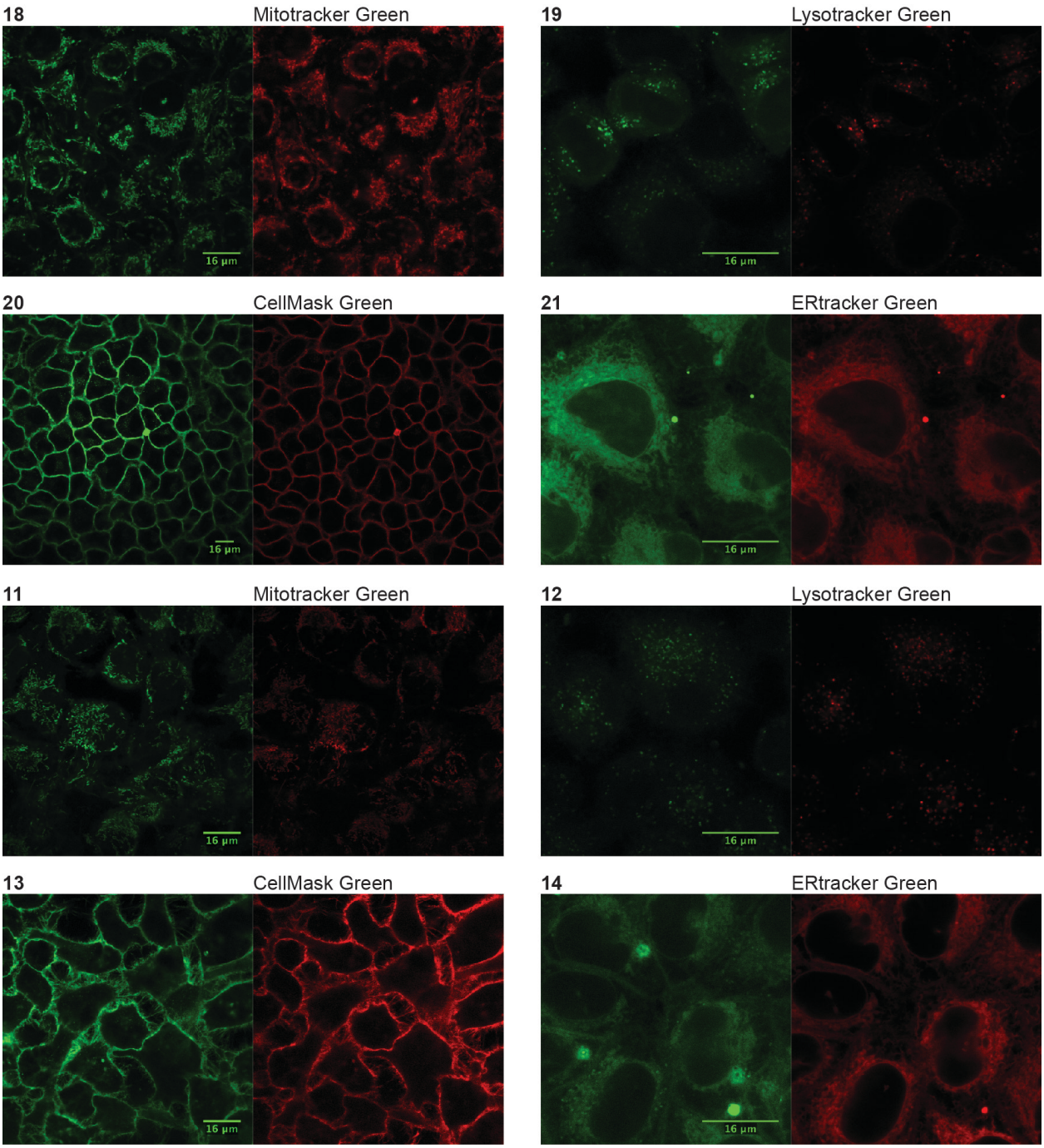

Figure S5. Source images for 2D histograms in Figures 1, S4. Left panels (green lookup-table) show the subcellular localization of organelle-targeted caged lipids, right panels (red lookup-table) show the respective organelle markers.

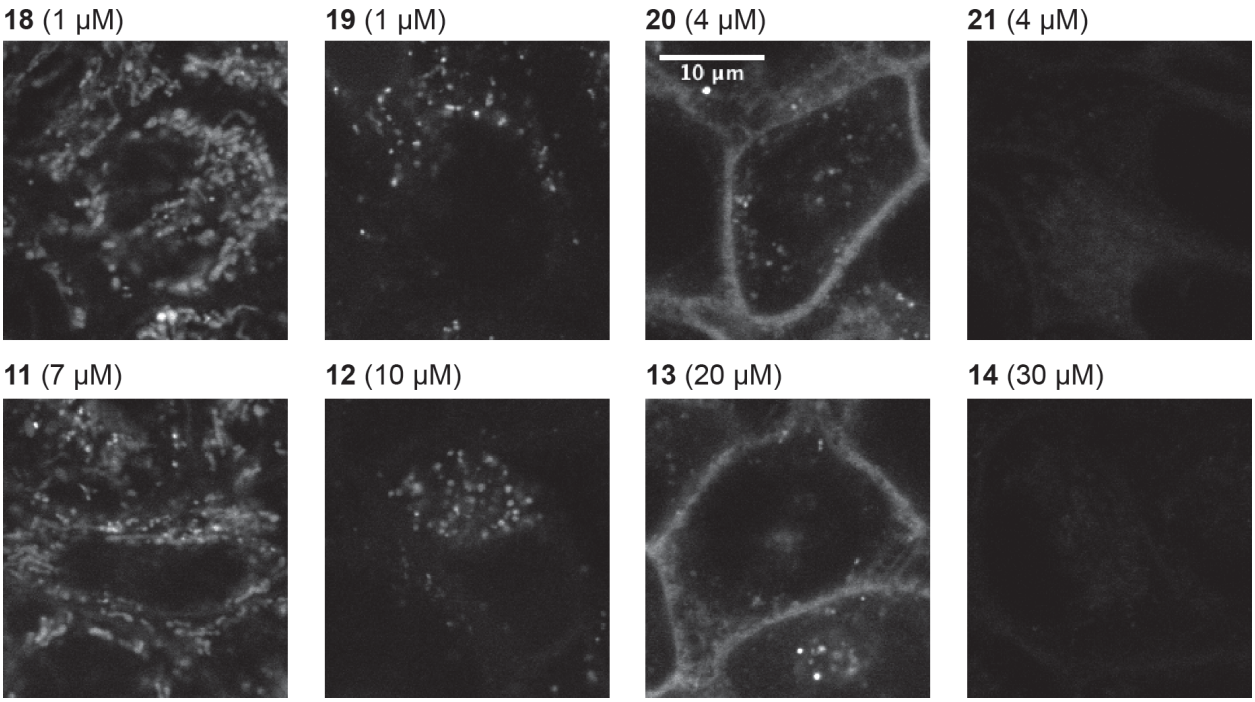

Figure S6. Comparison of compound uptake under conditions used for calcium imaging experiments. Compounds **11**-**14** and **18**-**21** were applied as specified above (compare section Loading procedures of caged compounds and organelle markers). Similar focus planes were chosen by calibrating on a transiently expressed red fluorescent R-GECO construct. Coumarin fluorescence was captured using identical acquisition settings for all compounds.

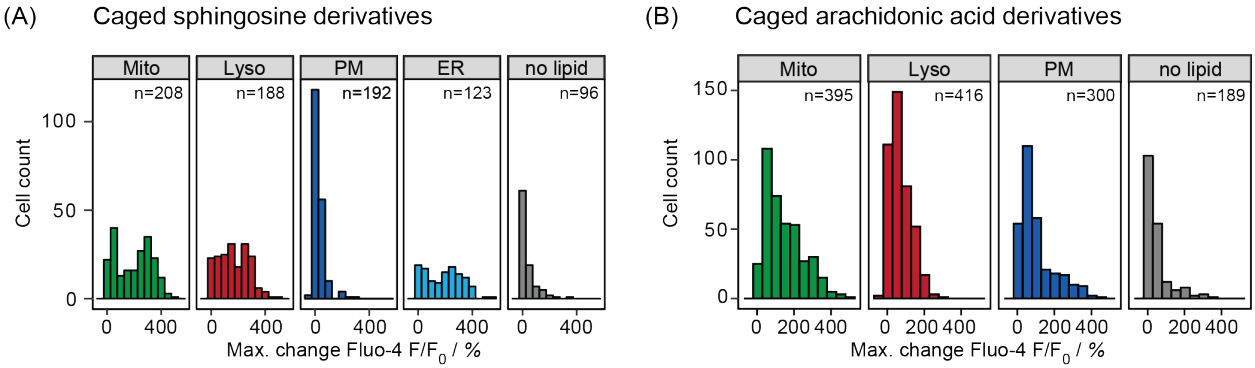

Figure S7. Comparison of the distribution of maximal Ca^{2+} responses for utilized compounds. (A) Histogram depicting maximal Ca^{2+} amplitudes in response to sphingosine uncaging from organelle-targeted probes **18**-**21**. Response distributions stemming from photorelease in mitochondria (**18**), the ER (**21**) and in lysosomes (**19**) are very similar, whereas irradiation of unloaded control cells and sphingosine uncaging at the plasma membrane (**20**) do not elicit responses. (B) Histogram depicting maximal Ca^{2+} amplitudes in response to arachidonic acid uncaging from organelle-targeted probes **11**-**14**.

Supplementary Methods

General synthetic procedures

All chemicals were obtained from commercial sources (Acros, Sigma-Aldrich, TCI chemicals, TRC Canada, Carbosynth, Alfa Aesar, Roth, Fluka or Merck) and were used without further purification. Organelle markers were purchased from Thermo Fisher Scientific. Solvents for flash chromatography were obtained from VWR and dry solvents were obtained from Sigma. Deuterated solvents were obtained from Deutero GmbH, Karlsruhe, Germany. TLC was performed on precoated plates of silica gel (Merck, 60 F254) using UV light (254 or 365 nm) or a solution of phosphomolybdic acid in EtOH (10 g phosphomolybdic acid, in 100 ml EtOH) for analysis. Preparative column chromatography was performed using silica gel from Merck, Darmstadt, Germany (silica 60, grain size 0.063-0.200 mm) with a pressure of 1.5 bar. Detailed purification conditions are given for the respective compounds. ^{1}H-, ^{13}C-, ^{31}P- and ^{19}F-NMR-spectra were measured on 400 MHz Advance^{TM} III HD Nanobay Bruker spectrometer. Chemical shifts of ^{1}H- and ^{13}C-NMR-spectra are referenced indirectly to tetramethylsilane. *J* values are given in Hz and chemical shifts in ppm. Splitting patterns are designated as follows: s, singlet; d, doublet; t, triplet; q, quartet; m, multiplet; b, broad. ^{13}C-NMR-spectra were broadband hydrogen decoupled. Mass spectra (ESI) were recorded using a QExactive instrument (Thermo Fisher Scientific) equipped 660 with a robotic nanoflow ion source. FTMS spectra were acquired with the target mass resolution of m/z 200=140000. The spectra were evaluated using the Xcalibur Qual 662 Browser software.

Photophysical characterization of caged compounds

Absorbance and fluorescence were measured using a TECAN Spark® 20M Multimode microplate reader (Plates: Microplate, 384 Well, PS, small volume, lobase, med. binding, black, μCLEAR®). For absorbance, the detection range was set to 200-500 nm, the spectral resolution to 2 nm and the averaging time to 0.1 s. The path length of the cuvette was 0.1989 cm (*d*), baseline correction was carried out by subtraction of the background signal of an ethanol sample. Extinction coefficients were determined by plotting the maxima of a serial dilution, using a linear fit to determine the slope (*m*) and calculated as following:

$$\varepsilon = \frac{m}{d} * 1000$$

Fluorescence spectra were recorded with 5-nm resolution. Excitation wavelength for all coumarin derivatives was 380 nm and emission collection at 400-600 nm, with a step size of 2 nm, and 40 μs integration. All spectra were recorded in ethanol at an analyte concentration of 62.5 μM and are background corrected for ethanol. Quantum Yields (QYs) where calculated as following:

$$QY = QY_{ref} \frac{\eta^2}{\eta_{ref}^2} \frac{A_{ref}}{A} \frac{I}{I_{ref}}$$

where QY_{ref} is the QY of the reference compound (coumarin 1, QY=0.73)[1], η is the refractive index of the solvent (ethanol for all samples and the reference), *A* is the absorbance at the

excitation wavelength, *I* is the integrated fluorescence intensity. Spectra were recorded using a concentration range from 0.065 mM to 0.5 mM. To observe the effect of pH on the fluorescence of the caged compounds, spectra of four representative compounds (the un-clicked derivatives **6** and **17** and the lysosomal targeted derivatives **12** and **19**) were acquired at room temperature at 50 µM concentration in PBS buffer adjusted with 3% HCl to the respective pH value 7.4, 7, 6 and 5. The spectra as well as the data are shown in Figure S1.

Determination of photocleavage efficiency in vitro

Photocleavage efficiency after exposure of caged compounds to UV light was analyzed by high performance liquid chromatography (HPLC), using a Knauer Azura system (AZURA P 2.1L pump, ASM 2.1L assistant, DAD 6.1 and a Sedere Sedex 85 ELSD detector) with a reverse phase Knauer Eurosphere II 100-5 C_4 column. Newly synthesized compounds **6**, **11**-**14** and **17**-**21** were compared to previously reported caged arachidonate and sphingosine derivatives **22** and **23**, which are equipped with the 7-(diethylamino)-4-(hydroxymethyl)-coumarin group. UV irradiation was carried out using a 1000 W Mercury-Xenon lamp equipped with a 335 nm high pass filter. Irradiation samples were prepared by diluting 20 µl of 10 mM stock solutions of the respective caged compounds in DMSO with 180 µl MeOH in a 250 µl transparent Eppendorf tube. Samples were placed in a stand 20 cm away from the light source. For each compound a sample was illuminated for 1, 3 and 5 min, respectively. Samples were analyzed by semi-preparative reversed phase-HPLC directly after illumination (conditions below). Elution conditions were chosen to enable analysis of the photo-liberated parent molecules and the caged precursors during the same HPLC run (Table S1). Eluting compounds were detected by light scattering using a Sedere Sedex 85 ELSD detector and retention times (R_t) of the free parent molecules sphingosine (**15**) and arachidonic acid (**5**) and their caged counterparts were determined. During the analysis of the 5 min UV irradiation sample set, peaks matching the retention times of arachidonate and sphingosine were collected and analyzed by high resolution mass spectrometry to confirm the identity of the photo-liberated molecules. Results of the photocleavage analysis are summarized in table S2. Elution profiles are exemplary shown for arachidonate, sphingosine, and compounds **14** and **21** before and after 3 min UV irradiation in Figure S2.

Time (min)	**% of solvent B**	**Flowrate (ml/min)**
0	0	3
2-18	0→100, linear gradient	3
18-25	100	3
25-26	100→0, linear gradient	3
26-30	0	3

Table S1. HPLC gradient for the HPLC uncaging assay. Solvent **A** (500 ml MeOH; 500 ml water; 10 mM triethyl ammonium acetate); Solvent **B** (500 ml 2-propanol; 200 ml acetonitrile; 200 ml tetrahydrofuran; 100 ml methanol; 10 mM triethyl ammonium acetate).

	R_t (min) prior illumination	R_t (min) liberated molecule	Mass (Da) of caged compound	Mass (Da) liberated molecule	Standards R_t (min)/ mass (Da)	Complete photo cleavage after (min)
Cou-AA	17.8	14.7	533.3505	303.2334 $[AA-H]^-$	14.7/ 304.2402	3
6	17.4	14.8	557.3505	303.2331 $[AA-H]^-$	14,7/ 304.2402	3
11	17.5	14.7	917.5129	303.2332 $[AA-H]^-$	14.7/ 304.2402	5
12	18.1	14.7	685.4567	303.2331 $[AA-H]^-$	14.7/ 304.2402	5
13	13.2	14.7	834.2979	303.2331 $[AA-H]^-$	14.7/ 304.2402	5
14	17.1	14.7	851.4045	303.2331 $[AA-H]^-$	14.7/ 304.2402	3
Cou-SPH	16.4	16.5	572.3825	358.2966 $[SPH+Ac]^-$	16.7/ 299.2824	5
17	16.2	16.5	596.3825	358.2966 $[SPH+Ac]^-$	16.7/ 299.2824	5
18	16.1	16.6	956.5449	358.2967 $[SPH+Ac]^-$	16.7/ 299.2824	5
19	17.0	16.5	724.4887	358.2967 $[SPH+Ac]^-$	16.7/ 299.2824	5
20	12.9	16.5	873.330	358.2968 $[SPH+Ac]^-$	16.7/ 299.2824	5
21	15.9	16.6	890.4365	358.2968 $[SPH+Ac]^-$	16.7/ 299.2824	5

Table S2. HPLC analysis of photocleavage efficiency. Retention times of the caged molecules prior to irradiation with a 1000 W Mercury-Xenon (335 nm high-pass filter) are displayed as well as the retention times of the peaks detected after irradiation. The latter match the retention times of the respective standard (sphingosine or arachidonic acid) in each case. Molecular identity after uncaging was confirmed by HRMS, masses could either be assigned to arachidonate $[AA-H]^-$, or sphingosine with acetate $[SPH+Ac]^-$.

Cell culture and cDNA transfection

All live cell experiments were carried out either in HeLa 'Kyoto' or in HeLa CCL2 cells. Cells were cultured in high-glucose DMEM (31966-021, Life Technologies) supplied with 10 % fetal bovine serum (10270-106, Life Technologies) and 100 µg ml^{-1} antibiotic Penicillin-Streptomycin (10 000 U/mL, 15140-122, Life Technologies). For colocalization analysis and assessment of compound uptake (Figures 1, S3-S6), cells were directly seeded in 8 well Lab-Tek microscope dishes (155411, Thermo Scientific. 100 000 cells (in 450 µl DMEM) were seeded into each well. For transfections, wells contained a transfection cocktail of 0.5 µl Fugene 6 (E2693, Promega), with 20 µl Opti-MEM (11058-021, Life Technologies) and 100 ng cDNA (R-GECO). Cells were imaged 24 h after transfection. For calcium imaging experiments (Figures 2, S6), cells were seeded in full medium into eight-well microscope dishes (80826, Ibidi) and used without transfection 24-48h after seeding.

Life cell imaging

For co-localization analysis and assessment of compound uptake (Figures 1, S3-S6), cells were imaged in eight-well Lab-Tek microscope dishes (155411, Thermo Scientific) using an Olympus Fluoview 1000 confocal laser scanning microscope with an Olympus UPlanSApochromat 60x 1.35 Oil objective at 37 °C and 5% CO_2 in imaging buffer containing 20 mM HEPES, 115 mM NaCl, 1.2 mM $CaCl_2$, 1.2 mM $MgCl_2$, 1.2 mM K_2HPO_4, 10 mM glucose. Microscope settings were adjusted to generate images displaying background fluorescence values slightly larger than zero in order to capture the complete signal stemming from the respective fluorescent dyes. Coumarin dyes were excited with the 405 nm laser and emitted light was collected between 425 and 475 nm. Organelle markers were excited with 488 nm laser and emitted light was collected at 500–550 nm. Images were acquired with the software FV10-ASW 1.7.

Loading procedures of caged compounds and organelle markers

Conditions used for data shown in Figures 1, S3-S5:

Caged lipids were stored as 10 mM DMSO stock solutions, whereas organelle markers were stored as 1 mM DMSO stock solutions. Caged lipid loading solutions for cellular uptake were generated by appropriate dilution with imaging buffer. HeLa cells were grown to 95% confluence in 8-well Lab-Tek dishes. The growth medium was removed prior to compound loading, and the cells were washed with imaging buffer (1 x 200 µl per well). Subsequently, the cells were treated with the respective caged lipid loading solutions (200 µl per well) for the time indicated in Table S1. The loading solution was removed, the cells washed with imaging buffer (1 x 200 µl per well) and subsequently treated with a solution of the respective organelle marker in imaging buffer. The organelle marker concentrations for each case are given in Table S3. The subcellular distributions of caged lipid probes and organelle markers were assessed using dual color confocal fluorescence microscopy on an Olympus FV1000 setup (see previous section for details). The two channels were acquired in sequential mode (line wise) to avoid bleed-through.

Compound	Loading concentration (µM)	Loading time (min)	Organelle marker	Loading concentration (nM)	Left on
6	10	10	none	-	-
11	20	10	Mitotracker green	500	yes
12	5	10	Lysotracker green	100	yes
13	100	10	CellMask Green	100	yes
14	30	20	ERtracker green	100	yes
17	10	10	None	-	-
18	5	10	Mitotracker green	750	yes
19	0.5	10	Lysotracker green	100	yes
20	10	10	CellMask green	100	yes
21	20	20	ERtracker green	100	yes
22	10	10	None	-	-
23	10	10	None	-	-

Table S3. Loading conditions for the caged lipids / organelle markers shown in Figures 2, S3, S4.

Conditions used for data shown in Figures 2, S6, S7:

Caged lipids were stored as 10 mM DMSO stock solutions. Caged lipid loading solutions for cellular uptake were generated by appropriate dilution with imaging buffer. HeLa cells were grown to 50% confluence in 8-well Lab-Tek dishes. The growth medium was removed prior to compound loading, and the cells were washed with imaging buffer (1 x 200 µl per well). Subsequently, the cells were treated with the respective caged lipid loading solutions (200 µl per well) and incubated for 10 min at 37 °C. The loading solution was removed, the cells washed twice with imaging buffer, either kept at 37 °C for additional 20 min (for assessment of compound uptake) or incubated with Fluo-4-AM (5 µM Fluo-4-AM in imaging buffer) at 37 °C for 20 min. Prior to imaging, the cells were washed once more with imaging buffer. The optimized loading conditions chosen for calcium imaging are displayed in Table S4, comparable loading was achieved for compounds **11**-**13** and **18**-**20**, whereas incorporation of compounds **14** and **21** was found to be either slightly (**21**) or significantly (**14**) less efficient (compare Figure S6).

Compound	Loading concentration (µM)	Loading time (min)
11	7	10 + 20
12	10	10 + 20
13	20	10 + 20
14	30	10 + 20
18	1	10 + 20
19	1	10 + 20
20	4	10 + 20
21	4	10 + 20

Table S4. Loading conditions for lipid uncaging and calcium imaging experiments.

Colocalization analysis

The colocalization plugin Coloc2 for the ImageJ/Fiji software was used to generate 2D histograms and to determine Pearson correlation coefficients and Manders overlap coefficients. Non-corrected and non-thresholded images of caged lipid probes and respective organelle markers were loaded into the plugin. Mean Pearson correlation coefficients for each caged lipid/organelle marker pair were determined from the entire dataset. Thresholding was carried out automatically using the "automatic-biscetion" settings. Images were not included for the calculation of mean average thresholded Manders overlap coefficients, if the automatic threshold determination failed to reduce bias introduced by manually chosen threshold values.

Confocal time lapse live cell microscopy and uncaging assay

For calcium imaging experiments (Figures 2, S7), cells loaded with caged compounds and Fluo-4-AM (as described above) were imaged in eight-well microscopy dishes (80826, Ibidi) using a Zeiss LSM800 confocal microscope with a Plan-Apochromat 63x/1.40 Oil objective at ambient temperature in imaging buffer containing 20 mM HEPES, 115 mM NaCl, 1.8 mM $CaCl_2$, 1.2 mM $MgCl_2$, 1.2 mM K_2HPO_4, 10 mM glucose. Coumarin dyes were excited using a 405 nm laser (at 1.0% laser power) and emission was collected between 400 nm and 590 nm. The calcium dye Fluo-4 was excited using a 488 nm laser (at 1.2%) and emitted light was collected between 400 and 590 nm. Coumarin and Fluo-4 fluorescence was acquired sequentially in line-mode. Time-lapse images were acquired using the Zen Blue software and the Experiment Designer plug-in set at one frame per second. Uncaging was performed after acquiring a 10 frames baseline, using widefield-illumination of the whole field-of-view by the 385 nm LED of the Colibri 7 module set to 30 % power for 1.5 s. After uncaging, time-lapse images of Coumarin and Fluo-4 fluorescence were acquired for 60 more frames. In the end, baseline and post-uncaging frames were stitched using the Timestitch function in the Experiment Designer plug-in and the resulting time-lapses were exported as .czi files.

Data analysis of calcium time lapses

The acquired time lapse series were analyzed with the Fiji software using the FluoQ macro[2] set to the following parameters:

Background subtraction method:	Do not remove background
Noise reduction / smoothing method:	None
Threshold method:	Interactively with ImageJ's built-in threshold window
ROI segmentation:	Semi-automatically with binary mask modification
Calculate amplitude changes:	Using maximum observed amplitude change

The maximum amplitude values were calculated by subjecting the raw traces to a central moving average. The maximal amplitude $\mathrm{x}_{\mathrm{response}}^{\mathrm{max}}$ of these smoothed traces was used to calculate the amplitude change in percent$\%\Delta_x^{max}$according to the following formula:

$$\%\Delta_x^{max} = \frac{x_{response}^{max} - \bar{x}_{baseline}}{|\bar{x}_{baseline}|} * 100$$

The resulting intensity series/amplitude values represent mean values of whole cells and were further analyzed using R. Figures 2 and S7 were prepared using the ggplot2 package[3].

Synthetic procedures and analytical data of synthesized compounds

Compounds **2**,**8**,**22** and **23** were synthesized according to literature [4]

(7-(Ethylamino)-2-oxo-2H-chromen-4-yl)methyl acetate (**3**):

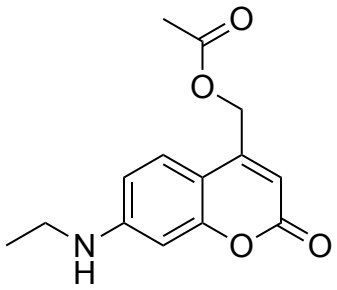

9.38 g (40.2 mmol) of (7-amino-2-oxo-2H-chromen-4-yl) methyl acetate (**2**) were suspended in 500 ml THF with freshly activated molecular sieve (3Å) under an inert argon atmosphere at room temperature. 3.4 ml (60.4 mmol, 1.5 eq) acetaldehyde were added directly and after 3 h 16.8 g (79.4 mmol, 2.0 eq) of sodium triacetoxyborohydride were added. After 4.5 h the reaction was quenched by adding 100 ml of a saturated ammonium chloride solution. The solution was decanted and the volatiles were removed under reduced pressure. 100 ml water were added and the aqueous layer was extracted with chloroform (3x 150 ml). The combined organic layers were dried over sodium sulfate and the solvents were removed under reduced pressure. The product was purified by flash chromatography with ethyl acetate/cyclohexane (1:1), yielding 6.98 g (66%) of a yellow solid.

^{1}H NMR (400 MHz, DMSO-d6): δ = 7.39 (d, J=8.8 Hz, 1 H), 6.71 (t, J=5.1 Hz, 1 H), 6.59 (dd, J=8.8, 2.2 Hz, 1 H), 6.41 (d, J=2.2 Hz, 1 H), 5.96 (s, 1 H), 5.24 (s, 2 H), 3.12 (qd, J=7.2, 5.1 Hz, 2 H), 2.16 (s, 3 H), 1.17 (t, J=7.2 Hz, 3 H) ppm.

^{13}C NMR (101 MHz, DMSO-d6): δ = 169.97, 160.60, 155.89, 152.56, 150.80, 125.14, 110.38, 105.63, 104.69, 96.23, 61.12, 36.96, 20.51, 13.97 ppm.

HR-MS (ESI positive) m/z calculated for $C_{14}H_{15}NO_4$: 261.1001; found: 262.1075 $[M+H]^+$.

(7-(But-3-yn-1-yl(ethyl)amino)-2-oxo-2H-chromen-4-yl)methyl acetate (**4**):

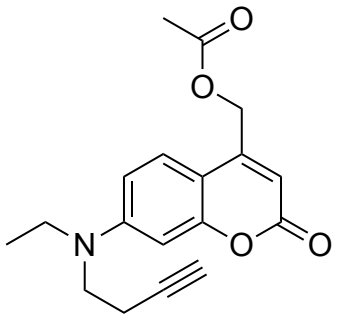

0.77 g (2.95 mmol) of **3** were dissolved in 15 ml DMF. Subsequently, a catalytic amount of TBAI and 3.2 ml (18.4 mmol, 6.4 eq) DIPEA and 1.8 ml (10.2 mmol, 3.5 eq) 3-butynyl tosylate were added. The reaction was heated to 130 °C and after 2 h 1.5 ml (8.5 mmol, 2.9 eq) 3-butynyl tosylate, after 5 h 5 ml (28.3 mmol, 9.8 eq) 3-butynyl tosylate and 3 ml (17.2 mmol, 5.9 eq) DIPEA and after 25 h 5 ml (28.3 mmol, 9.8 eq) 3-butynyl tosylate and 2 ml (11.5 mmol, 4 eq) DIPEA were added. After 47 h the reaction was stopped by cooling to room temperature. 200 ml water were added and the aqueous layer was extracted with chloroform (3x 150 ml). The combined organic layers were dried over sodium sulfate, filtered and the solvents were removed under reduced pressure. The crude product was purified by flash chromatography with ethyl acetate/cyclohexane (1:1), yielding 310 mg (34%) of an orange oil.

^{1}H NMR (400 MHz, $CDCl_3$): δ = 7.27 (d, *J* = 9.1 Hz, 1H), 6.63 – 6.53 (m, 1H), 6.48 (s, 1H), 6.09 (s, 1H), 5.18 (s, 2H), 3.53 (t, *J* = 7.2 Hz, 2H), 3.45 (q, *J* = 6.9 Hz, 2H), 2.51 – 2.38 (m, 2H), 2.16 (s, 3H), 2.04 – 1.98 (m, 1H), 1.18 (t, *J* = 7.0 Hz, 3H) ppm.

^{13}C NMR (101 MHz, $CDCl_3$): δ = 170.11, 161.50, 156.04, 150.23, 149.33, 124.49, 108.72, 106.89, 106.50, 98.08, 81.11, 70.38, 61.22, 49.24, 45.45, 20.68, 17.28, 12.15 ppm.

HR-MS (ESI positive) m/z calculated for $C_{18}H_{19}NO_4$: 313.1314; found: 314.1381 $[M+H]^+$.

7-(But-3-yn-1-yl(ethyl)amino)-4-(hydroxymethyl)-2H-chromen-2-one (**1**):

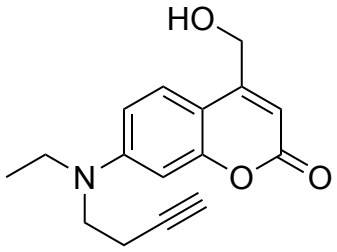

98.2 mg (0.31 mmol) of **4** were dissolved in 30 ml of a 3 % solution of KOH in MeOH (734.8 mg, 13.1 mmol, 41.8 eq). After stirring at room temperature for 5 min, the reaction was stopped by adding 50 ml of a saturated ammonium chloride solution the reaction mixture was extracted with chloroform (3x 150 ml). The combined organic layers were dried over sodium sulfate, filtered and the solvent was removed under reduced pressure. The product was purified by flash chromatography with ethyl acetate/cyclohexane (1:1), yielding 75 mg (89 %) of a dark yellow oil.

^{1}H NMR (400 MHz, $CDCl_3$): δ = 7.36 (d, *J* = 9.0 Hz, 1H), 6.61 (dd, *J* = 9.0, 2.6 Hz, 1H), 6.55 (d, *J* = 2.5 Hz, 1H), 6.32 (s, 1H), 4.86 (s, 2H), 3.58 (t, *J* = 7.3 Hz, 2H), 3.50 (q, *J* = 7.1 Hz, 2H), 2.51 (td, *J* = 7.4, 2.6 Hz, 2H), 2.06 (t, *J* = 2.6 Hz, 1H), 1.23 (t, *J* = 7.1 Hz, 3H) ppm.

^{13}C NMR (101 MHz, $CDCl_3$): δ = 162.48, 156.18, 154.66, 150.14, 124.67, 108.92, 107.21, 106.34, 98.47, 81.28, 70.47, 61.09, 49.56, 45.74, 17.48, 12.34 ppm.

HR-MS (ESI positive) m/z found: calculated for $C_{16}H_{17}NO_3$: 271.1208; found: 272.1278 $[M+H]^+$.

(7-(but-3-yn-1-yl(ethyl)amino)-2-oxo-2H-chromen-4-yl)methyl-(5Z,8Z,11Z,14Z)-icosa-5,8,11,14-tetraenoate (**6**):

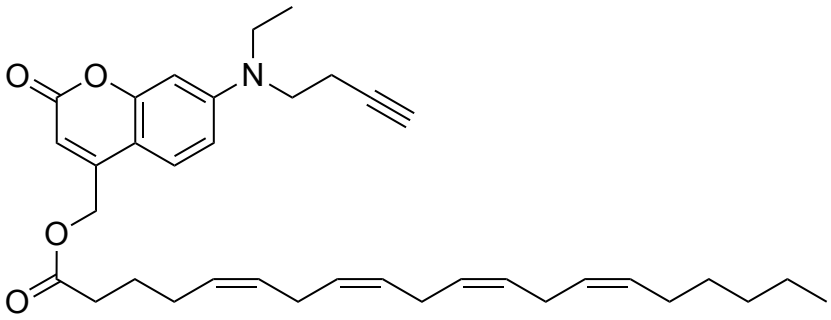

123 mg arachidonic acid (0.404 mmol, 1.1 eq), 120 mg EDC hydrochloride (0.626 mmol, 1.7 eq) and 30 mg DMAP (0.246 mmol, 0.7 eq) were dissolved in 6 ml dry DCM under an inert argon atmosphere. After 10 min, a solution of 100 mg **1** (0.369 mmol, 1 eq) in 5 ml dry DCM was added. After 4 h the reaction was stopped by removal of all volatiles. The crude product was purified by flash chromatography using 1% MeOH in DCM. Impure fractions were further purified by flash chromatography using ethyl acetate/cyclohexane (2:8). Pure fractions were combined to yield 180 mg (0.323 mmol, 88 %) of a yellow oil.

^{1}H NMR (400 MHz, $CDCl_3$): δ = 7.29 (d, J = 9.0 Hz, 1H), 6.58 (dd, J = 9.0, 2.6 Hz, 1H), 6.52 (d, J = 2.6 Hz, 1H), 5.46 – 5.29 (m, 8H), 5.20 (d, J = 1.3 Hz, 2H), 3.55 (t, J = 7.3 Hz, 2H), 3.47 (q, J = 7.1 Hz, 2H), 2.81 (dt, J = 11.8, 5.7 Hz, 6H), 2.53 – 2.40 (m, 4H), 2.14 (q, J = 7.0 Hz, 2H), 2.07 – 1.98 (m, 3H), 1.77 (q, J = 7.4 Hz, 2H), 1.37 – 1.22 (m, 6H), 1.20 (t, J = 7.1 Hz, 3H), 0.87 (t, J = 6.7 Hz, 3H) ppm.

^{13}C NMR (101 MHz, $CDCl_3$): δ = 173.04, 161.85, 156.42, 150.55, 149.67, 130.74, 129.42, 128.91, 128.85, 128.54, 128.33, 128.11, 127.81, 124.80, 109.01, 107.41, 106.94, 98.54, 81.37, 77.68, 77.36, 77.04, 70.66, 61.44, 49.62, 45.81, 33.71, 31.79, 29.59, 27.49, 26.79, 25.92, 24.95, 22.84, 17.64, 14.35, 12.49 ppm.

HR-MS (ESI positive) m/z found: calculated for $C_{36}H_{47}NO_4$: 557.3505; found: 558.357 $[M+H]^+$.

(4-Azidobutyl) triphenyl phosphonium bromide (**7**)

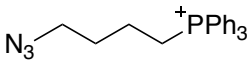

2.39 g of 4-bromo-butyl-triphenyl-phosphonium bromide (5 mmol, 1.0 eq) and 0.325 g NaN_3 (5 mmol, 1.0 eq) were dissolved in 50 ml dry DMF under an inert argon atmosphere. After heating to reflux for 14 h, all volatiles were removed and the crude product was dissolved in 300 ml of a 1:1 mixture of water and DCM. The aqueous phase was extracted with DCM (2x 100 ml) and the combined organic layers were dried over sodium sulfate. The solvent was removed under reduced pressure and analytically pure product (2.17 g, 4.95 mmol, 98.5%) was obtained as a colorless solid.

^{1}H NMR (400 MHz, $CDCl_3$): δ = 7.79 – 7.57 (m, 15H), 3.84 – 3.69 (m, 2H), 3.33 (t, J = 6.3 Hz, 2H), 1.91 (p, J = 6.7 Hz, 2H), 1.70 – 1.55 (m, 2H) ppm.

^{13}C NMR (101 MHz, $CDCl_3$): δ = 135.03, 135.00, 133.59, 133.49, 130.51, 130.38, 118.37, 117.52, 50.49, 50.47, 29.18, 29.01, 22.37, 21.86, 19.75, 19.71ppm.

^{31}P NMR (162 MHz, $CDCl_3$): δ = 24.16 ppm.

HR-MS (ESI positive) m/z calculated for $C_{22}H_{23}N_3P^+$: 360.163; found: 360.163 $[M]^+$.

4-Azidobenzene-1,3-disulfonate (**9**)

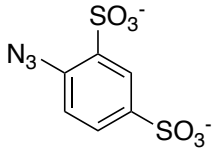

8.46 g aniline-2,4-disulfonic acid (33.4 mmol) were suspended in 15 ml water and cooled with an ice bath. 7.5 ml (13.8 g, 141 mmol, 4.2 eq) of precooled conc. H_2SO_4 were added dropwise. Subsequently, an aqueous solution of $NaNO_2$ (3 g, 43.5 mmol, 1.3 eq in 12 ml water) was added dropwise. After 30 min, 5 ml water were added before an ice-cold solution of NaN_3 (4.34 g, 66.8 mmol, 2 eq in 15 ml water) was added dropwise. The mixture was allowed to reach room temperature and concentrated by removing 20 ml of the solvent under reduced pressure. The product was crystallized at 4ºC and formed a grey suspension. After filtration, 10 ml of ice cold MeOH were added to the mother liquor to trigger further precipitation and the resulting suspension was filtered. The combined solid material was washed twice with ice cold MeOH and 4.92 g of a grey solid were obtained (17.6 mmol, 53 %).
Prior to the use in the click reactions, the protonated acid was neutralized by dissolving 0.5 g in 5 ml water and subsequent addition of 700 µl of a 1 M ammonium formate solution. The resulting solution was filtered and applied to gradient HILIC-HPLC (solvent A: 5 % water in MeOH and solvent B: 40 % MeOH in water with 25 mM ammonium formate). The neutralized compound eluted in a broad peak from 6.5 min to 8.5 min and product-containing fractions were collected

when significant ELSD signals (above 250 mV) were detected. The solvents were removed under reduced pressure and the remaining solid was dried under high vacuum for 24 h.

^{1}H NMR (400 MHz, D_2O): δ = 8.16 (s, 1H), 7.92 (d, J = 8.1 Hz, 1H), 7.48 (d, J = 8.4 Hz, 1H) ppm.

^{13}C NMR (101 MHz, D_2O): δ = 140.58, 138.45, 132.43, 129.93, 125.95, 120.80 ppm.

HR-MS (ESI negative) m/z found: calculated for $C_6H_3N_3O_6S_2^{2-}$: 276.9474; found: 277.954 $[M+H]^-$.

N-(3-azidopropyl)-2,3,4,5,6-pentafluorobenzamide (**10**)

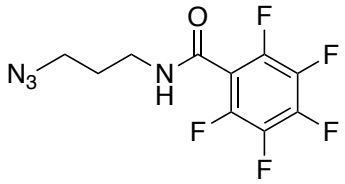

To a solution of 212 mg (1 mmol, 1 eq) pentafluorobenzoic acid in 5 ml THF and 10 ml DMF 525 µl (390 mg, 3.02 mmol) DIPEA, 500 mg HBTU (1.32 mmol) and 30 mg (0.211 mmol) oxyma pure were added. After 3 min, 125 mg (1.25 mmol, 1.3 eq) 3-azidopropylamine were added. After 3 h, the reaction was stopped by removing all volatiles under reduced pressure. The crude product was purified by flash chromatography using ethyl acetate/cyclohexane (3:7). 185 mg of a colorless solid were obtained (0.63 mmol, 63 %).

^{1}H NMR (400 MHz, $CDCl_3$) δ 7.03 (s, 1H), 3.49 – 3.35 (m, 4H), 1.83 (p, J = 6.6 Hz, 2H).

^{13}C NMR (101 MHz, $CDCl_3$): δ = 157.82, 145.30, 143.56, 142.79, 141.00, 138.89, 136.34, 111.60, 49.14, 37.93, 28.33 ppm. Signal of the fluorinated ^{13}C nuclei between 145.3 and 136.34 show distinct C-F coupling patterns.

^{19}F NMR (376 MHz, $CDCl_3$): δ = -141.17 – -141.34 (m), -150.92 – -151.13 (m), -160.27 – -160.52 (m) ppm.

HR-MS (ESI positive) m/z found: calculated for $C_{10}H_7F_5N_4O$: 294.0540; found: 265.062 $[M+H]^+$

(4-(4-(2-(ethyl(4-((((5Z,8Z,11Z,14Z)-icosa-5,8,11,14-tetraenoyl)oxy)methyl)-2-oxo-2H-chromen-7-yl)amino)ethyl)-1H-1,2,3-triazol-1-yl)butyl)triphenylphosphonium (**11**)

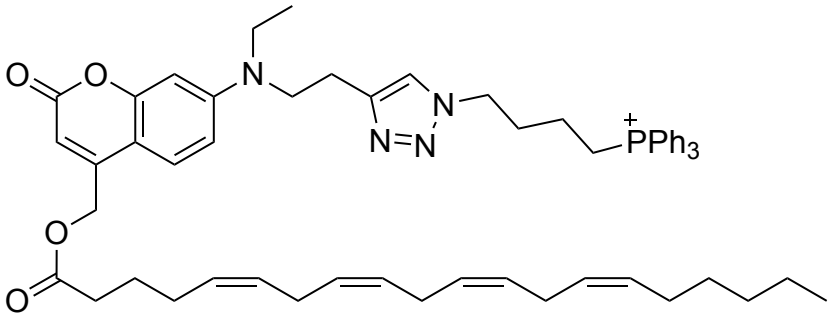

20 mg **6** (35.8 µmol, 1 eq), 20 mg **7** (45.5 µmol, 1.3 eq), 5 mg CuI (26.2 µmol, 0.7 eq) and 2 mg TBTA (3.7 µmol, 0.1 eq) were dissolved in 1 ml dry and degassed DMF. The reaction was stopped by removal of all volatiles after 2 h and the crude product was purified by flash chromatography with 10 % MeOH in chloroform, yielding 20 mg of a yellow solid (20.1 µmol, 56 %)

^{1}H NMR (400 MHz, $CDCl_3$): δ = 7.88 – 7.60 (m, 15H), 5.51 – 5.27 (m, 8H), 5.22 (d, J = 1.3 Hz, 2H), 4.59 (s, 2H), 3.81 (s, 2H), 3.65 (dd, J = 9.3, 6.3 Hz, 2H), 3.42 (q, J = 7.0 Hz, 2H), 2.96 (dd, J = 9.0, 6.6 Hz, 2H), 2.86 – 2.75 (m, 6H), 2.45 (t, J = 7.6 Hz, 2H), 2.29 (s, 2H), 2.15 (q, J = 7.0 Hz, 2H), 2.04 (q, J = 7.0 Hz, 2H), 1.77 (p, J = 7.5 Hz, 2H), 1.41 – 1.11 (m, 13H), 0.87 (t, J = 6.8 Hz, 4H) ppm.

^{13}C NMR (101 MHz, $CDCl_3$): δ = 173.14, 168.08, 162.15, 156.53, 150.97, 149.93, 144.68, 135.40, 135.37, 134.01, 133.91, 130.85, 130.82, 130.73, 129.46, 129.01, 128.92, 128.61, 128.42, 128.19, 127.88, 124.89, 123.22, 118.98, 118.12, 109.30, 106.91, 106.66, 98.34, 77.67, 77.36, 77.04, 61.55, 50.56, 48.79, 45.67, 33.81, 31.85, 30.49, 30.32, 30.05, 29.66, 27.56, 26.87, 25.98, 25.03, 24.09, 22.91, 21.34, 19.54, 14.42, 12.54 ppm.

^{31}P NMR (162 MHz, $CDCl_3$): δ = 24.52 ppm.

HR-MS (ESI positive) m/z found: calculated for $C_{58}H_{70}N_4O_4P^+$: 917.5129; found: 917.513 $[M]^+$.

(7-((2-(1-(3-(dimethylamino)propyl)-1H-1,2,3-triazol-4-yl)ethyl)(ethyl)amino)-2-oxo-2H-chromen-4-yl)methyl (5Z,8Z,11Z,14Z)-icosa-5,8,11,14-tetraenoate (**12**)

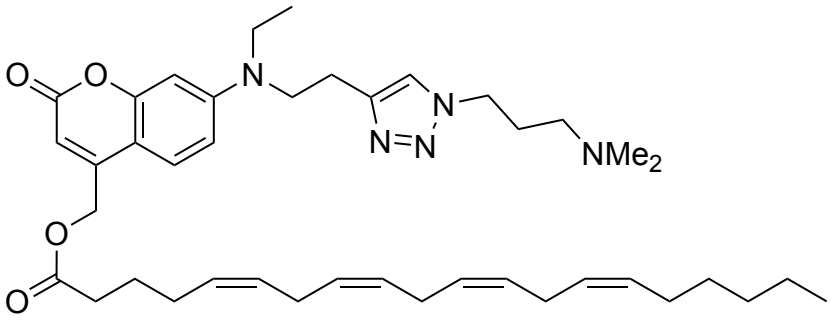

20 mg **6** (35.8 µmol, 1 eq), 9 mg **8** (70 µmol, 2.0 eq), 5 mg CuI (26.2 µmol, 0.7 eq) and 2 mg TBTA (3.7 µmol, 0.1 eq) were dissolved in 1 ml dry and degassed DMF. The reaction was stopped by removal of all volatiles after 2 h and the crude product was purified twice by flash chromatography using a gradient from 10-20 % MeOH in chloroform, yielding 21 mg of a yellow solid (30.6 µmol, 86 %)

^{1}H NMR (400 MHz, Methanol-d_4): δ = 7.49 (d, J = 9.1 Hz, 1H), 6.78 (dd, J = 9.1, 2.4 Hz, 1H), 6.09 (d, J = 1.2 Hz, 1H), 5.49 – 5.27 (m, 10H), 4.45 (t, J = 6.9 Hz, 2H), 3.75 (t, J = 7.1 Hz, 2H), 3.50 (q, J = 7.0 Hz, 2H), 3.06 (t, J = 7.3 Hz, 2H), 2.91 – 2.77 (m, 6H), 2.51 (t, J = 7.3 Hz, 2H), 2.43 (d, J = 8.8 Hz, 2H), 2.35 (s, 6H), 2.19 (q, J = 6.9 Hz, 2H), 2.08 (p, J = 7.8, 6.9 Hz, 4H), 1.78 (p, J = 7.3 Hz, 2H), 1.38 – 1.28 (m, 6H), 1.21 (t, J = 7.0 Hz, 3H), 0.91 (t, J = 6.8 Hz, 3H) ppm.

^{13}C NMR (101 MHz, Methanol-d_4) δ 175.10, 164.90, 158.30, 153.54, 153.35, 132.03, 130.95, 130.69, 130.27, 129.98, 129.74, 129.61, 127.12, 111.44, 108.47, 107.66, 99.59, 63.30, 51.83, 46.96, 34.98, 33.51, 31.31, 29.44, 29.04, 28.36, 27.43, 26.65, 25.43, 24.48, 15.30, 13.28 ppm.

HR-MS (ESI positive) m/z found: calculated for $C_{41}H_{59}N_5O_4$: 685.4567; found: 686.463 $[M+H]^+$.

4-(4-(2-(ethyl(4-((((5Z,8Z,11Z,14Z)-icosa-5,8,11,14-tetraenoyl)oxy)methyl)-2-oxo-2H-chromen-7-yl)amino)ethyl)-1H-1,2,3-triazol-1-yl)benzene-1,3-disulfonate (**13**)

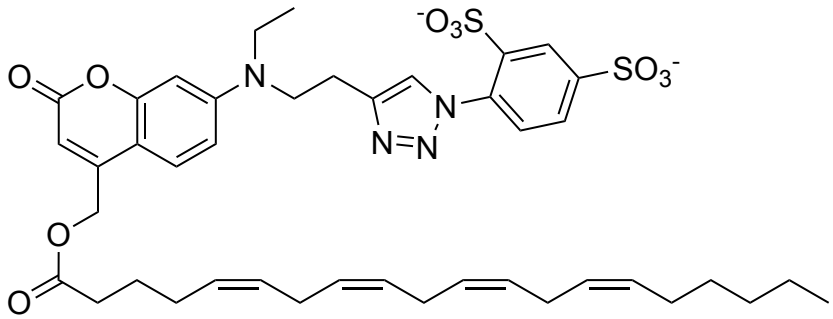

20 mg **6** (35.8 µmol, 1 eq), 12 mg **9** (38.3 µmol, 1.1 eq), 3 mg CuI (15.8 µmol, 0.4 eq) and 2 mg TBTA (3.7 µmol, 0.1 eq) were dissolved in 1 ml dry and degassed DMF. The reaction was stopped by removal of all volatiles after 2 h and the crude product was purified by silica column chromatography using 35 % MeOH in chloroform while increasing water content from 2-4 %. The product was obtained as a yellow solid (20 mg, 23 µmol, 64 %).

^{1}H NMR (400 MHz, Methanol-d_4): δ = 8.68 (d, J = 1.9 Hz, 1H), 8.07 (dd, J = 8.1, 2.0 Hz, 1H), 7.60 (d, J = 8.1 Hz, 1H), 7.53 (d, J = 9.0 Hz, 1H), 6.86 (dd, J = 9.1, 2.2 Hz, 1H), 6.66 (s, 1H), 6.10 (s, 1H), 5.50 – 5.26 (m, 9H), 3.84 (t, J = 6.8 Hz, 2H), 3.55 (q, J = 7.0 Hz, 2H), 3.15 (d, J = 8.4 Hz, 2H), 2.84 (dp, J = 10.8, 5.8, 5.1 Hz, 5H), 2.52 (t, J = 7.3 Hz, 2H), 2.19 (q, J = 6.9 Hz, 2H), 2.06 (q, J = 6.8 Hz, 2H), 1.78 (p, J = 7.3 Hz, 2H), 1.42 – 1.28 (m, 6H), 1.24 (t, J = 7.0 Hz, 3H), 0.91 (t, J = 6.7 Hz, 3H) ppm.

^{13}C NMR (101 MHz, Methanol-d_4): δ = 175.15, 165.05, 158.34, 153.63, 153.37, 148.64, 142.11, 137.31, 132.02, 130.93, 130.69, 130.48, 130.26, 130.10, 129.97, 129.73, 129.60, 128.85, 127.19,

111.57, 108.43, 107.55, 99.59, 63.35, 51.85, 47.20, 34.99, 33.49, 31.30, 29.02, 28.35, 27.42, 26.65, 25.40, 24.46, 15.28, 13.32 ppm.

HR-MS (ESI negative) m/z found: calculated for $C_{42}H_{50}N_4O_{10}S_2^{2-}$: 834.2979; found: 835.306 $[M+H]^-$.

(7-(ethyl(2-(1-(3-(perfluorobenzamido)propyl)-1H-1,2,3-triazol-4-yl)ethyl)amino)-2-oxo-2H-chromen-4-yl)methyl (5Z,8Z,11Z,14Z)-icosa-5,8,11,14-tetraenoate (**14**)

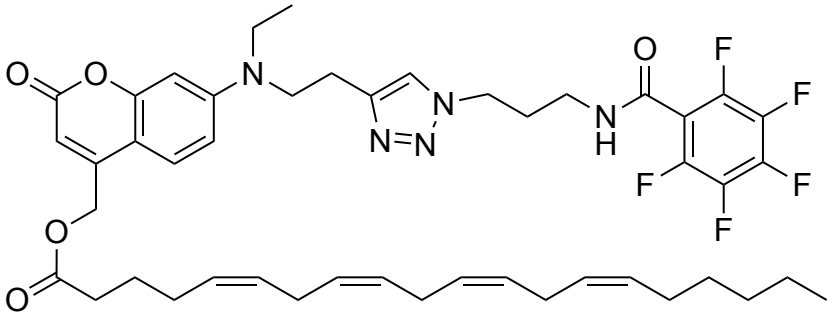

25 mg **6** (44.8 µmol, 1 eq), 20 mg **10** (67.9 µmol, 1.5 eq), 5 mg CuI (26.2 µmol, 0.6 eq) and 2 mg TBTA (3.7 µmol, 0.1 eq) were dissolved in 3 ml dry and degassed $CHCl_3$. The reaction was stopped after 1 h and the reaction mix directly subjected to flash chromatography using ethyl acetate/cyclohexane (2:1). The product was obtained as a yellow solid (25.9 mg, 30.4 µmol, 68 %).

^{1}H NMR (400 MHz, $CDCl_3$): δ = 7.50 (s, 1H), 7.28 (d, J = 9.0 Hz, 1H), 7.17 (t, J = 5.9 Hz, 1H), 6.61 (dd, J = 9.0, 2.5 Hz, 1H), 6.42 (d, J = 2.5 Hz, 1H), 5.46 – 5.27 (m, 8H), 5.25 – 5.16 (m, 2H), 4.46 (t, J = 6.5 Hz, 2H), 3.68 (t, J = 7.3 Hz, 2H), 3.44 (p, J = 7.4, 6.9 Hz, 4H), 3.00 (t, J = 7.3 Hz, 2H), 2.87 – 2.72 (m, 6H), 2.45 (t, J = 7.6 Hz, 2H), 2.27 – 2.09 (m, 4H), 2.04 (q, J = 7.0 Hz, 2H), 1.77 (q, J = 7.5 Hz, 2H), 1.36 – 1.23 (m, 7H), 1.18 (t, J = 7.0 Hz, 4H), 0.87 (t, J = 6.7 Hz, 3H) ppm.

^{13}C NMR (101 MHz, $CDCl_3$): δ = 172.94, 162.04, 158.06, 156.15, 150.76, 149.99, 144.82, 143.62, 142.87, 141.05, 138.98, 136.61, 130.61, 129.28, 128.73, 128.72, 128.41, 128.17, 127.95, 127.64, 124.66, 122.31, 109.15, 106.62, 98.19, 61.21, 50.27, 47.59, 45.44, 37.28, 33.54, 31.62, 29.95, 29.43, 27.33, 26.62, 25.75, 24.78, 23.86, 22.68, 14.17, 12.25 ppm.

^{19}F NMR (376 MHz, $CDCl_3$): δ = -140.64 – -140.80 (m), -150.79 – -150.98 (m), -159.94 – -160.17 (m) ppm.

HR-MS (ESI positive) m/z found: calculated for $C_{46}H_{54}F_5N_5O_5$: 851.4045; found: 852.414 $[M+H]^+$.

(7-(but-3-yn-1-yl(ethyl)amino)-2-oxo-2H-chromen-4-yl)methyl (E)-(1,3-dihydroxyoctadec-4-en-2-yl)carbamate (**17**)

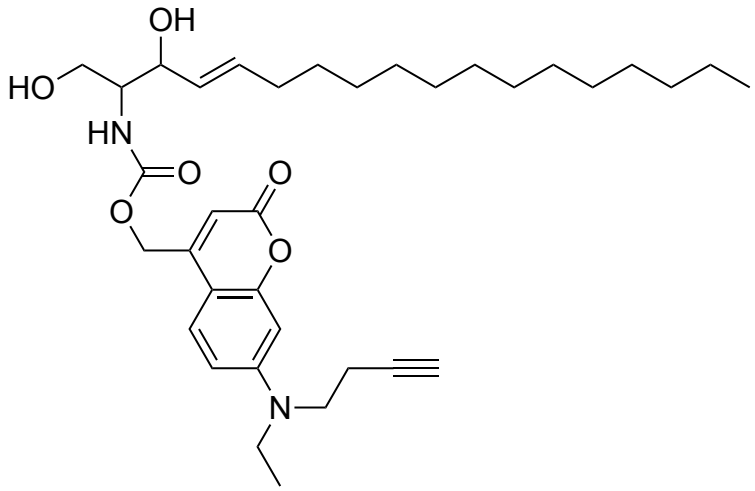

A solution of 100 mg **1** (369 µmol) in 4 ml dry THF with 200 µl DIPEA (1.15 mmol) under an inert argon atmosphere was cooled with an ice bath. Phosgene (600 µl of a solution in toluene, 1.22 mmol) was added dropwise and the reaction mixture was stirred for 2 h in the dark. 200 ml of an ethyl acetate/water (1:1) mix were added, the layers were separated, and the organic layer was washed with brine and dried over sodium sulfate. After removal of volatiles, 140 mg of the crude coumarin chloroformate were obtained and dissolved in 2 ml dry THF. This solution was added dropwise to a solution of D-erythro-sphingosine (**15**, 80 mg, 267 µmol) and DIPEA (200 µl, 1.15 mmol) in 4 ml dry THF at RT. After 2 h in the dark, the reaction was stopped by dilution with 100 ml ethyl acetate. The resulting mixture was washed twice with 100 ml citric acid (5% w/v, 2x 100 ml) and twice with saturated $NaHCO_3$ (2x 100 ml), the organic layer subsequently dried over sodium sulfate and the solvents removed under reduced pressure. The crude product was purified by silica gel column chromatography using ethyl acetate/cyclohexane (4:1) and 106 mg (178 µmol, 67 %) of a yellow solid were obtained.

^{1}H NMR (400 MHz, $CDCl_3$): δ = 7.29 (d, J = 9.0 Hz, 1H), 6.58 (dd, J = 9.0, 2.6 Hz, 1H), 6.51 (d, J = 2.5 Hz, 1H), 6.15 (s, 1H), 5.99 (d, J = 8.4 Hz, 1H), 5.80 (dt, J = 14.2, 6.7 Hz, 1H), 5.54 (dd, J = 15.5, 6.3 Hz, 1H), 5.21 (s, 2H), 4.39 (t, J = 5.2 Hz, 1H), 3.89 (ddd, J = 101.2, 11.5, 3.5 Hz, 2H), 3.68 (dt, J = 8.3, 3.8 Hz, 1H), 3.55 (t, J = 7.3 Hz, 2H), 3.47 (q, J = 7.1 Hz, 2H), 2.48 (td, J = 7.3, 2.7 Hz, 2H), 2.12 – 1.96 (m, 3H), 1.42 – 1.11 (m, 26H), 0.87 (t, J = 6.7 Hz, 3H) ppm.

^{13}C NMR (101 MHz, $CDCl_3$): δ = 162.46, 156.32, 155.91, 150.85, 150.57, 134.60, 129.02, 124.82, 109.20, 106.96, 106.70, 98.54, 81.44, 77.68, 77.36, 77.04, 74.93, 70.71, 62.47, 62.10, 56.13, 49.68, 45.88, 32.63, 32.25, 30.03, 29.99, 29.97, 29.84, 29.69, 29.57, 29.45, 23.02, 17.69, 14.45, 12.54 ppm.

HR-MS (ESI positive) m/z found: calculated for $C_{35}H_{52}N_2O_6$: 596.3825; found: 597.3906 $[M+H]^+$.

(E)-(4-(5-(2-((4-((((1,3-dihydroxyoctadec-4-en-2-yl)carbamoyl)oxy)methyl)-2-oxo-2H-chromen-7-yl)(ethyl)amino)ethyl)-1H-1,2,3-triazol-1-yl)butyl)triphenylphosphonium (**18**)

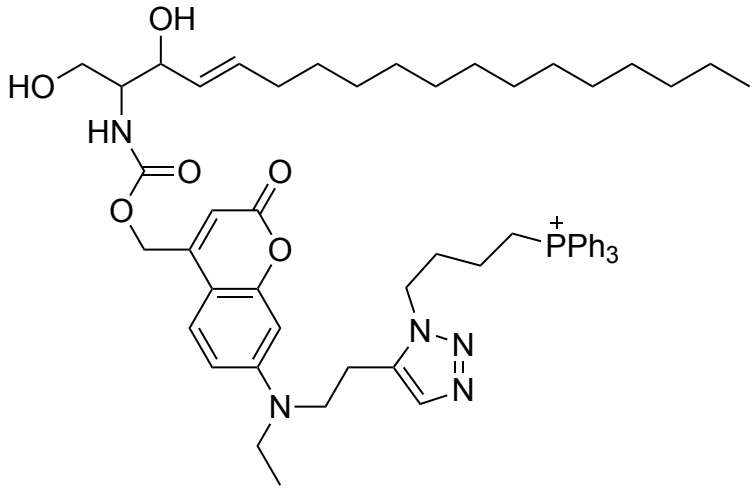

25 mg **17** (41.9 µmol, 1 eq), 22 mg **7** (50 µmol, 1.2 eq), 10 mg CuI (52.5 µmol, 1.3 eq) and 2 mg TBTA (3.7 µmol, 0.1 eq) were dissolved in 2 ml dry and degassed chloroform. After 2 h the reaction was stopped and the reaction mix was directly purified by silica column chromatography using chloroform/methanol/water (65/35/2). Impure fractions were further purified with 35 % MeOH in chloroform. The pure fractions were combined and the solvents were removed under reduced pressure. The obtained yield was 27 mg of a yellow solid (28.4 µmol, 68 %).

^{1}H NMR (400 MHz, DMSO-d_6) δ 7.94 – 7.73 (m, 16H), 6.70 (dd, J = 9.1, 2.5 Hz, 1H), 6.55 (d, J = 2.5 Hz, 1H), 5.55 (dt, J = 15.2, 6.5 Hz, 1H), 5.40 (dd, J = 15.4, 6.9 Hz, 1H), 5.19 (q, J = 16.0 Hz, 2H), 4.88 (d, J = 5.2 Hz, 1H), 4.55 (t, J = 5.5 Hz, 1H), 4.40 (t, J = 6.8 Hz, 2H), 3.89 (q, J = 6.7 Hz, 1H), 3.71 – 3.37 (m, 9H), 2.87 (t, J = 7.5 Hz, 2H), 2.03 – 1.87 (m, 4H), 1.56 – 1.45 (m, 2H), 1.28 – 1.12 (m, 22H), 1.07 (t, J = 6.9 Hz, 3H), 0.83 (t, J = 6.8 Hz, 3H).

^{13}C NMR (101 MHz, DMSO-d_6) δ 160.67, 155.60, 155.32, 151.92, 143.77, 134.92, 133.62, 133.52, 131.10, 130.32, 130.29, 130.19, 125.18, 122.71, 118.84, 118.76, 117.98, 117.90, 108.76, 105.54, 104.62, 97.06, 71.31, 60.60, 60.51, 57.81, 49.42, 47.93, 44.57, 31.65, 31.25, 29.04, 29.02, 28.98, 28.81, 28.73, 28.67, 28.53, 23.20, 22.05, 19.95, 19.45, 19.04, 19.00, 13.92, 12.04.

^{31}P NMR (162 MHz, DMSO-d_6) δ 23.99.

HR-MS (ESI positive) m/z found: calculated for $C_{57}H_{75}N_5O_6P^+$: 956.5449; found: 956.545 $[M]^+$

(7-((2-(1-(3-(dimethylamino)propyl)-1H-1,2,3-triazol-5-yl)ethyl)(ethyl)amino)-2-oxo-2H-chromen-4-yl)methyl (E)-(1,3-dihydroxyoctadec-4-en-2-yl)carbamate (**19**)

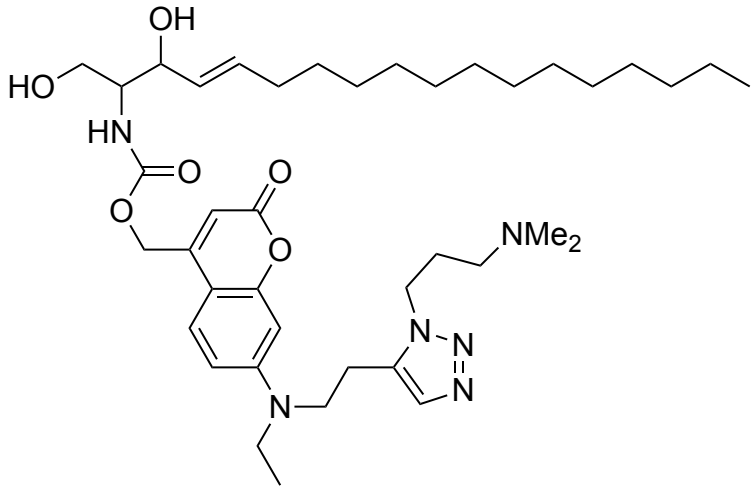

30 mg **17** (50.3 µmol, 1 eq), 11.4 mg **8** (89 µmol, 1.8 eq), 5 mg CuI (26.2 µmol, 0.5 eq) and 2 mg TBTA (3.7 µmol, 0.1 eq) were dissolved in 2 ml dry and degassed DMF. The reaction was stopped by removal of all volatiles after 2 h. The crude product was purified by flash chromatography using 20 % MeOH in chloroform to yield 18 mg of a yellow solid (24.8 µmol, 49 %).

^{1}H NMR (400 MHz, Methanol-d_4): δ = 7.87 (s, 1H), 7.46 (d, J = 9.0 Hz, 1H), 6.76 (dd, 1H), 6.56 (d, J = 2.0 Hz, 1H), 6.12 (s, 1H), 5.71 (dt, J = 14.1, 6.7 Hz, 1H), 5.49 (dd, J = 15.4, 7.5 Hz, 1H), 5.29 (q, 2H), 4.45 (t, J = 6.8 Hz, 2H), 4.06 (t, J = 7.4 Hz, 1H), 3.83 – 3.57 (m, 5H), 3.48 (q, J = 6.9 Hz, 2H), 3.03 (t, J = 7.2 Hz, 2H), 2.64 (t, 2H), 2.48 (s, 6H), 2.15 (p, J = 6.8 Hz, 2H), 2.02 (q, J = 6.7 Hz, 2H), 1.35 – 1.16 (m, 27H), 0.88 (t, J = 6.8 Hz, 3H) ppm.

^{13}C NMR (101 MHz, Methanol-d_4): δ = 164.23, 157.88, 157.33, 153.72, 152.42, 134.96, 131.12, 126.04, 110.59, 107.50, 106.05, 98.70, 73.91, 62.69, 62.51, 58.81, 56.71, 50.99, 46.10, 44.69, 33.35, 33.06, 30.80, 30.79, 30.78, 30.75, 30.71, 30.46, 30.36, 30.27, 27.91, 24.56, 23.72, 14.44, 12.45 ppm.

HR-MS (ESI positive) m/z found: calculated for $C_{40}H_{64}N_6O_6$: 724.4887; found: 725.497 $[M+H]^+$.

(E)-4-(4-(2-((4-((((1,3-dihydroxyoctadec-4-en-2-yl)carbamoyl)oxy)methyl)-2-oxo-2H-chromen-7-yl)(ethyl)amino)ethyl)-1H-1,2,3-triazol-1-yl)benzene-1,3-disulfonate (**20**)

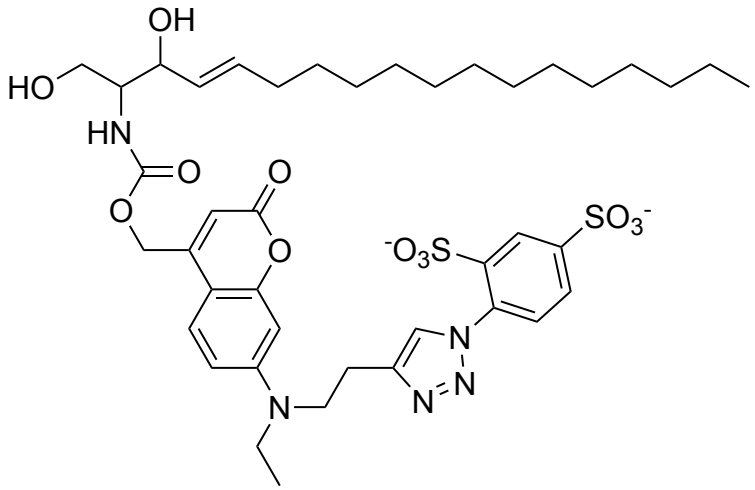

30 mg **17** (50.3 µmol, 1 eq), 33 mg **9** (105 µmol, 2.1 eq), 5 mg CuI (26.2 µmol, 0.5 eq) and 2 mg TBTA (3.7 µmol, 0.1 eq) were dissolved in 2 ml dry and degassed DMF. The reaction was stopped by removal of all volatiles after 2 h and the residue was purified by flash chromatography using chloroform/methanol/water (65/35/4). The product was obtained as a yellow solid (20 mg, 22 µmol, 44 %).

^{1}H NMR (400 MHz, Methanol-d_4): δ = 8.64 (d, J = 2.0 Hz, 1H), 8.40 (s, 1H), 8.05 (dd, J = 8.1, 2.0 Hz, 1H), 7.56 (d, J = 8.2 Hz, 1H), 7.49 (d, J = 9.0 Hz, 1H), 6.82 (dd, J = 9.2, 2.5 Hz, 1H), 6.62 (d, J = 2.5 Hz, 1H), 6.13 (s, 1H), 5.71 (dt, J = 14.3, 6.7 Hz, 1H), 5.49 (dd, J = 15.4, 7.5 Hz, 1H), 5.32 (q, J = 15.8 Hz, 2H), 4.06 (t, J = 7.4 Hz, 1H), 3.86 – 3.72 (m, 3H), 3.72 – 3.58 (m, 2H), 3.52 (q, J = 7.0 Hz, 2H), 3.11 (t, 2H), 2.02 (q, J = 7.2 Hz, 2H), 1.42 – 1.12 (m, 25H), 0.88 (t, J = 6.7 Hz, 3H) ppm.

^{13}C NMR (101 MHz, Methanol-d_4): δ = 164.35, 157.91, 157.38, 153.74, 152.46, 147.68, 145.16, 141.16, 136.45, 134.96, 131.09, 129.69, 129.28, 128.00, 127.82, 126.13, 110.71, 107.50, 106.04, 98.72, 73.93, 62.77, 62.53, 58.80, 50.99, 49.64, 49.43, 49.21, 49.00, 48.79, 48.58, 48.36, 46.31, 33.34, 33.06, 30.80, 30.75, 30.70, 30.47, 30.36, 30.27, 24.56, 23.72, 14.44, 12.47 ppm.

HR-MS (ESI positive) m/z found: calculated for $C_{41}H_{55}N_5O_{12}S_2^{2-}$: 873.330; found: 874.339 $[M+H]^-$
.

(7-(ethyl(2-(1-(3-(perfluorobenzamido)propyl)-1H-1,2,3-triazol-4-yl)ethyl)amino)-2-oxo-2H-chromen-4-yl)methyl (E)-(1,3-dihydroxyoctadec-4-en-2-yl)carbamate (**21**)

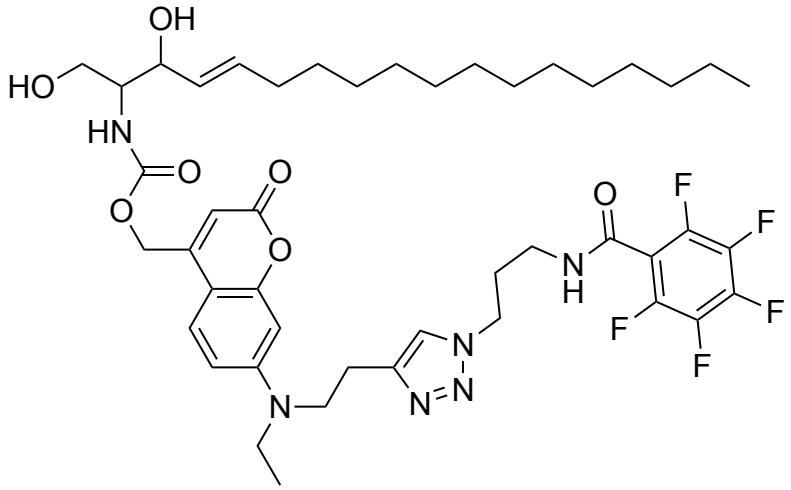

20 mg **17** (33.5 µmol, 1 eq), 20 mg **10** (68 µmol, 2 eq), 5 mg CuI (26.2 µmol, 0.8 eq) and 2 mg TBTA (3.7 µmol, 0.1 eq) were dissolved in 2 ml dry and degassed DMF. After 4 h the reaction was stopped by removal of all volatiles. The crude product was purified by silica column chromatography using 5% MeOH in chloroform. The obtained yield was 15 mg of a yellow solid (16.8 µmol, 50%).

^{1}H NMR (400 MHz, Methanol-d_4): δ 7.84 = (s, 1H), 7.45 (d, J = 9.0 Hz, 1H), 7.06 (N-H, partially exchanged with D), 6.74 (dd, J = 9.1, 2.5 Hz, 1H), 6.56 (d, J = 2.5 Hz, 1H), 5.71 (dt, J = 14.1, 6.7 Hz, 1H), 5.49 (dd, J = 15.4, 7.4 Hz, 1H), 5.38 – 5.14 (m, 2H), 4.46 (t, J = 6.9 Hz, 2H), 4.05 (t, J = 7.5 Hz, 1H), 3.82 – 3.56 (m, 5H), 3.47 (q, J = 7.0 Hz, 2H), 3.35 (t, J = 6.7 Hz, 2H), 3.03 (t, J = 7.3 Hz, 2H), 2.16 (p, J = 6.8 Hz, 2H), 2.02 (q, J = 7.1 Hz, 2H), 1.38 – 1.15 (m, 27H), 0.88 (t, J = 6.7 Hz, 3H) ppm.

^{13}C NMR (101 MHz, Methanol-d_4): δ = 164.28, 157.88, 157.36, 153.72, 152.44, 146.01, 134.96, 131.16, 126.01, 124.40, 110.57, 107.52, 106.05, 98.74, 73.92, 62.68, 62.49, 58.82, 50.99, 46.14, 38.01, 33.35, 33.08, 30.92, 30.81, 30.80, 30.76, 30.72, 30.48, 30.37, 30.28, 24.57, 23.73, 14.44, 12.41 ppm. Signals stemming from the pentafluoro benzamide structure (δ 145.3 - 136.34) were not well resolved due to the presence of complex fluorine-carbon coupling patterns.

^{19}F NMR (376 MHz, Methanol-d_4): δ = -143.84 – -143.98 (m), -155.02 – -155.19 (m), -163.54 – -163.76 (m) ppm.

HR-MS (ESI positive) m/z calculated for $C_{45}H_{59}F_5N_6O_7$: 890.4365; found: 891.443 $[M+H]^+$.

^{1}H and ^{13}C NMR spectra of new compounds

7-(But-3-yn-1-yl(ethyl)amino)-4-(hydroxymethyl)-2H-chromen-2-one (**1**) ^{1}H NMR:

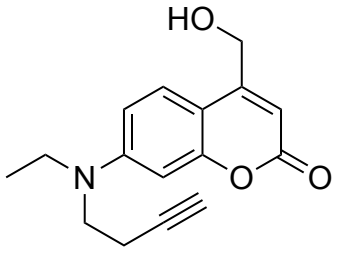

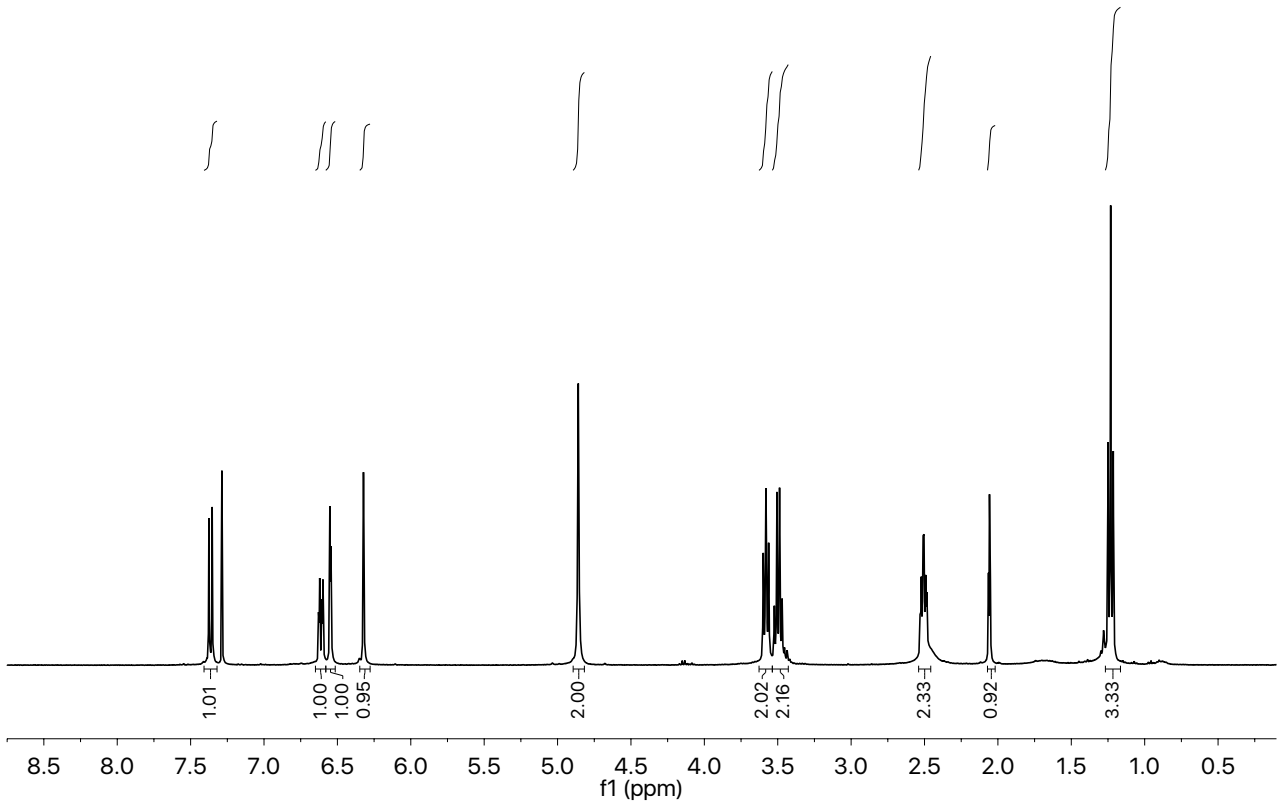

7-(But-3-yn-1-yl(ethyl)amino)-4-(hydroxymethyl)-2H-chromen-2-one (**1**) ^{13}C NMR:

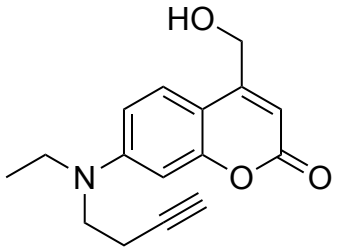

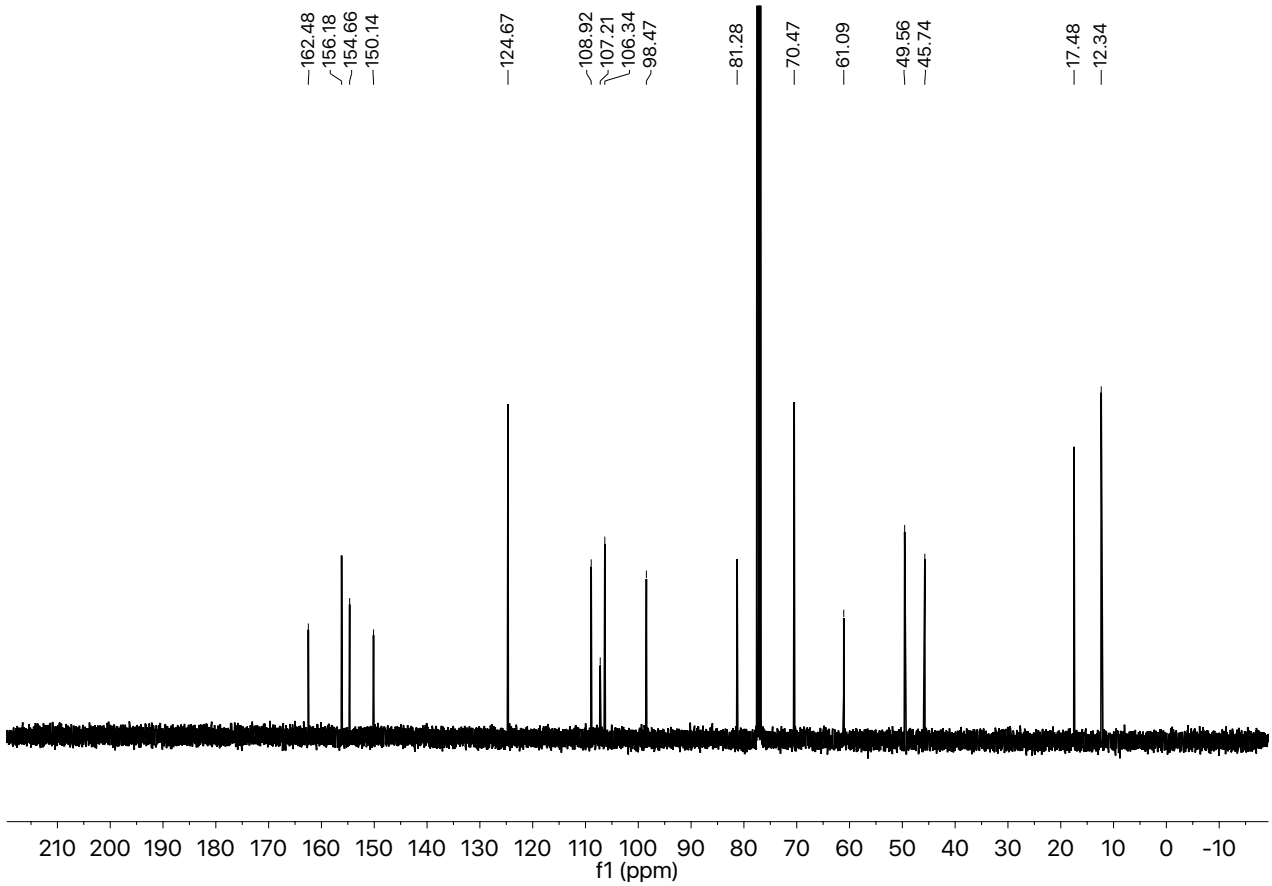

(7-(Ethylamino)-2-oxo-2H-chromen-4-yl)methyl acetate (**3**) ^{1}H NMR:

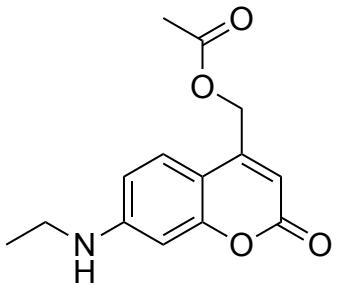

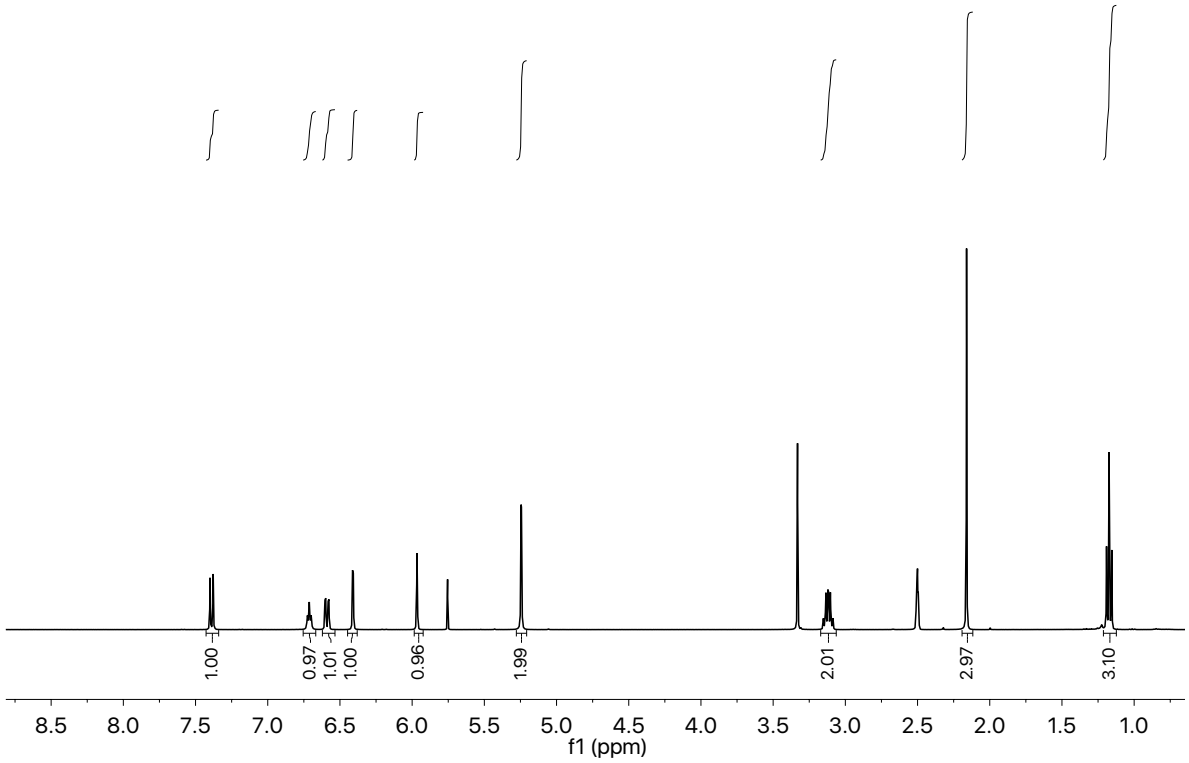

(7-(Ethylamino)-2-oxo-2H-chromen-4-yl)methyl acetate (**3**) ^{13}C NMR:

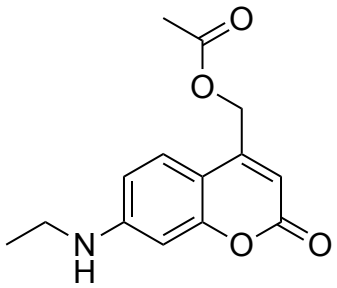

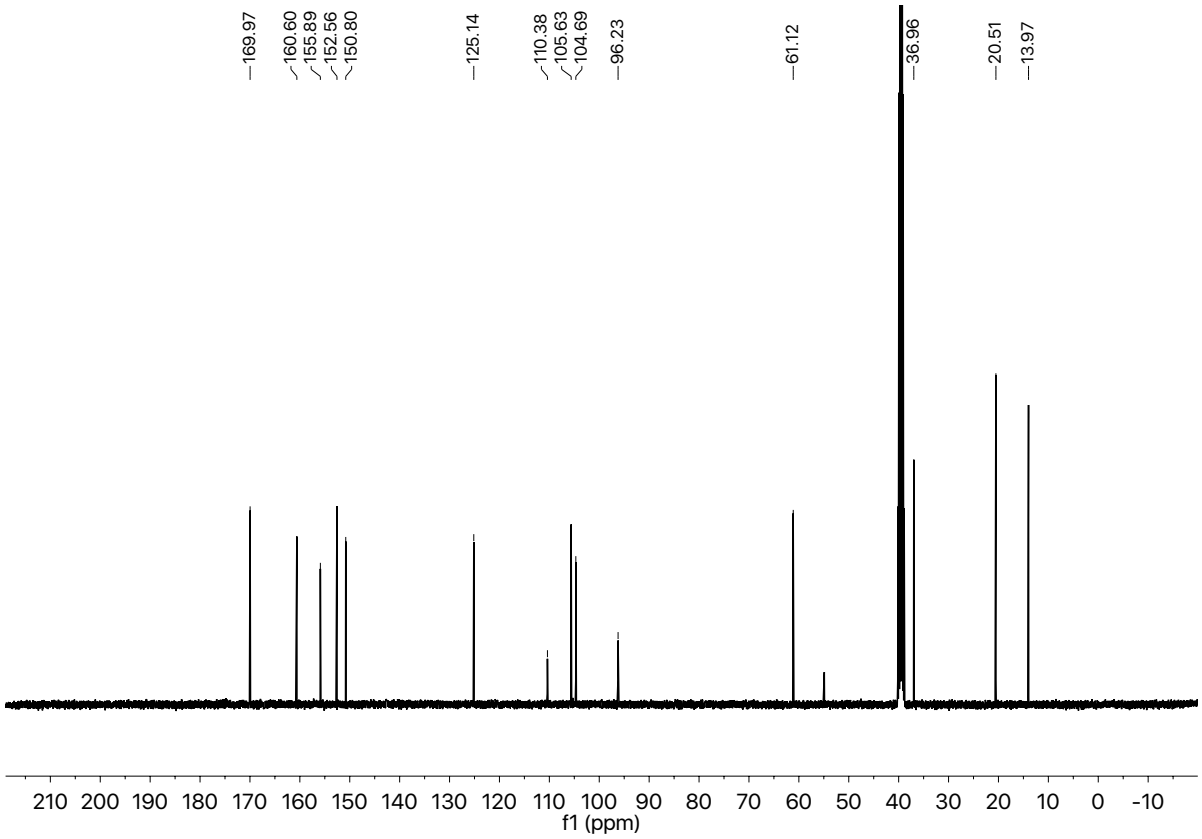

(7-(But-3-yn-1-yl(ethyl)amino)-2-oxo-2H-chromen-4-yl)methyl acetate (**4**) ^{1}H NMR:

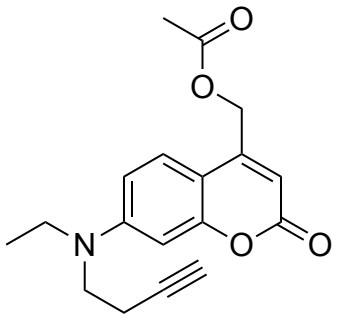

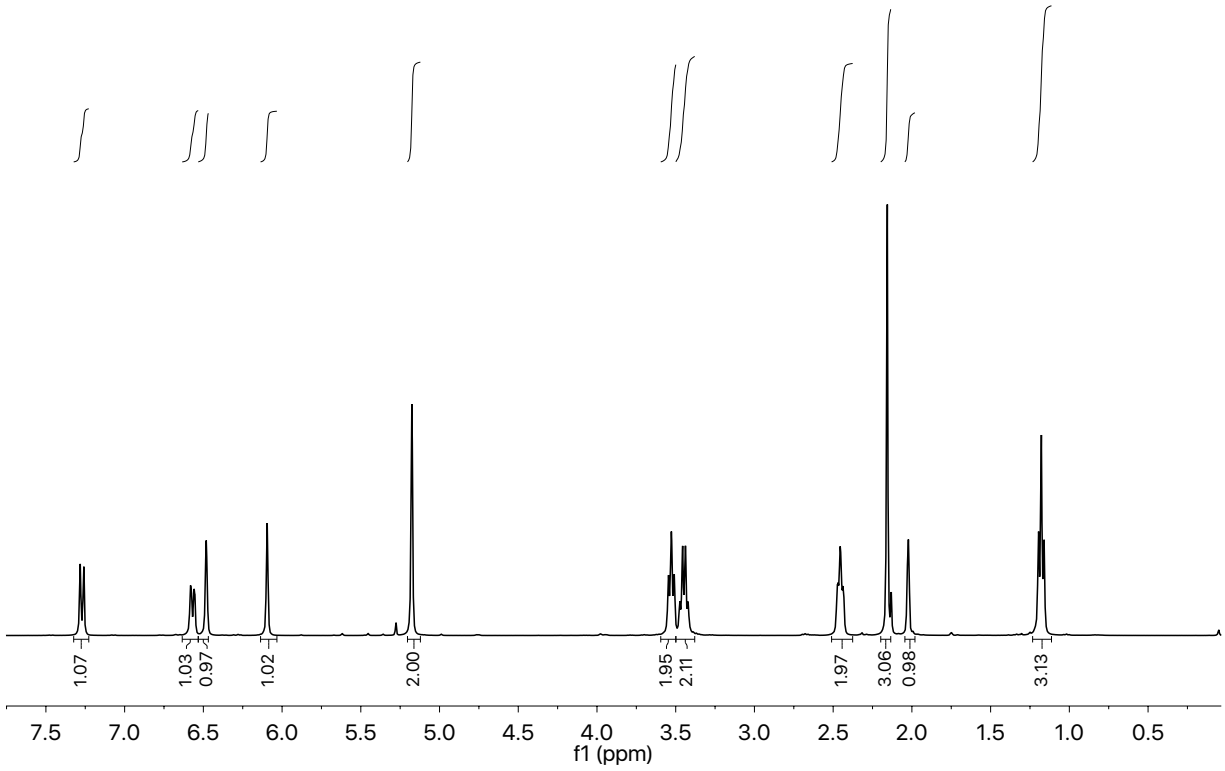

(7-(But-3-yn-1-yl(ethyl)amino)-2-oxo-2H-chromen-4-yl)methyl acetate (**4**) ^{13}C NMR:

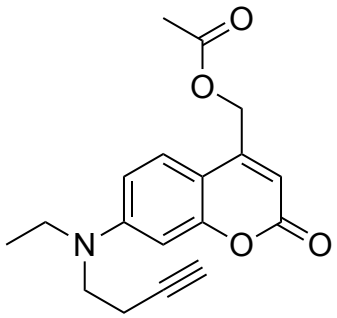

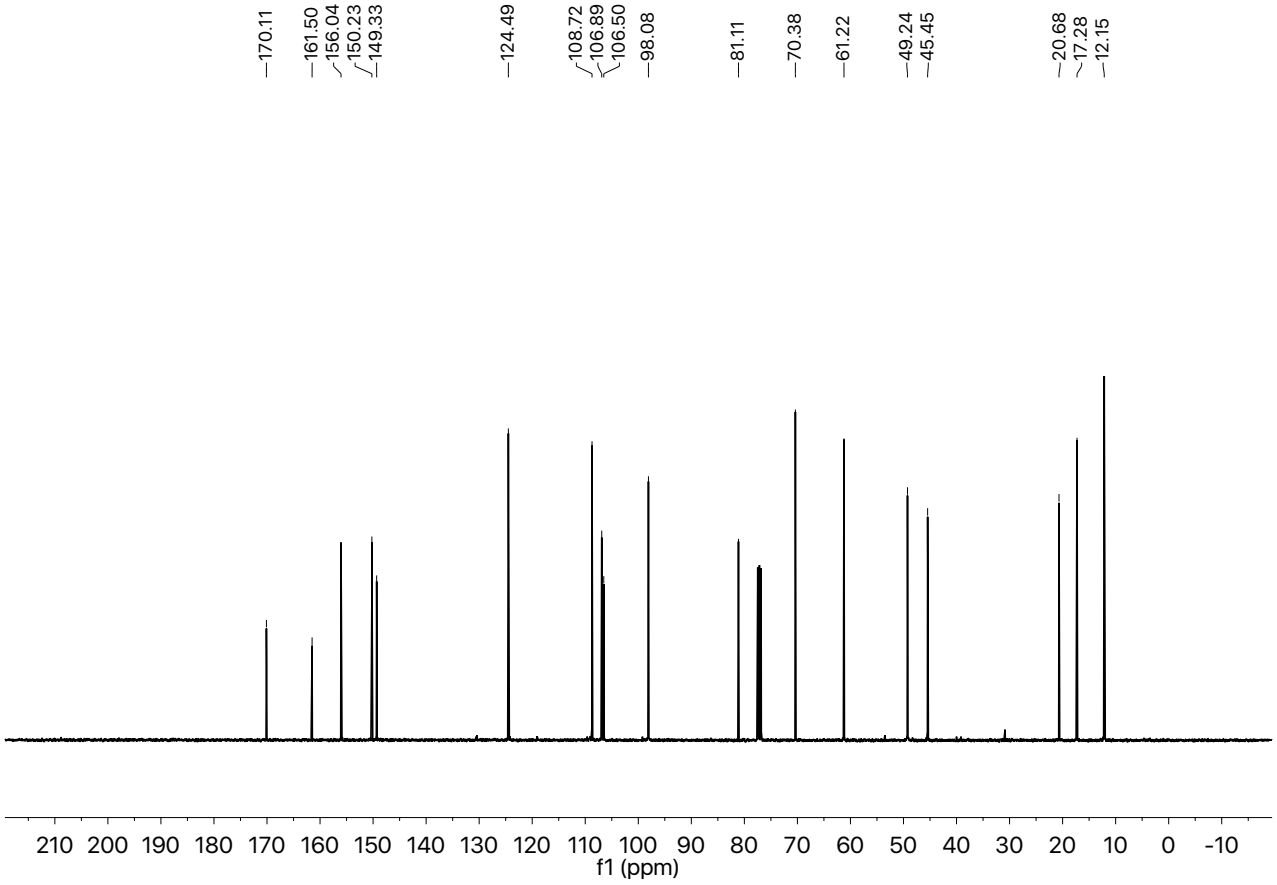

(7-(but-3-yn-1-yl(ethyl)amino)-2-oxo-2H-chromen-4-yl)methyl-(5Z,8Z,11Z,14Z)-icosa-5,8,11,14-tetraenoate (**6**) ^{1}H NMR:

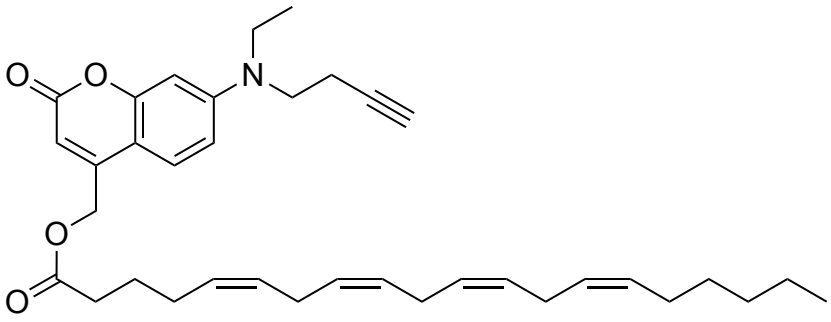

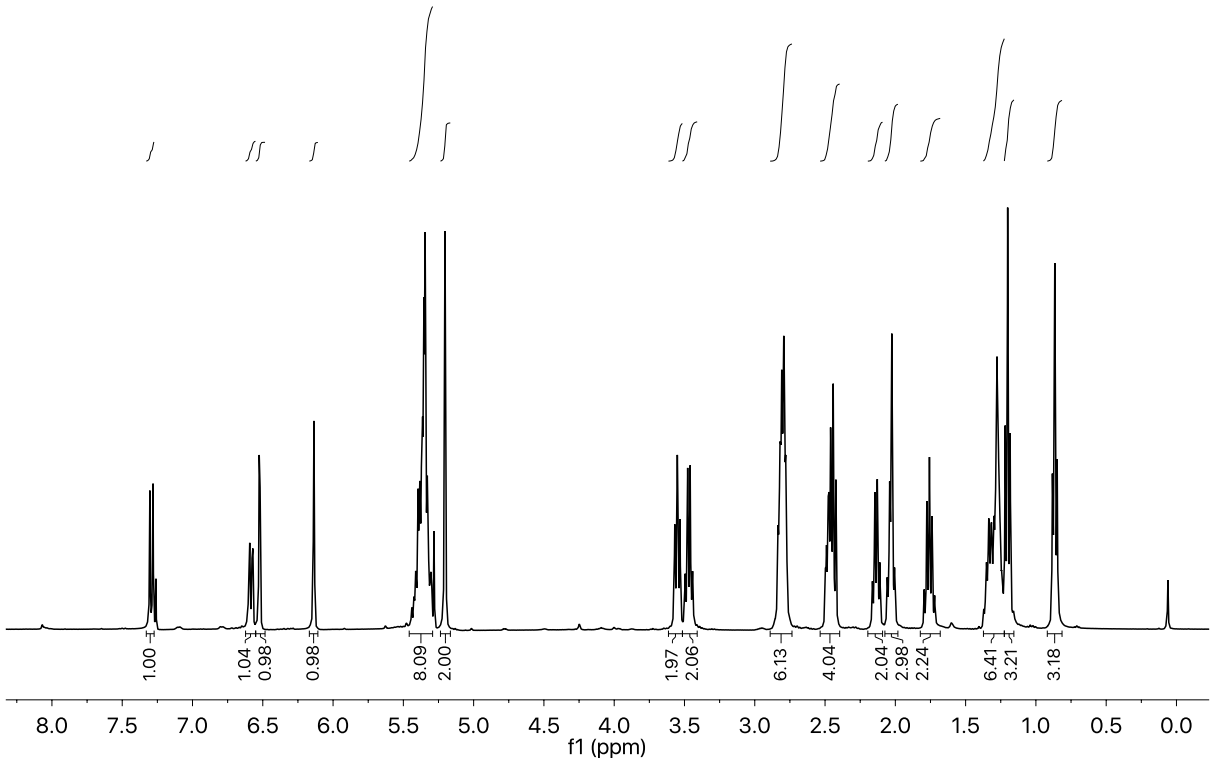

(7-(but-3-yn-1-yl(ethyl)amino)-2-oxo-2H-chromen-4-yl)methyl (5Z,8Z,11Z,14Z)-icosa-5,8,11,14-tetraenoate (**6**) ^{13}C NMR:

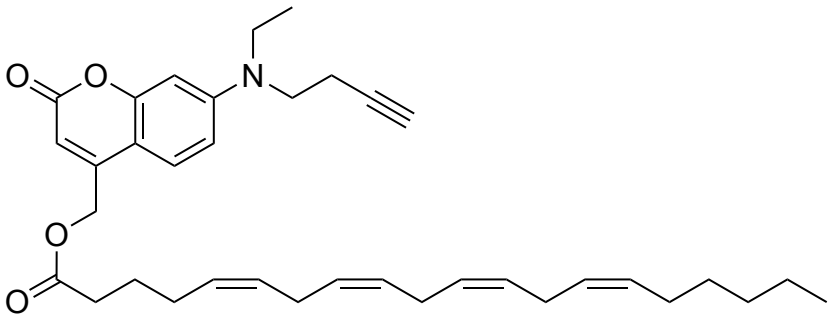

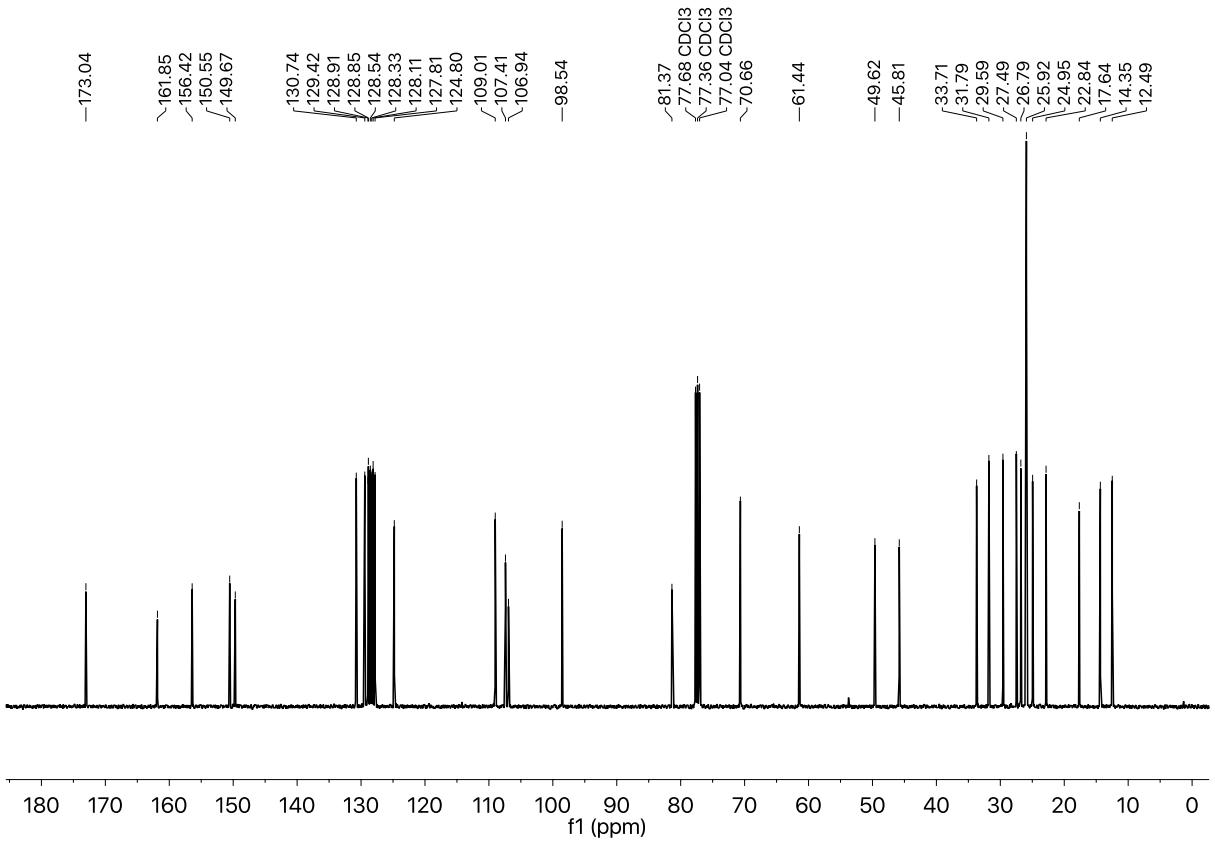

(4-azidobutyl)triphenylphosphonium (**7**) ^{1}H NMR:

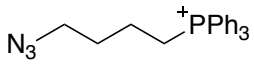

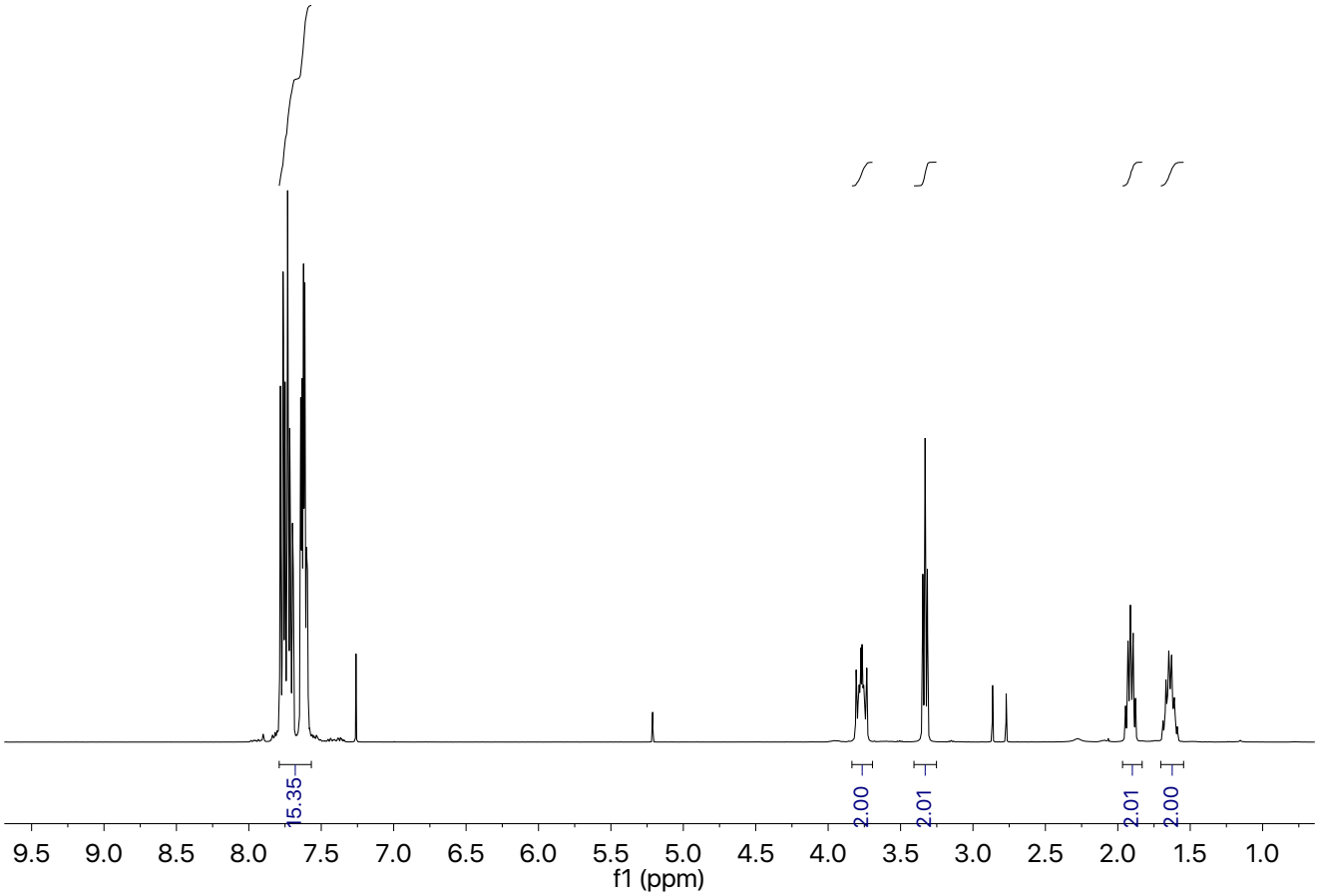

(4-azidobutyl)triphenylphosphonium (**7**) ^{13}C NMR:

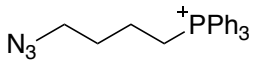

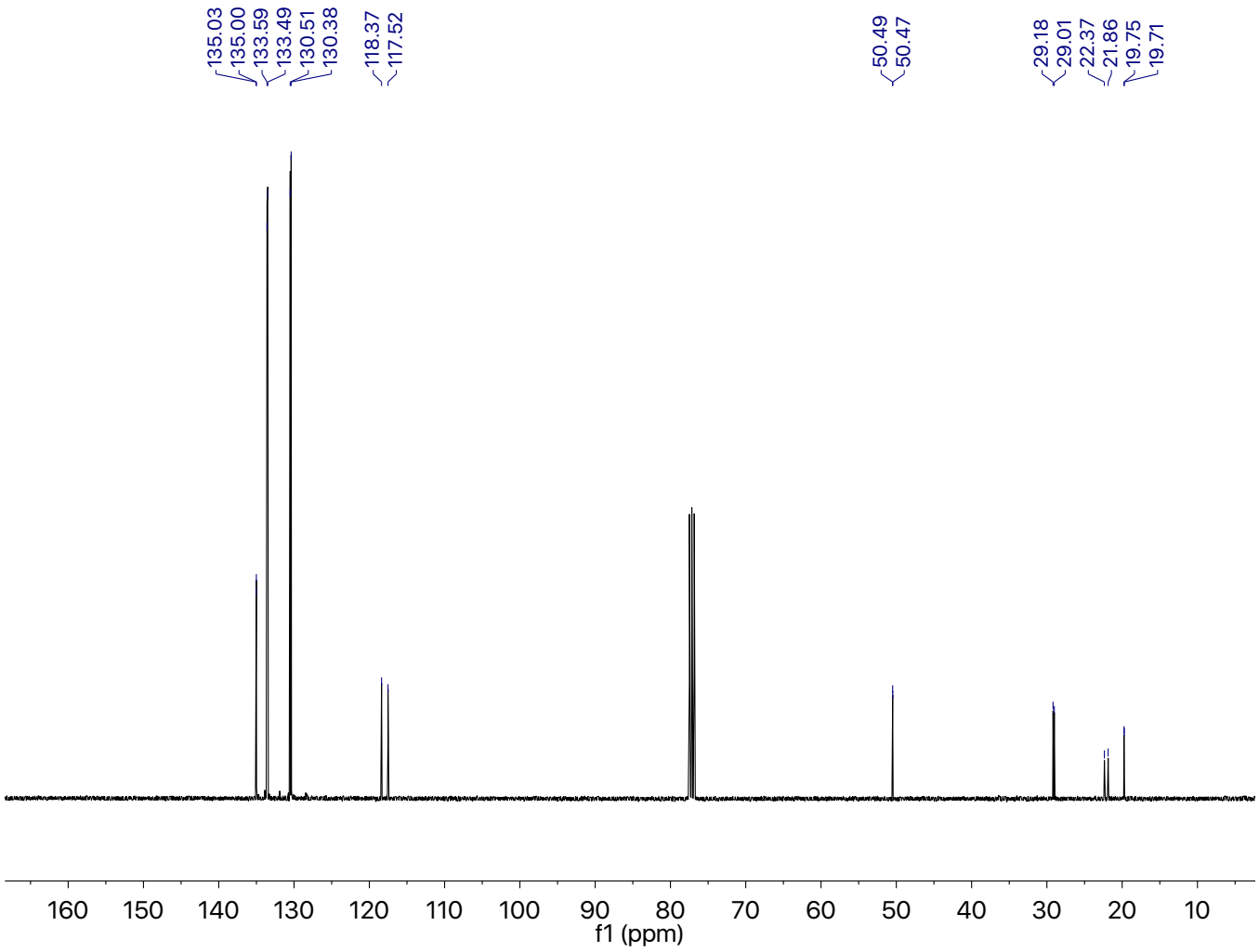

(4-azidobutyl)triphenylphosphonium (**7**) ^{31}P NMR:

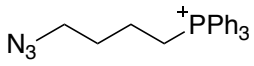

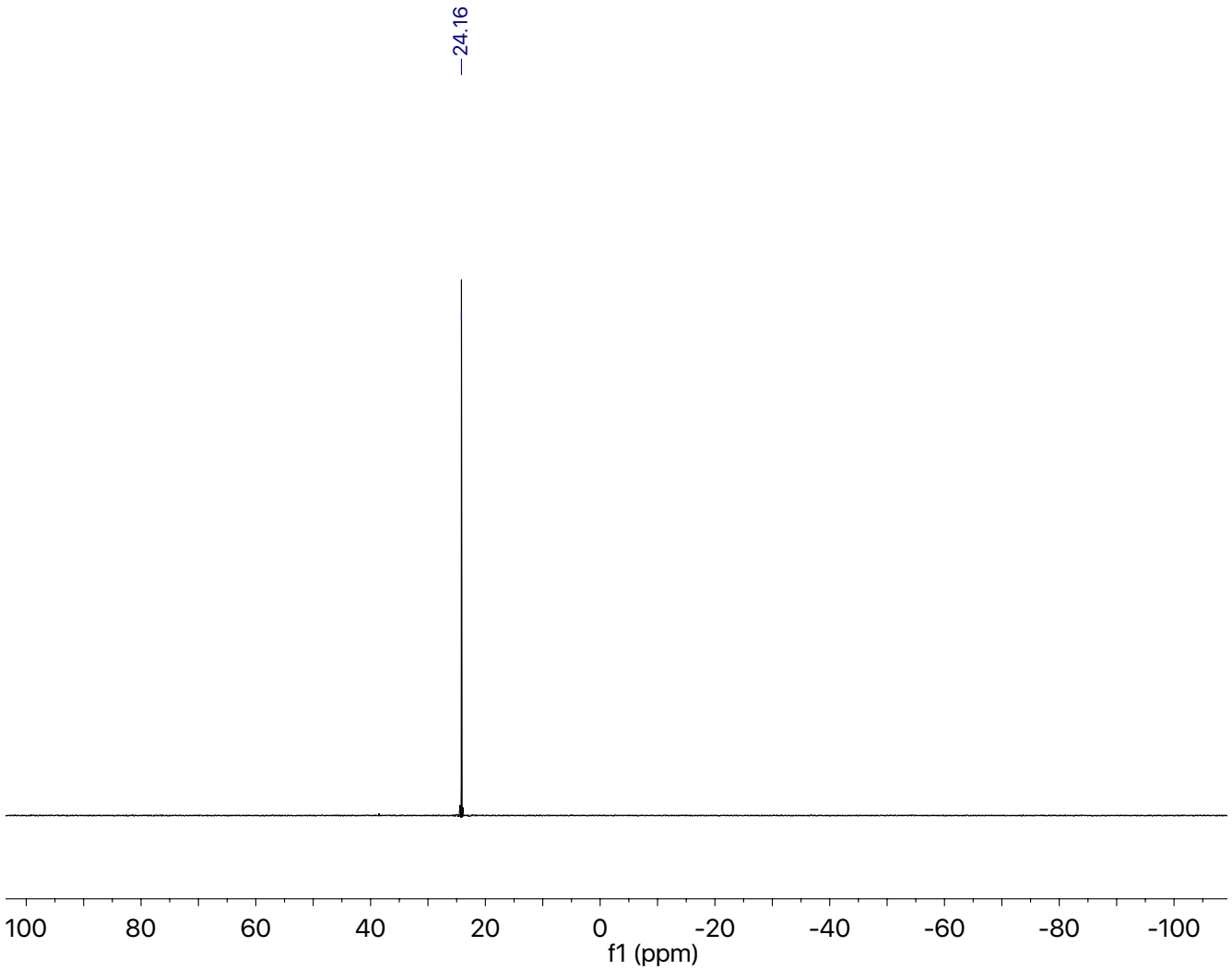

4-azidobenzene-1,3-disulfonate (**9**) ^{1}H NMR:

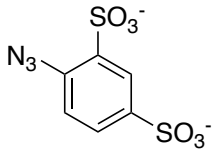

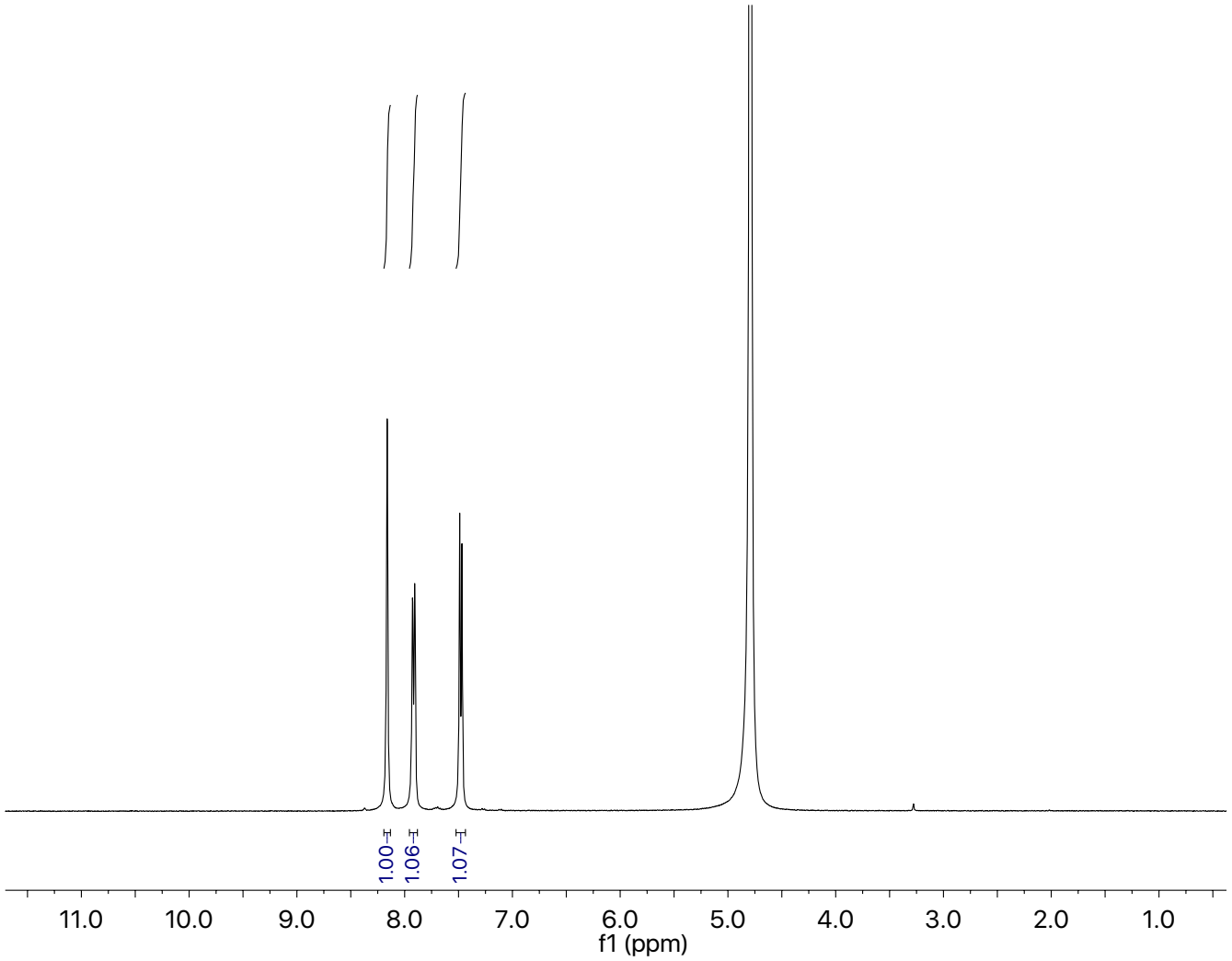

4-azidobenzene-1,3-disulfonate (**9**) ^{13}C NMR:

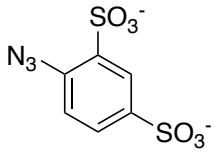

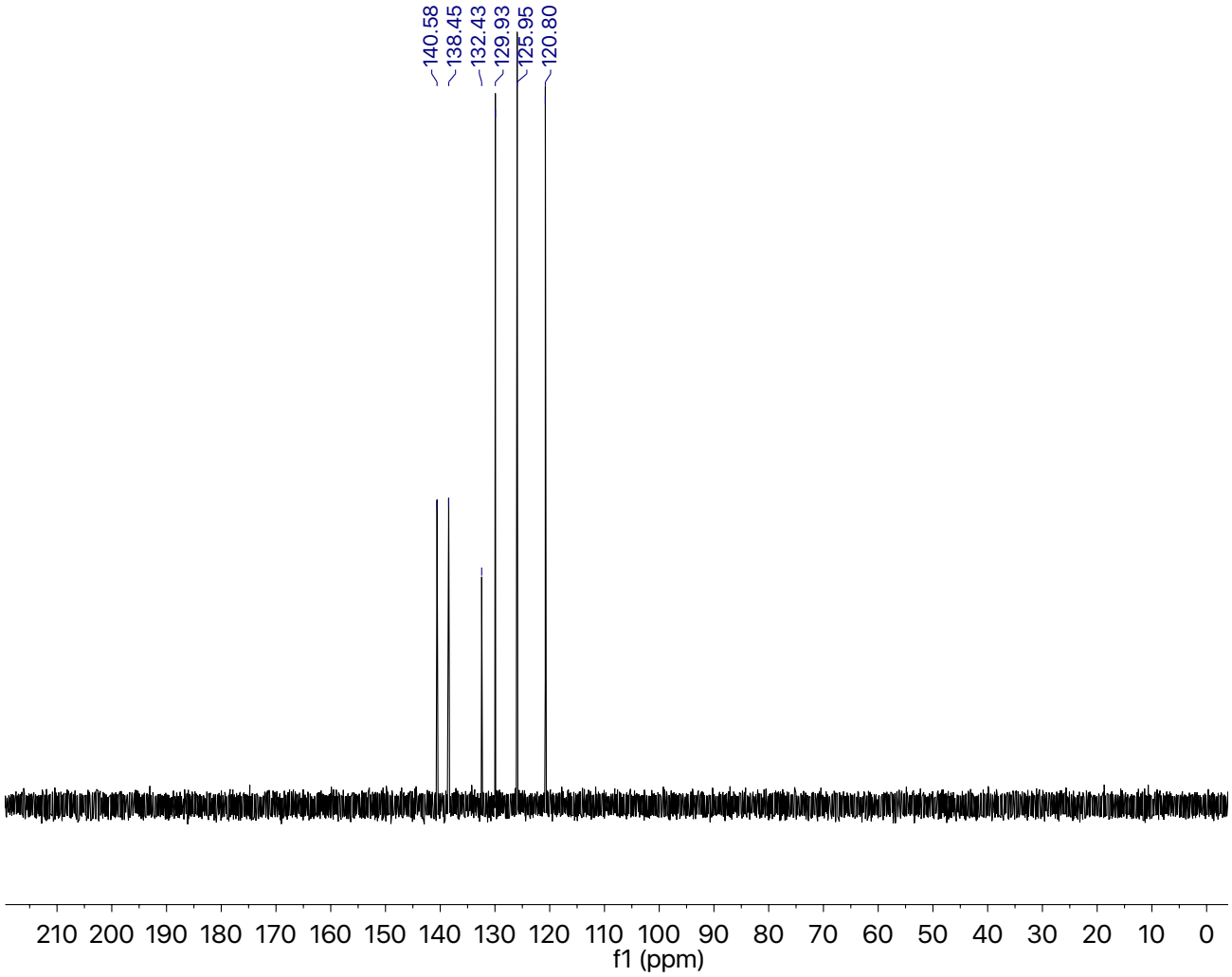

N-(3-azidopropyl)-2,3,4,5,6-pentafluorobenzamide (**10**) ^{1}H NMR:

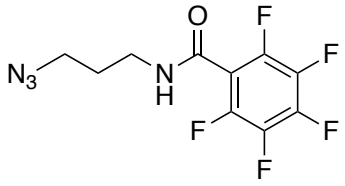

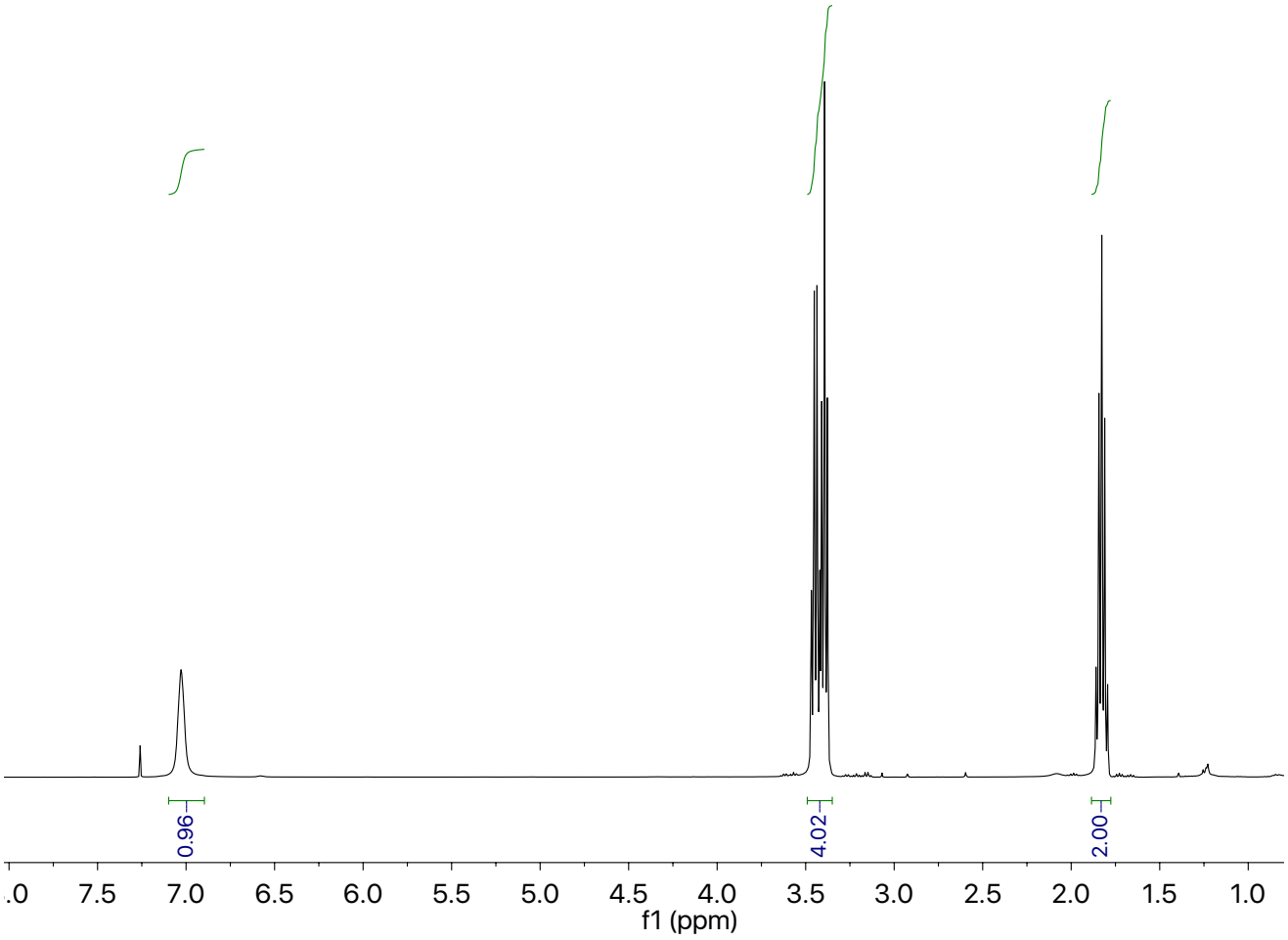

N-(3-azidopropyl)-2,3,4,5,6-pentafluorobenzamide (**10**) ^{13}C NMR:

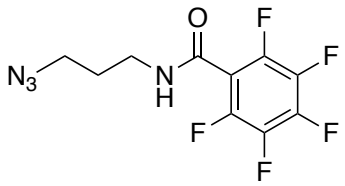

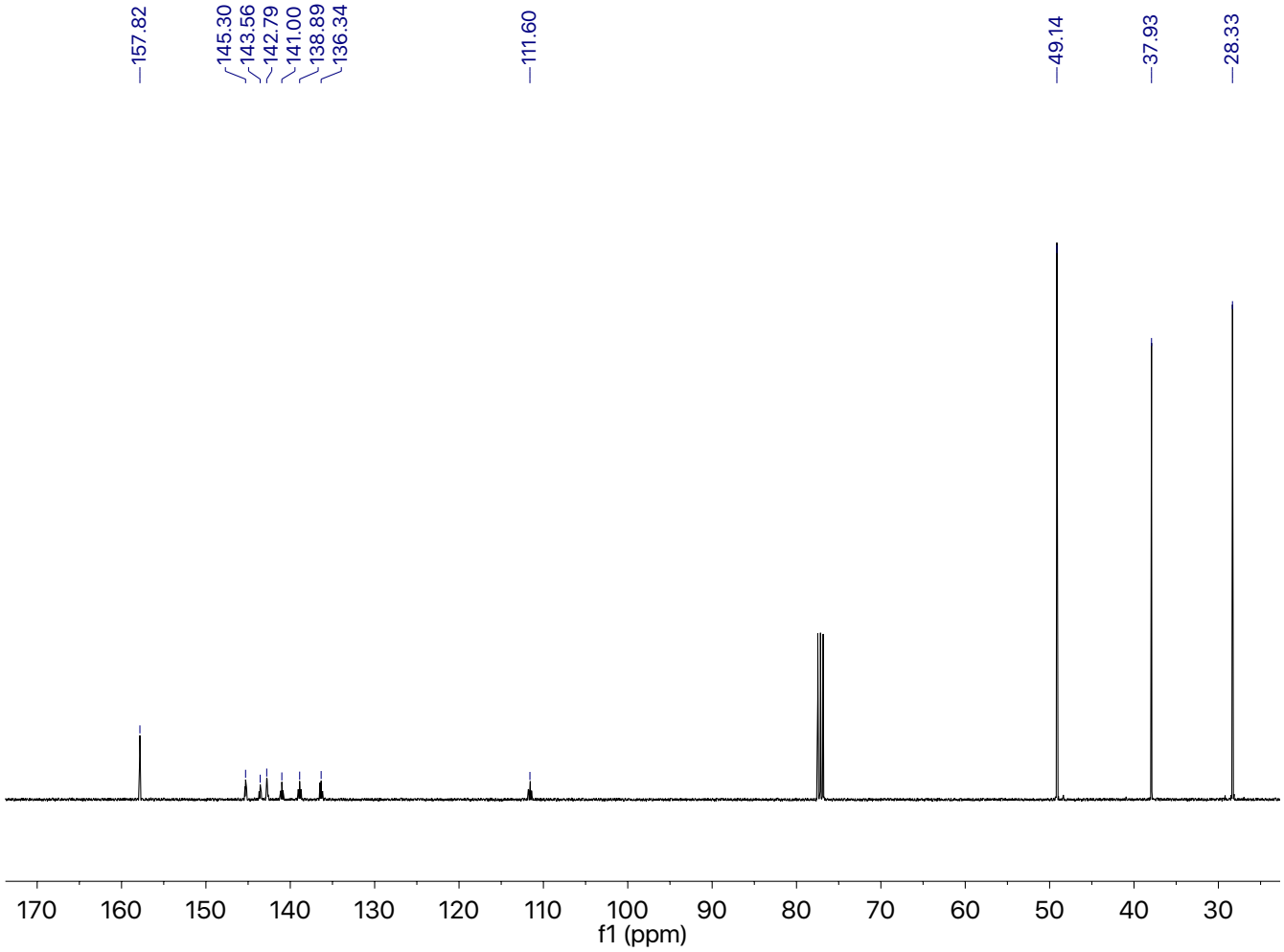

N-(3-azidopropyl)-2,3,4,5,6-pentafluorobenzamide (**10**) ^{19}F NMR:

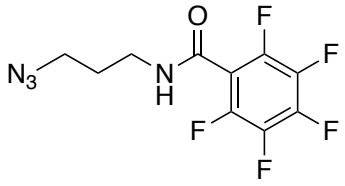

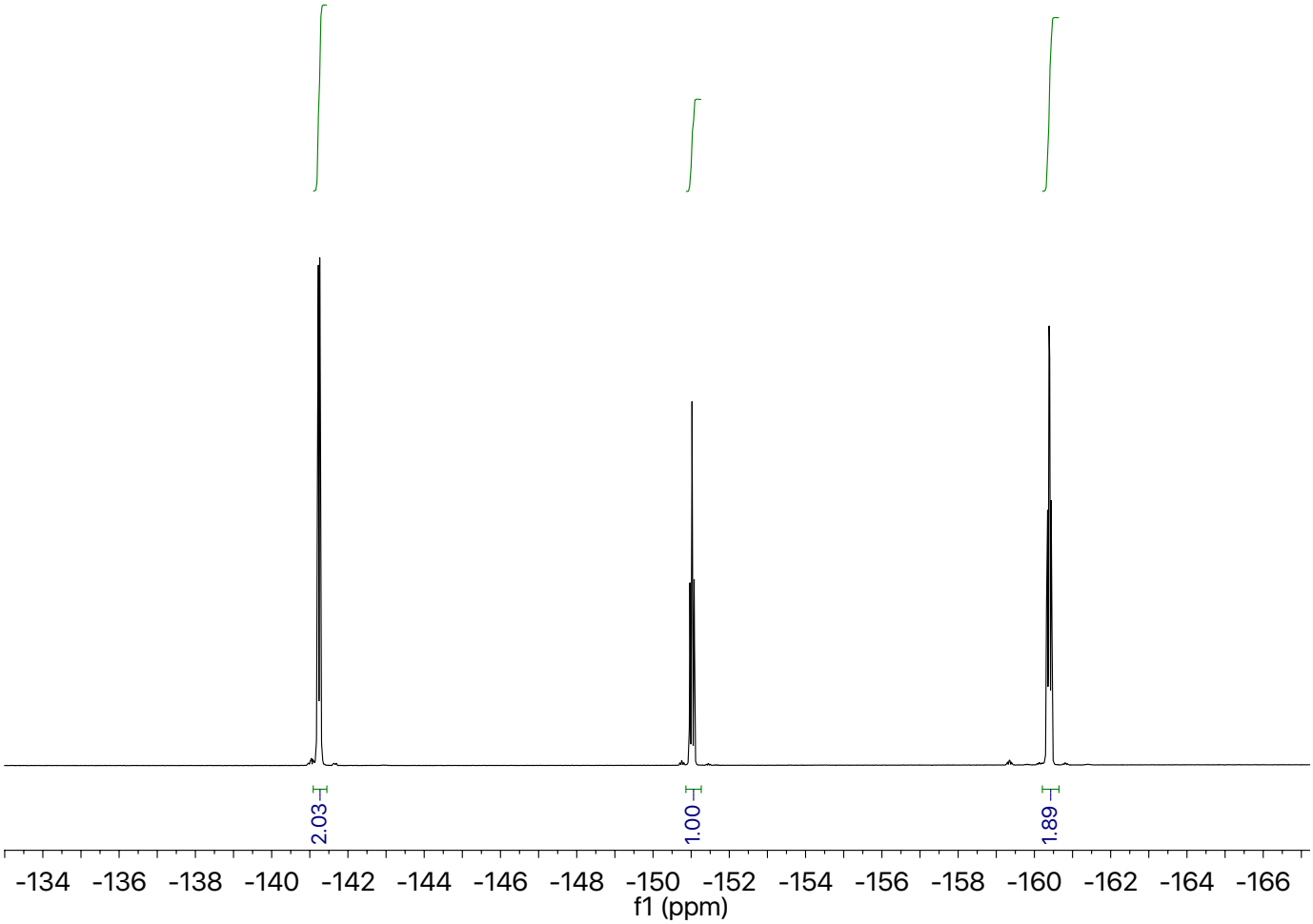

(4-(4-(2-(ethyl(4-((((5Z,8Z,11Z,14Z)-icosa-5,8,11,14-tetraenoyl)oxy)methyl)-2-oxo-2H-chromen-7-yl)amino)ethyl)-1H-1,2,3-triazol-1-yl)butyl)triphenylphosphonium (**11**) ^{1}H NMR:

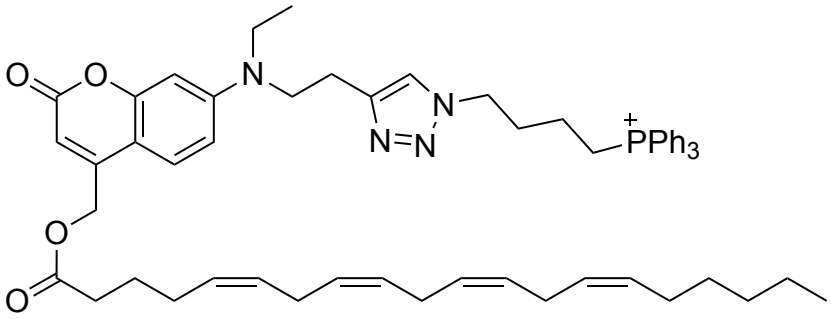

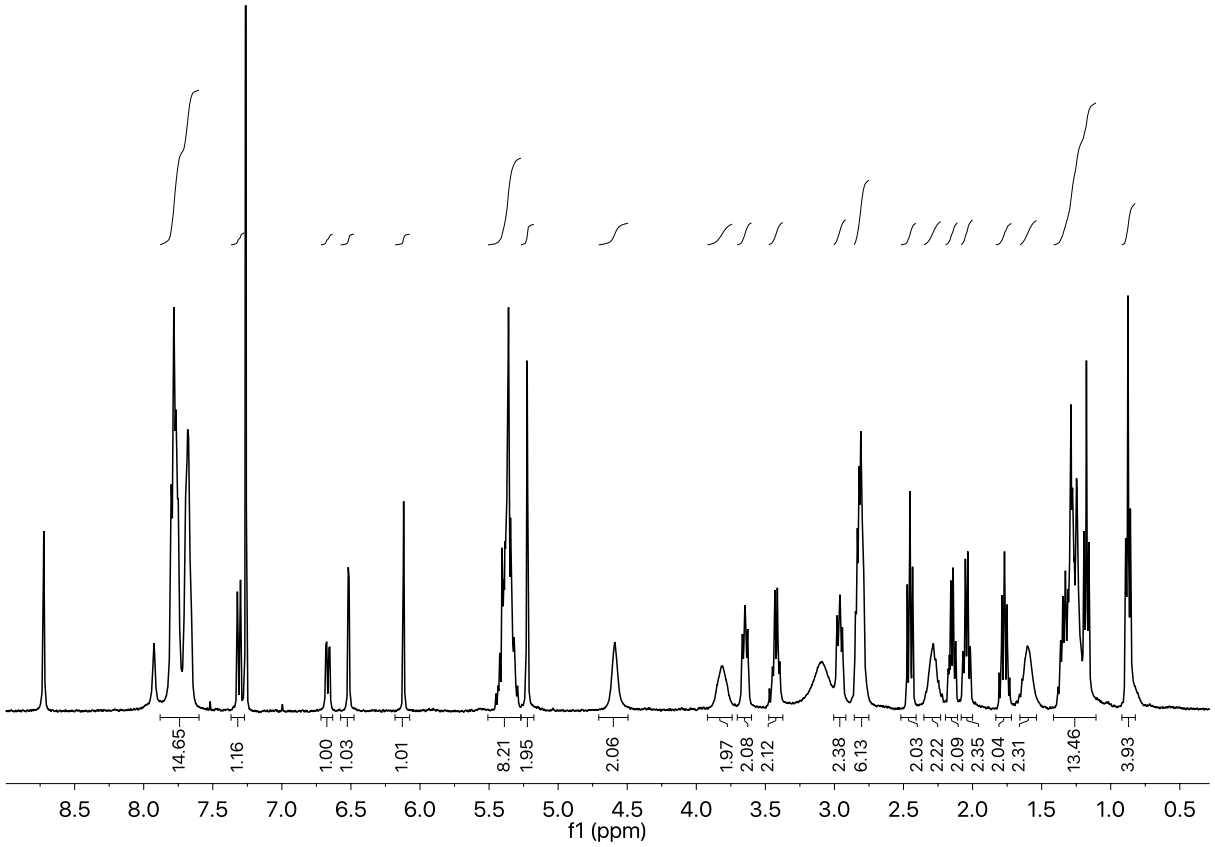

(4-(4-(2-(ethyl(4-((((5Z,8Z,11Z,14Z)-icosa-5,8,11,14-tetraenoyl)oxy)methyl)-2-oxo-2H-chromen-7-yl)amino)ethyl)-1H-1,2,3-triazol-1-yl)butyl)triphenylphosphonium (**11**) ^{13}C NMR:

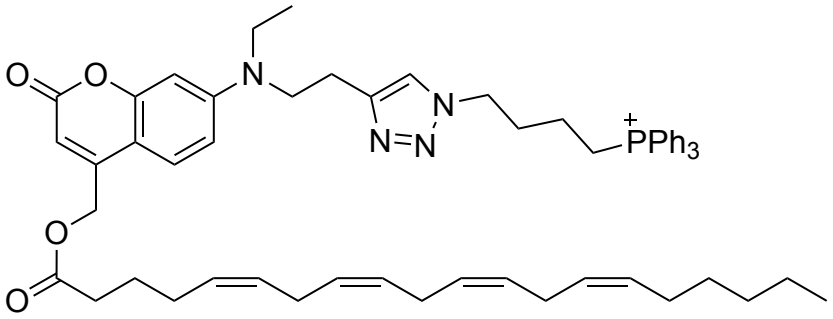

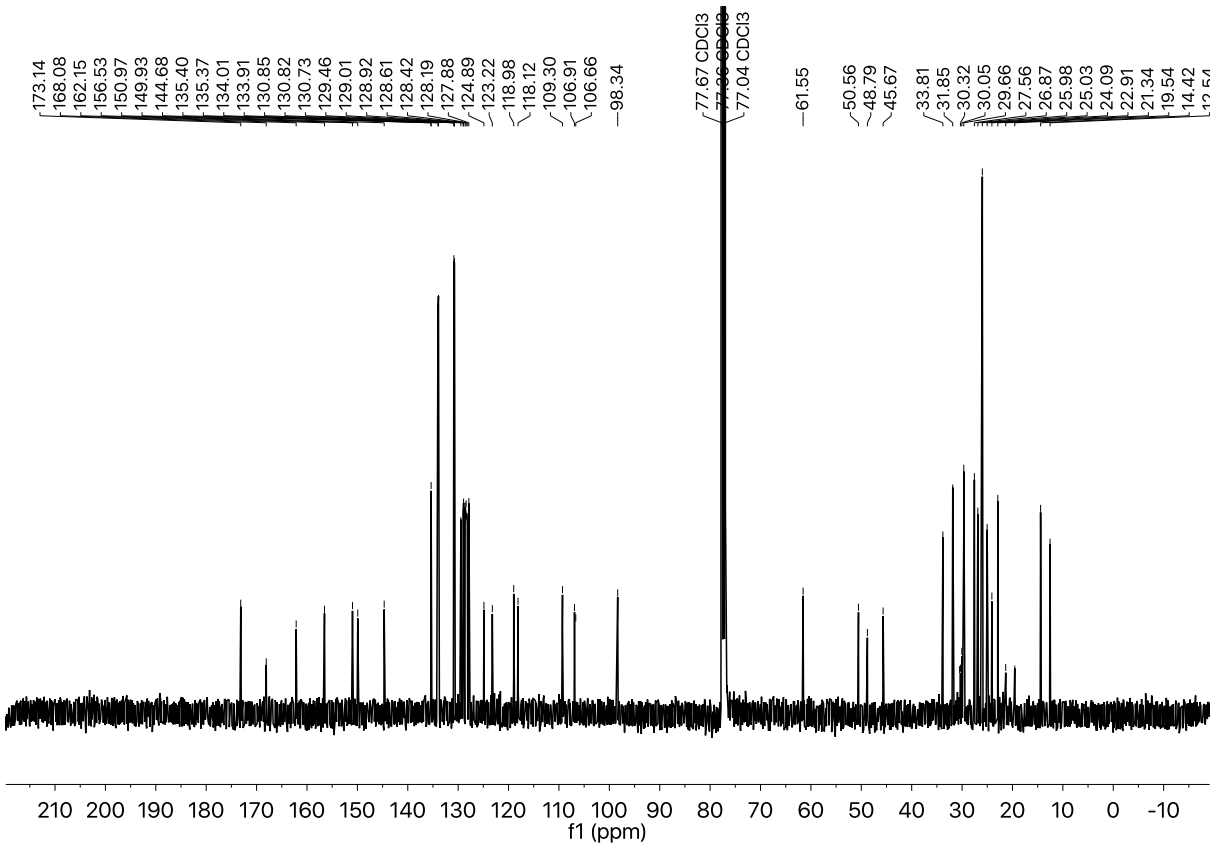

(4-(4-(2-(ethyl(4-((((5Z,8Z,11Z,14Z)-icosa-5,8,11,14-tetraenoyl)oxy)methyl)-2-oxo-2H-chromen-7-yl)amino)ethyl)-1H-1,2,3-triazol-1-yl)butyl)triphenylphosphonium (**11**) ^{31}P NMR:

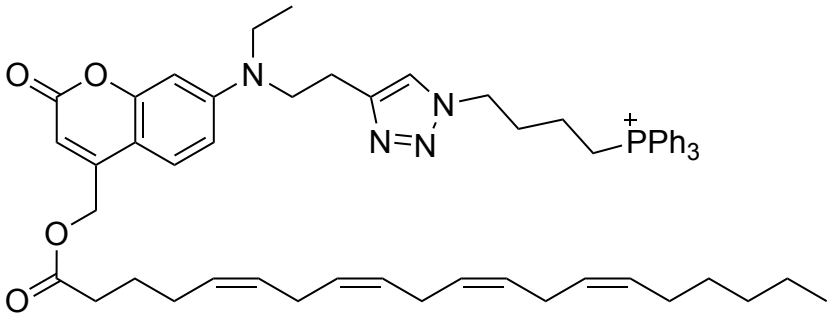

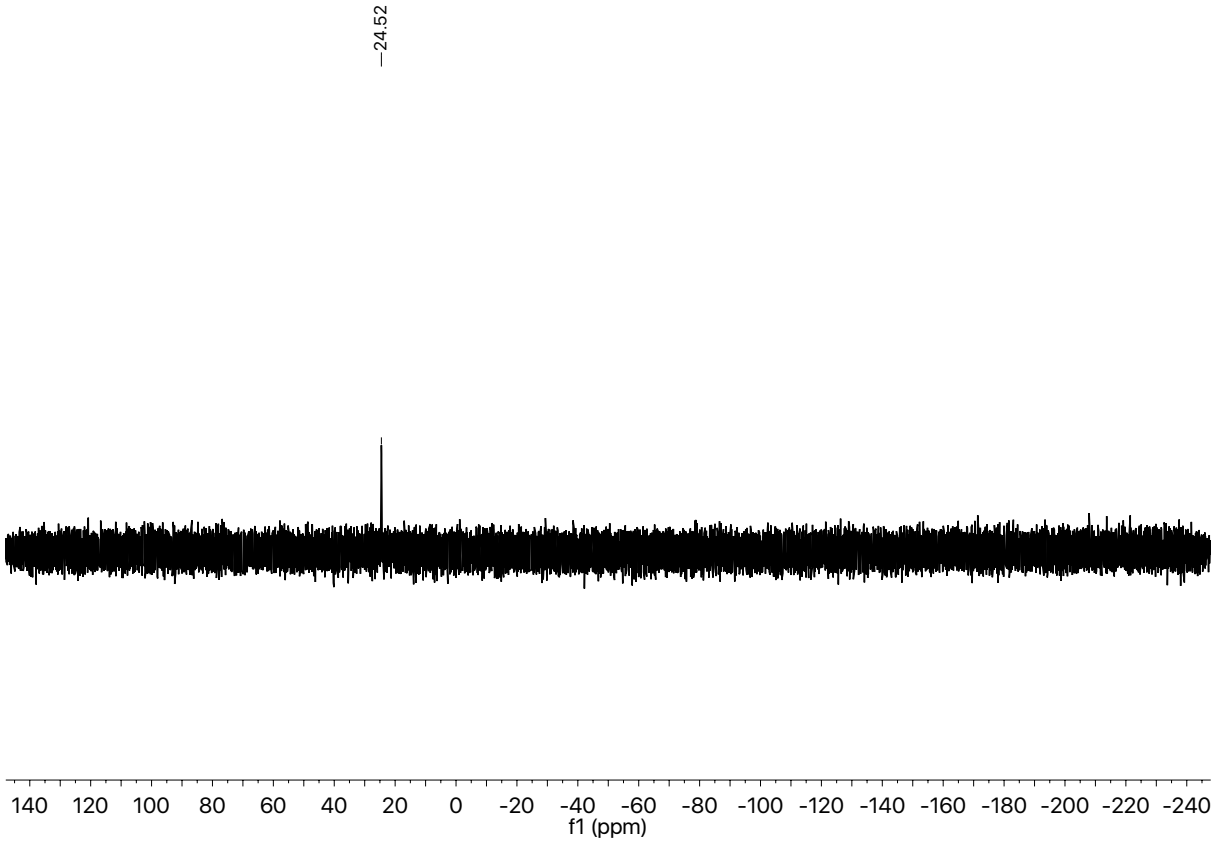

(7-((2-(1-(3-(dimethylamino)propyl)-1H-1,2,3-triazol-4-yl)ethyl)(ethyl)amino)-2-oxo-2H-chromen-4-yl)methyl (5Z,8Z,11Z,14Z)-icosa-5,8,11,14-tetraenoate (**12**) ^{1}H NMR:

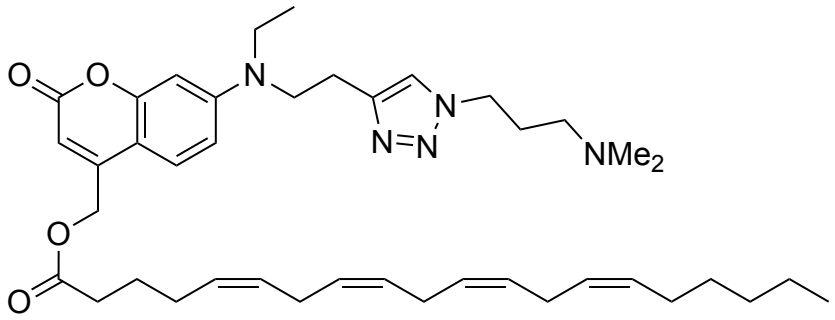

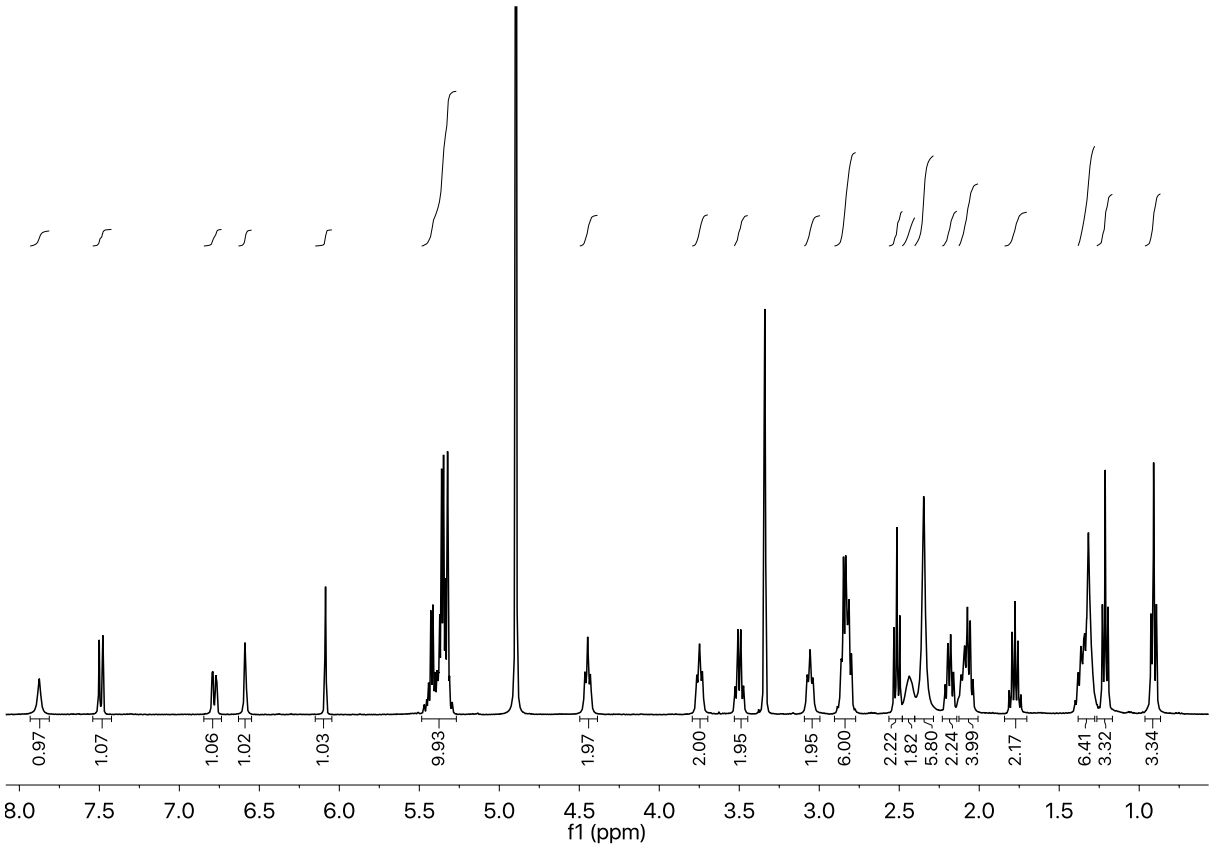

(7-((2-(1-(3-(dimethylamino)propyl)-1H-1,2,3-triazol-4-yl)ethyl)(ethyl)amino)-2-oxo-2H-chromen-4-yl)methyl (5Z,8Z,11Z,14Z)-icosa-5,8,11,14-tetraenoate (**12**) ^{13}C NMR:

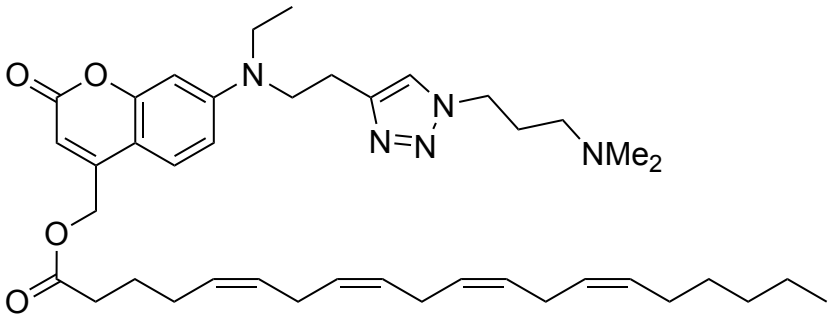

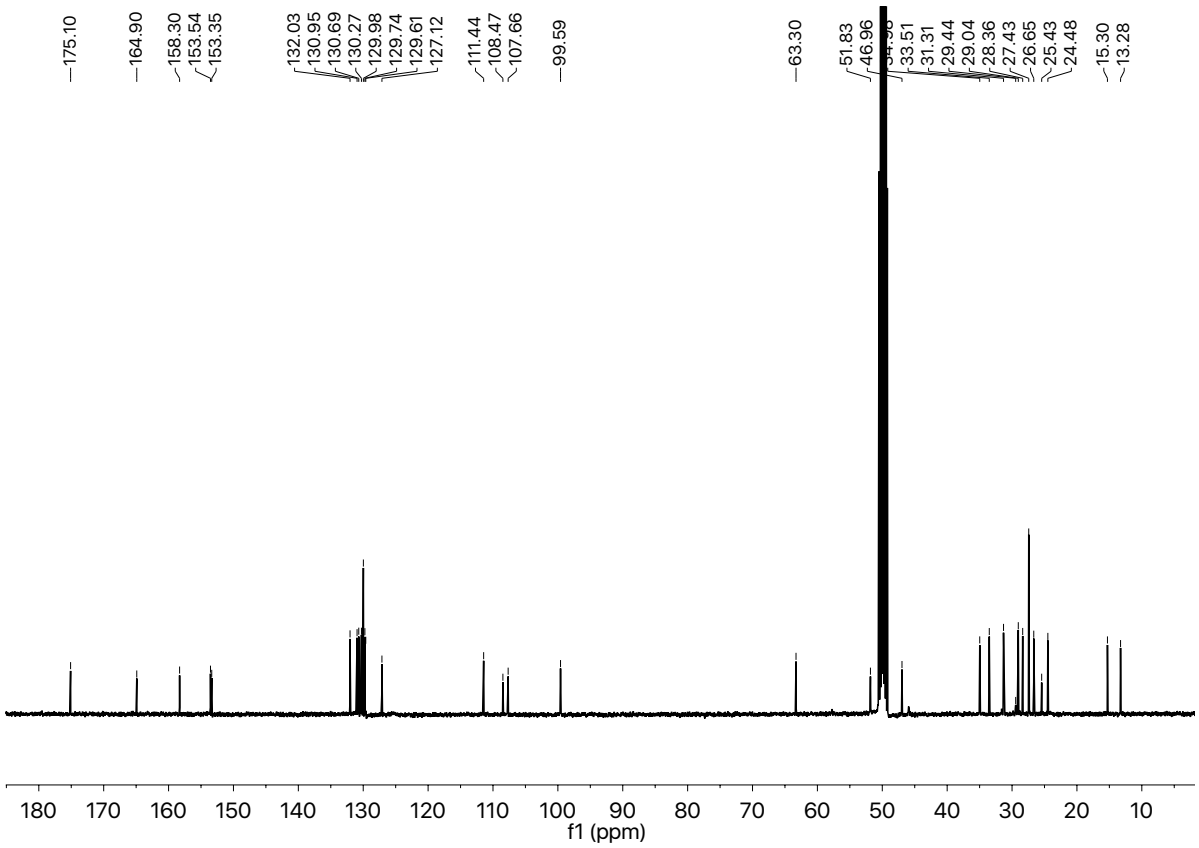

4-(4-(2-(ethyl(4-((((5Z,8Z,11Z,14Z)-icosa-5,8,11,14-tetraenoyl)oxy)methyl)-2-oxo-2H-chromen-7-yl)amino)ethyl)-1H-1,2,3-triazol-1-yl)benzene-1,3-disulfonate (**13**) ^{1}H NMR:

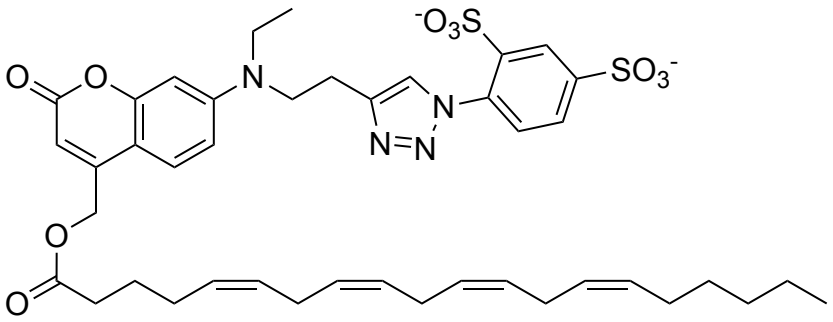

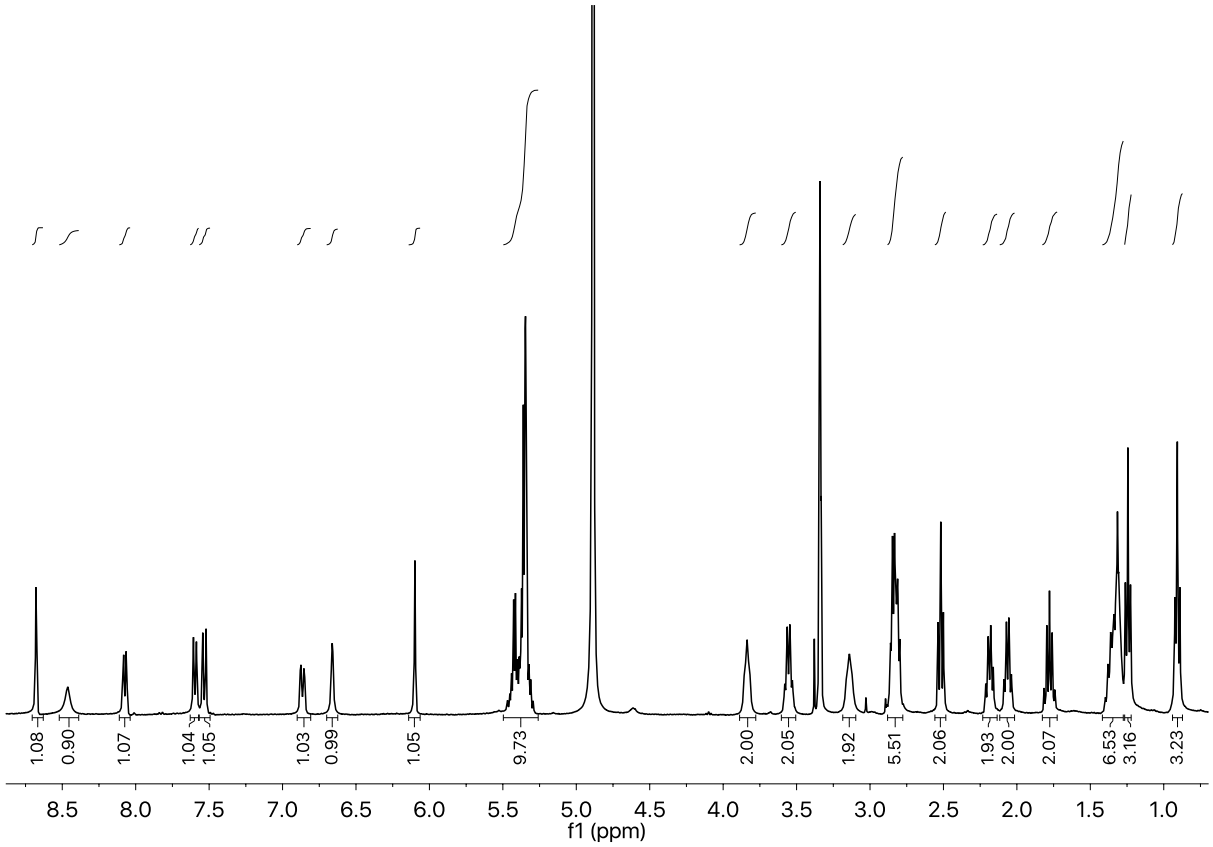

4-(4-(2-(ethyl(4-((((5Z,8Z,11Z,14Z)-icosa-5,8,11,14-tetraenoyl)oxy)methyl)-2-oxo-2H-chromen-7-yl)amino)ethyl)-1H-1,2,3-triazol-1-yl)benzene-1,3-disulfonate (**13**) ^{13}C NMR:

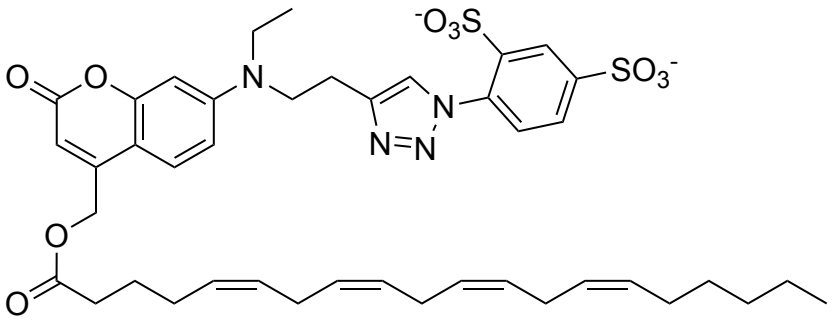

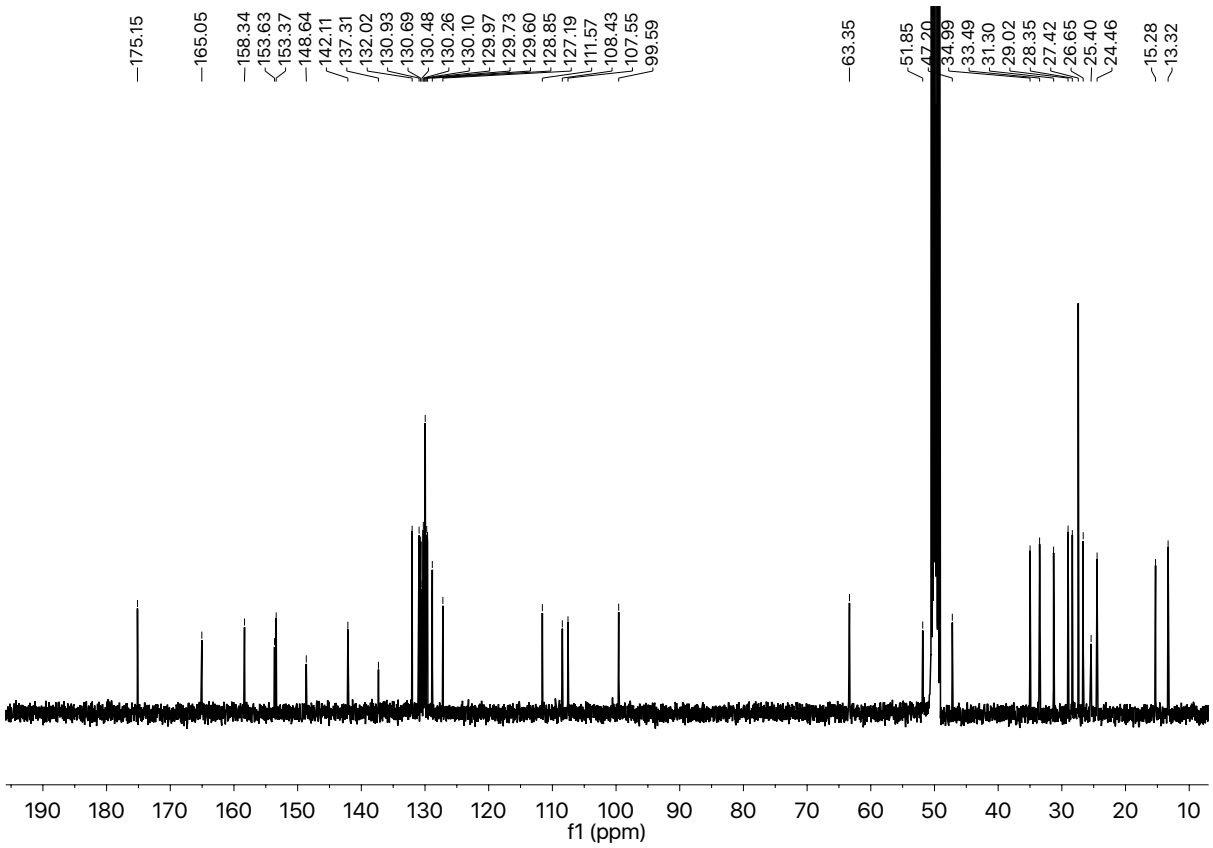

(7-(ethyl(2-(1-(3-(perfluorobenzamido)propyl)-1H-1,2,3-triazol-4-yl)ethyl)amino)-2-oxo-2H-chromen-4-yl)methyl (5Z,8Z,11Z,14Z)-icosa-5,8,11,14-tetraenoate (**14**) ^{1}H NMR:

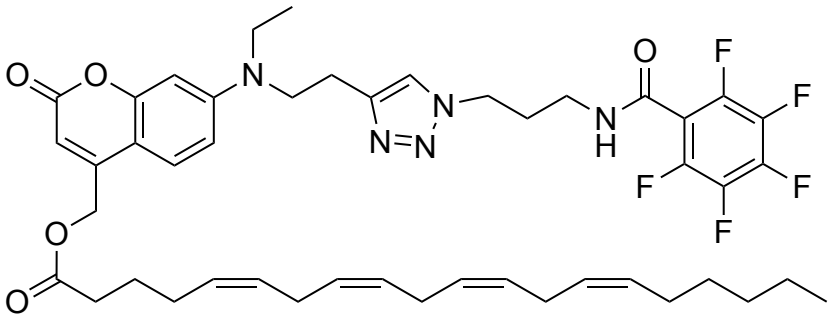

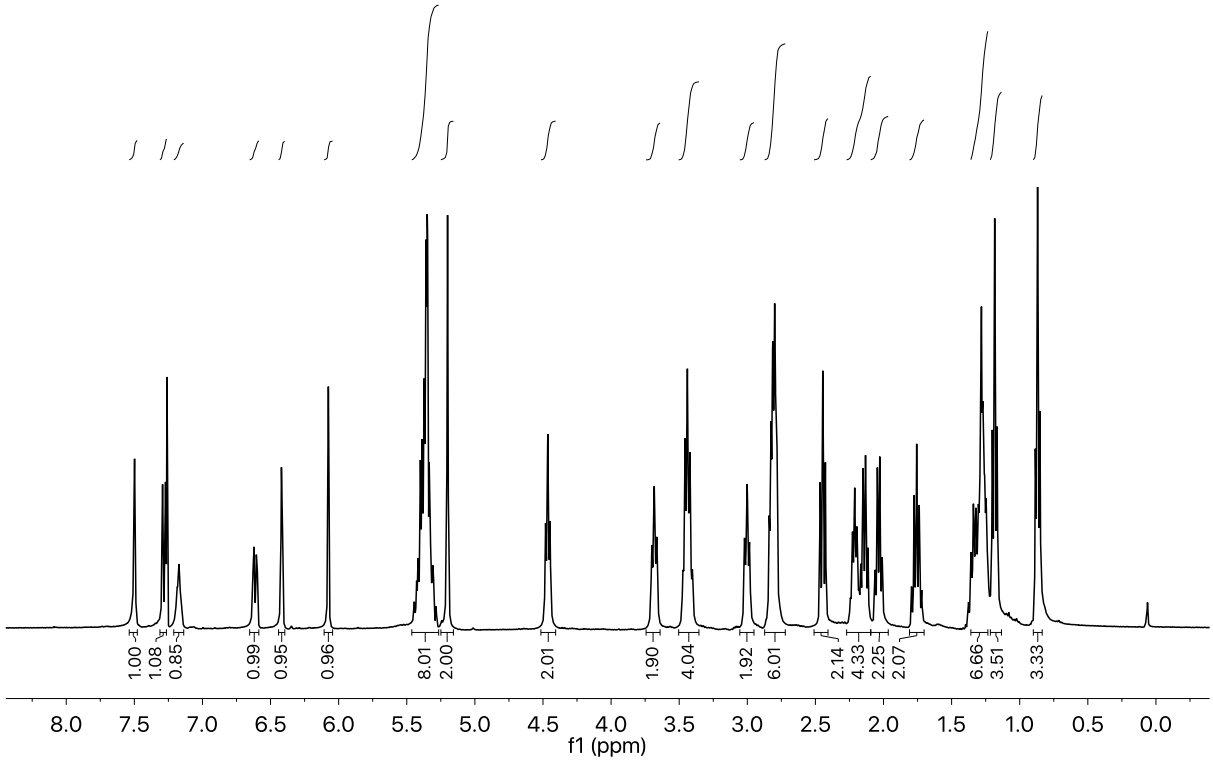

(7-(ethyl(2-(1-(3-(perfluorobenzamido)propyl)-1H-1,2,3-triazol-4-yl)ethyl)amino)-2-oxo-2H-chromen-4-yl)methyl (5Z,8Z,11Z,14Z)-icosa-5,8,11,14-tetraenoate (**14**) ^{13}C NMR:

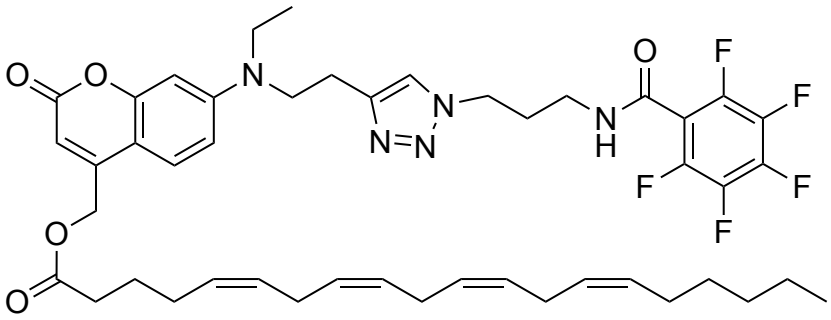

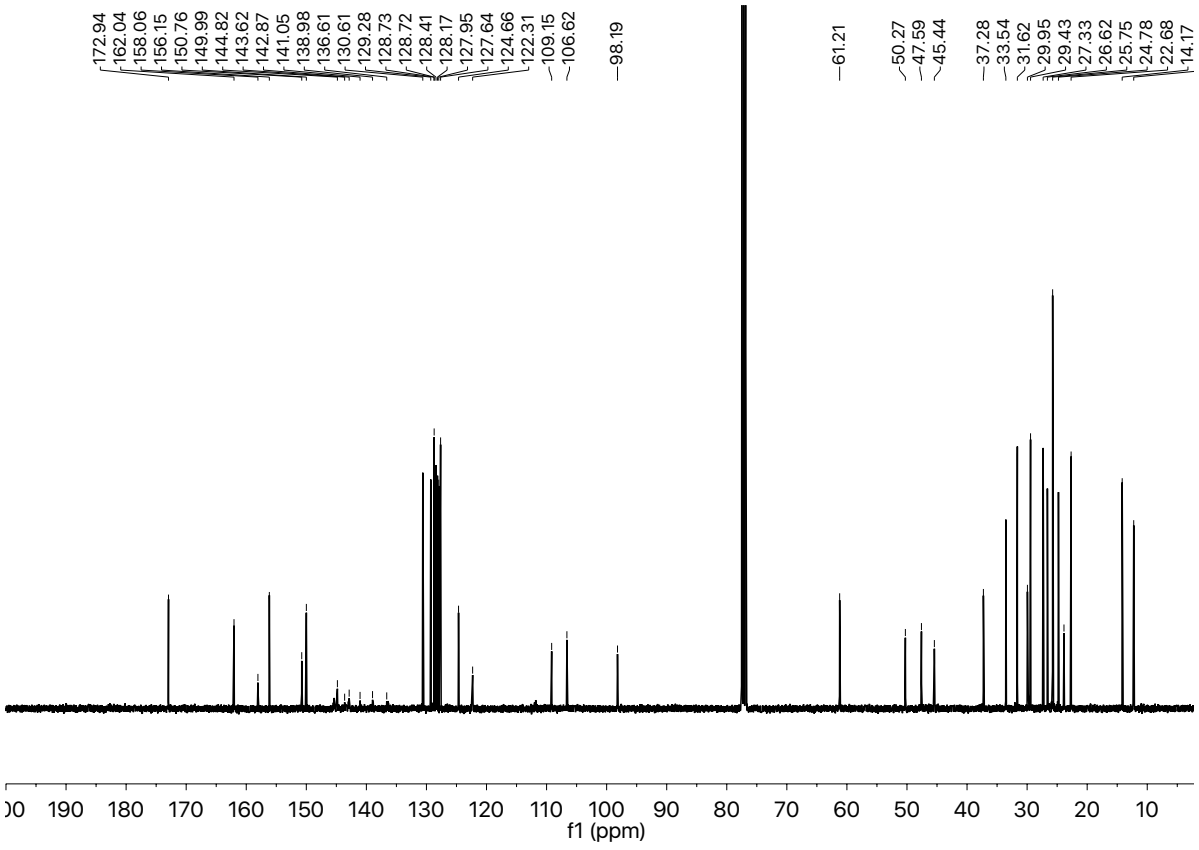

(7-(ethyl(2-(1-(3-(perfluorobenzamido)propyl)-1H-1,2,3-triazol-4-yl)ethyl)amino)-2-oxo-2H-chromen-4-yl)methyl (5Z,8Z,11Z,14Z)-icosa-5,8,11,14-tetraenoate (**14**) ^{19}F NMR:

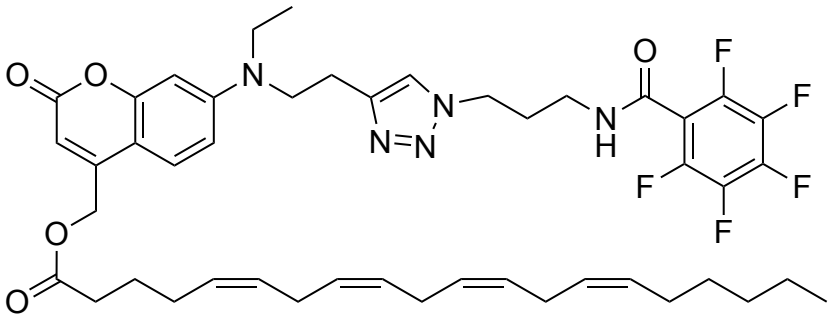

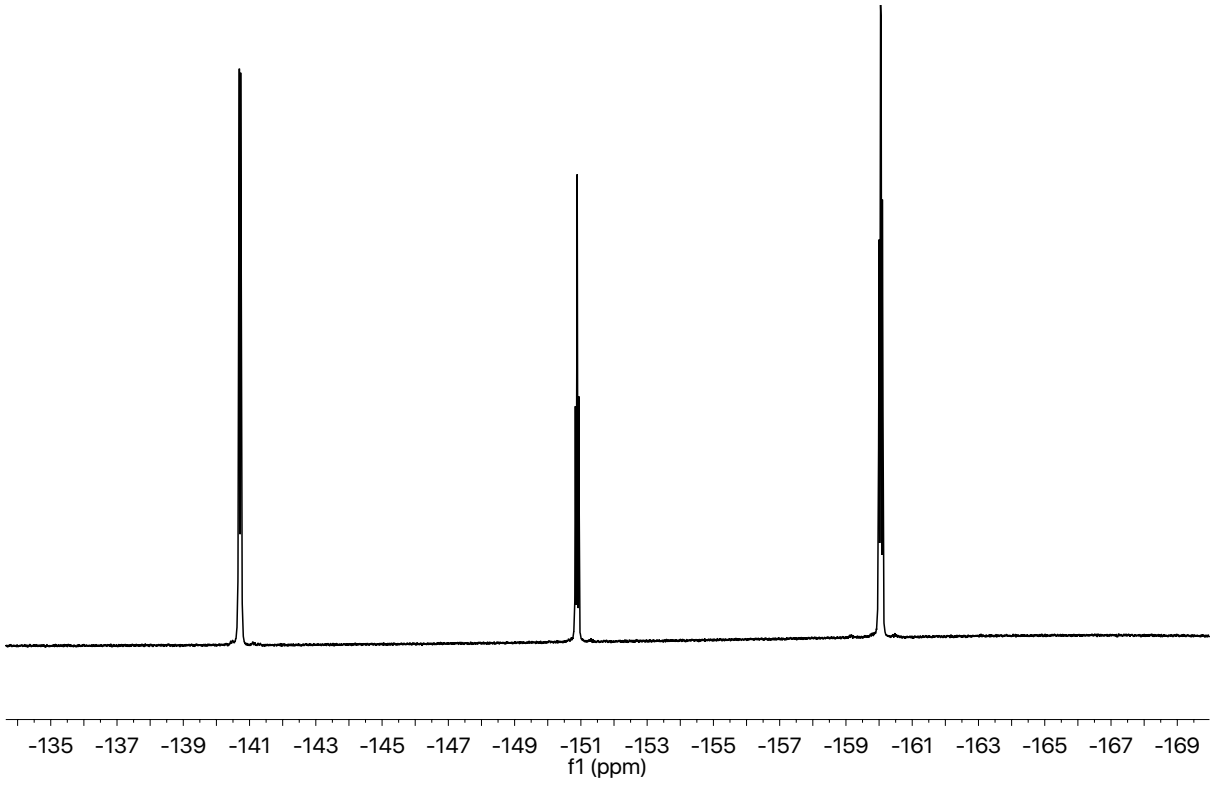

(7-(but-3-yn-1-yl(ethyl)amino)-2-oxo-2H-chromen-4-yl)methyl (E)-(1,3-dihydroxyoctadec-4-en-2-yl)carbamate (**17**) ^{1}H NMR:

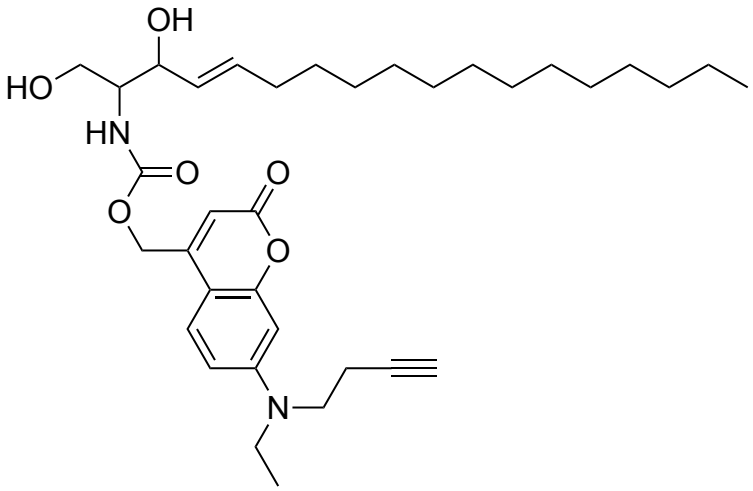

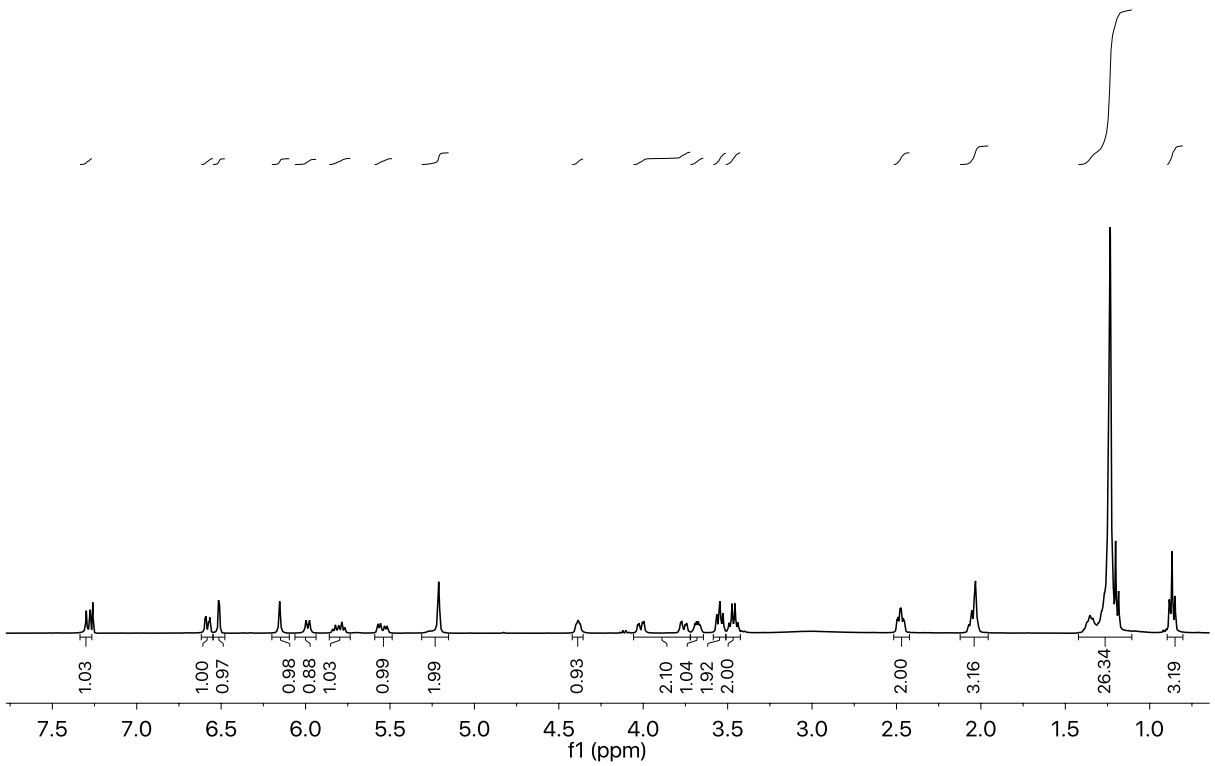

(7-(but-3-yn-1-yl(ethyl)amino)-2-oxo-2H-chromen-4-yl)methyl (E)-(1,3-dihydroxyoctadec-4-en-2-yl)carbamate (**17**) ^{13}C NMR:

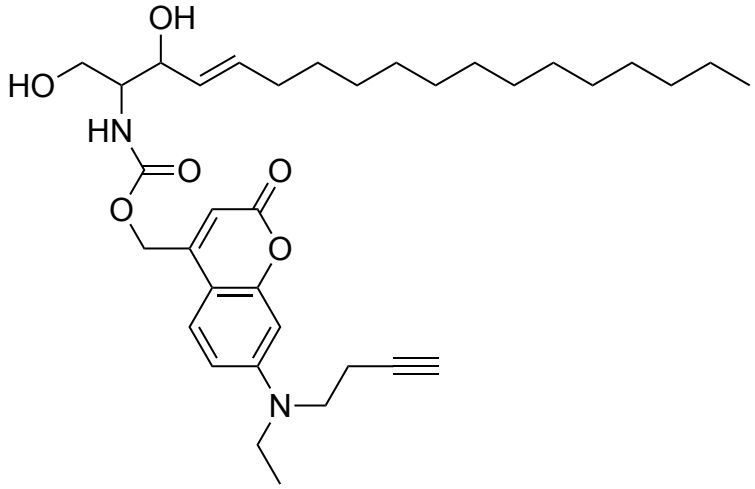

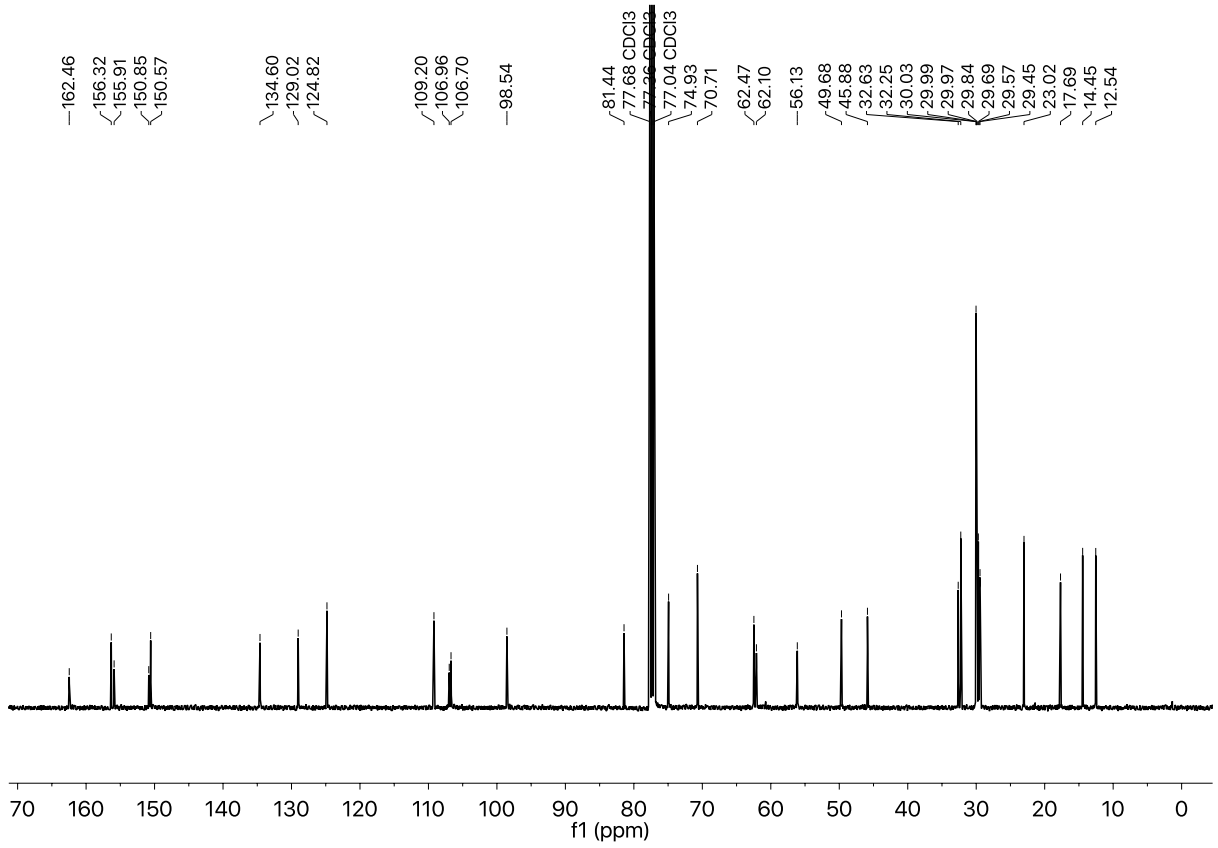

(E)-(4-(5-(2-((4-((((1,3-dihydroxyoctadec-4-en-2-yl)carbamoyl)oxy)methyl)-2-oxo-2H-chromen-7-yl)(ethyl)amino)ethyl)-1H-1,2,3-triazol-1-yl)butyl)triphenylphosphonium (**18**) ^{1}H NMR:

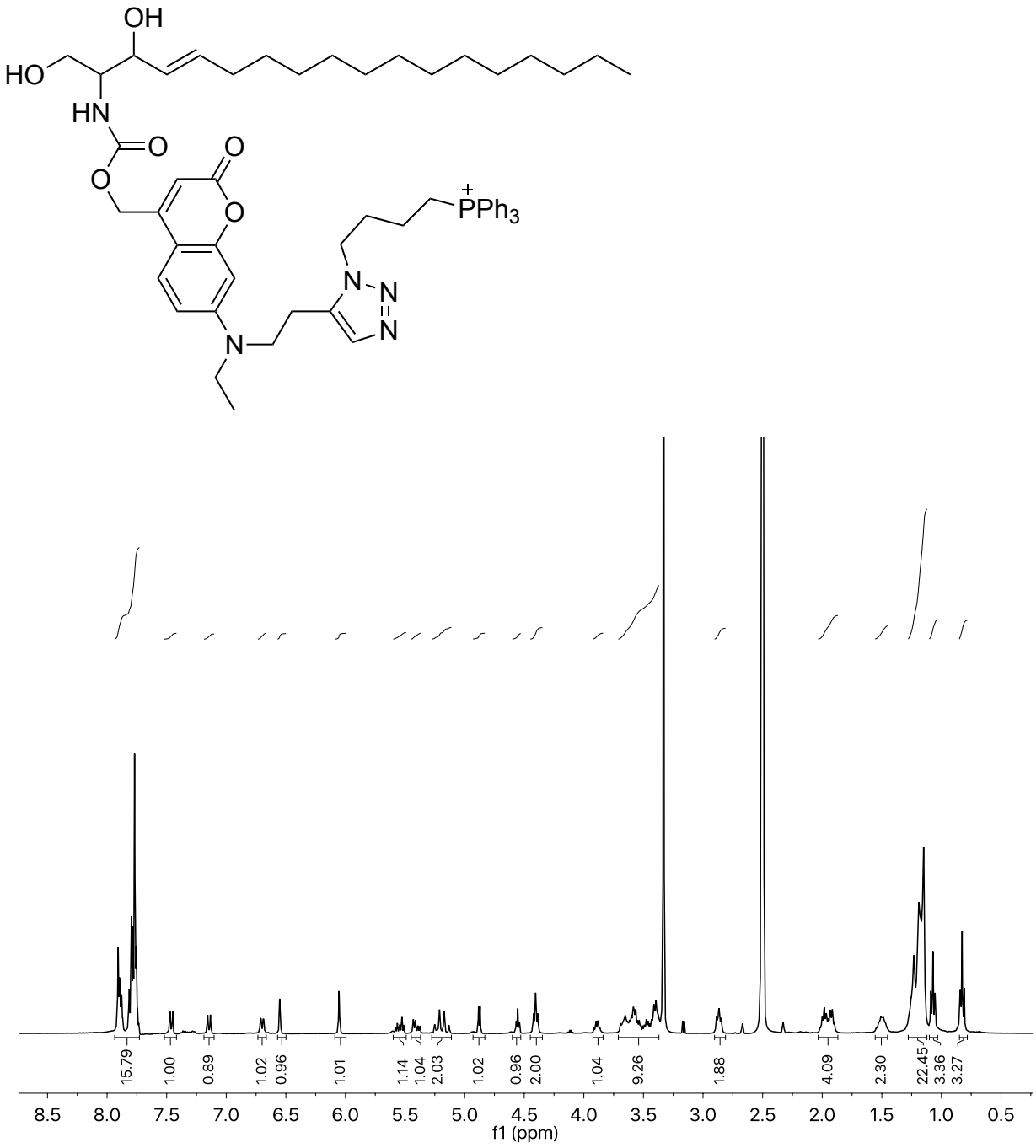

(E)-(4-(5-(2-((4-((((1,3-dihydroxyoctadec-4-en-2-yl)carbamoyl)oxy)methyl)-2-oxo-2H-chromen-7-yl)(ethyl)amino)ethyl)-1H-1,2,3-triazol-1-yl)butyl)triphenylphosphonium (**18**) ^{13}C NMR:

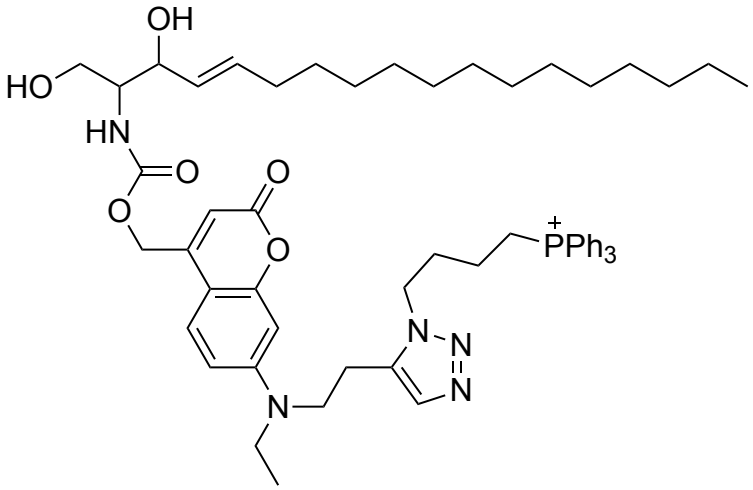

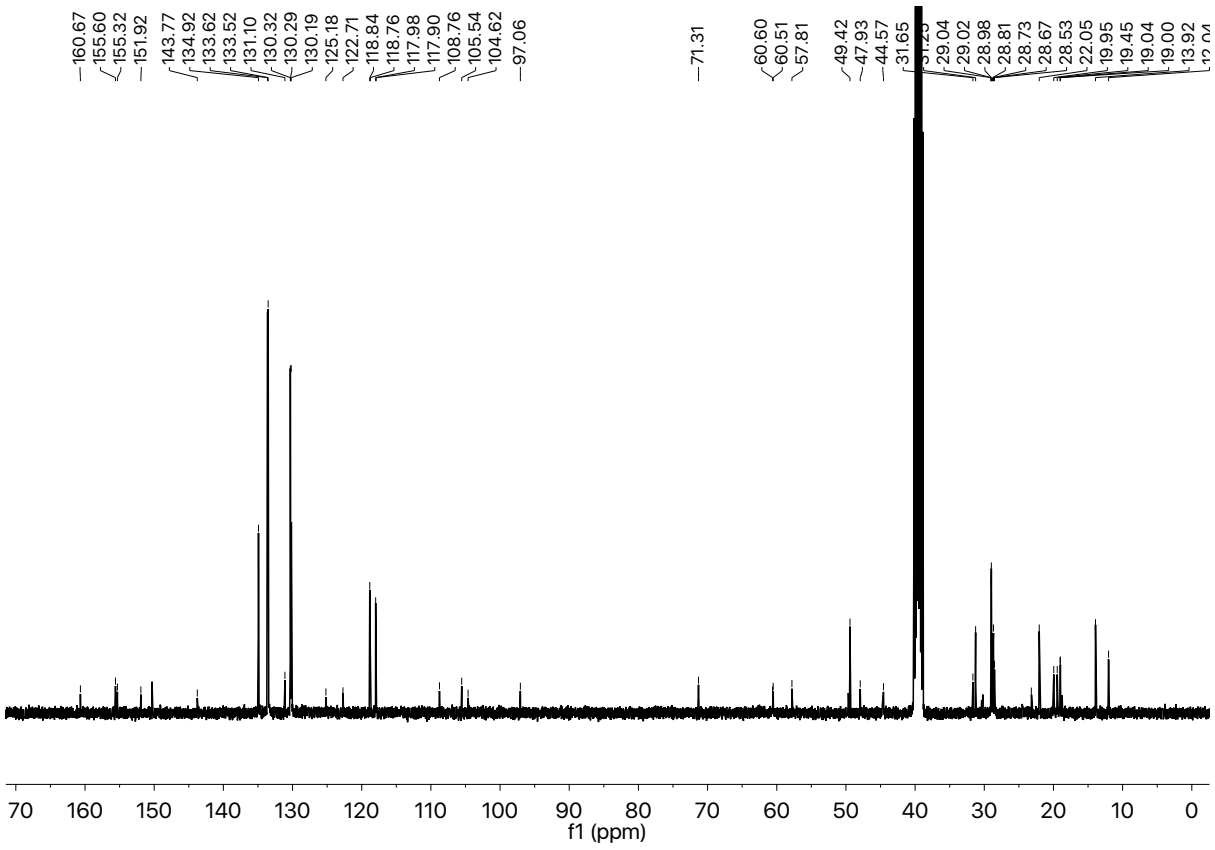

(E)-(4-(5-(2-((4-((((1,3-dihydroxyoctadec-4-en-2-yl)carbamoyl)oxy)methyl)-2-oxo-2H-chromen-7-yl)(ethyl)amino)ethyl)-1H-1,2,3-triazol-1-yl)butyl)triphenylphosphonium (**18**) ^{31}P NMR:

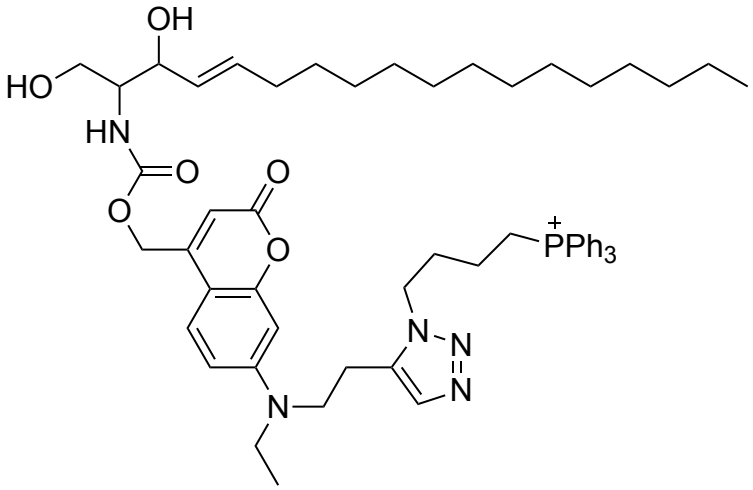

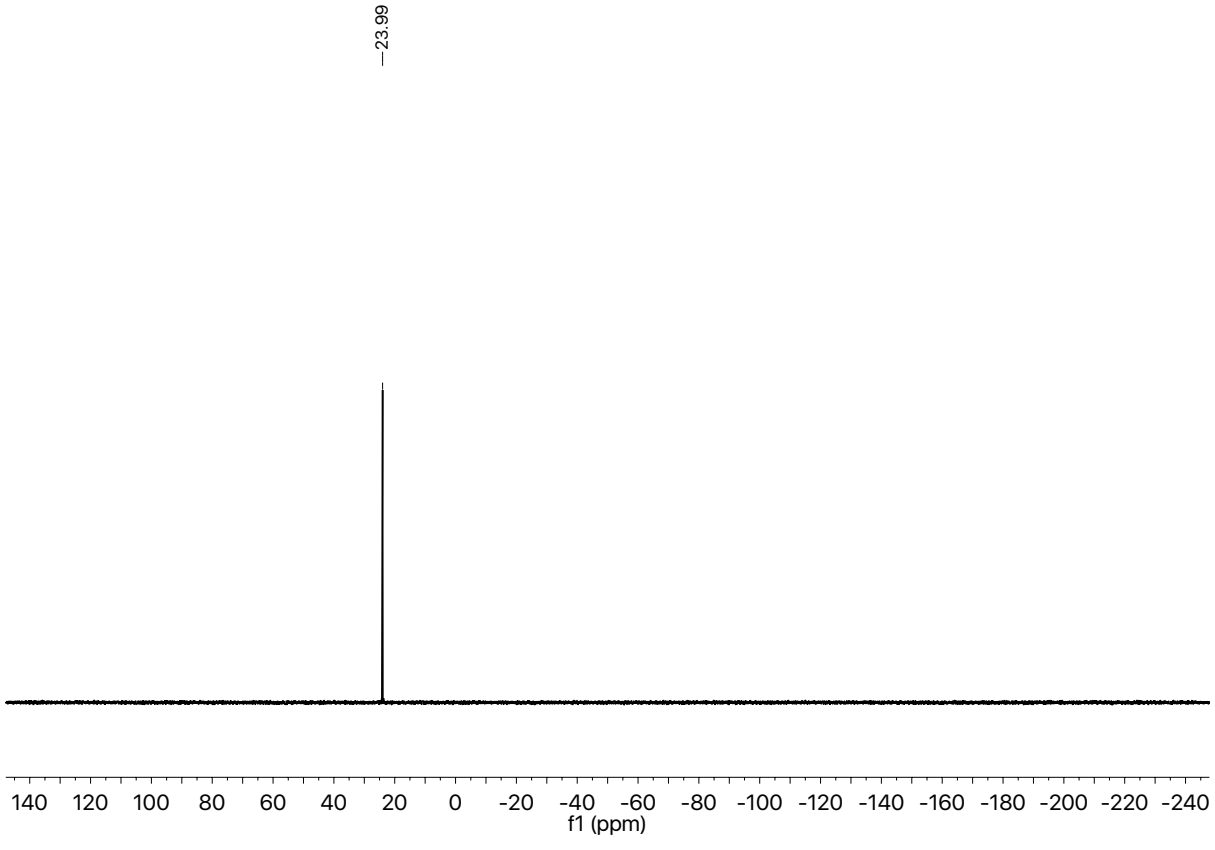

(7-((2-(1-(3-(dimethylamino)propyl)-1H-1,2,3-triazol-5-yl)ethyl)(ethyl)amino)-2-oxo-2H-chromen-4-yl)methyl (E)-(1,3-dihydroxyoctadec-4-en-2-yl)carbamate (**19**) ^{1}H NMR:

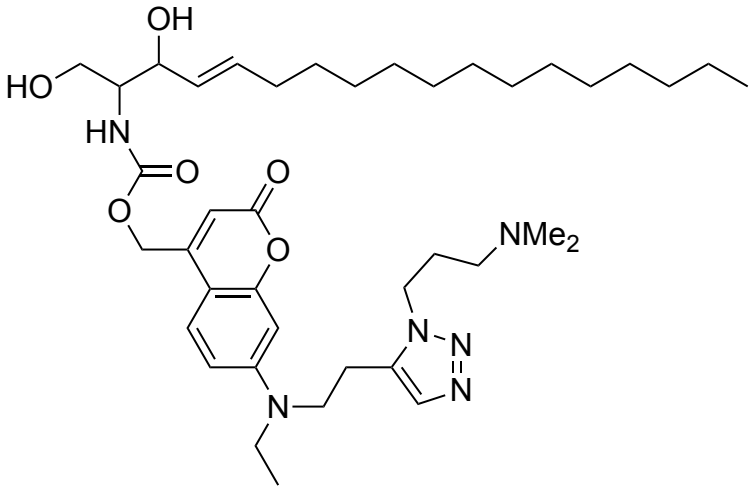

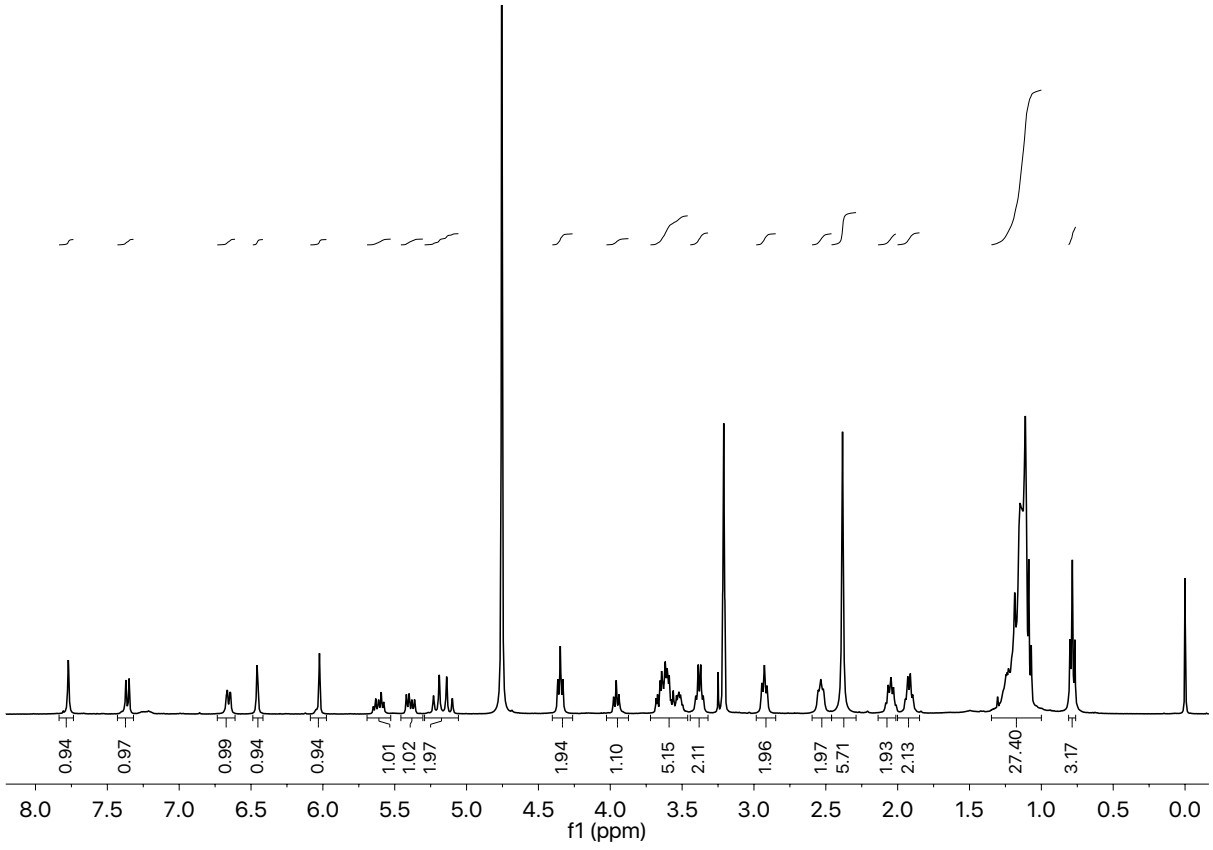

(7-((2-(1-(3-(dimethylamino)propyl)-1H-1,2,3-triazol-5-yl)ethyl)(ethyl)amino)-2-oxo-2H-chromen-4-yl)methyl (E)-(1,3-dihydroxyoctadec-4-en-2-yl)carbamate (**19**) ^{13}C NMR:

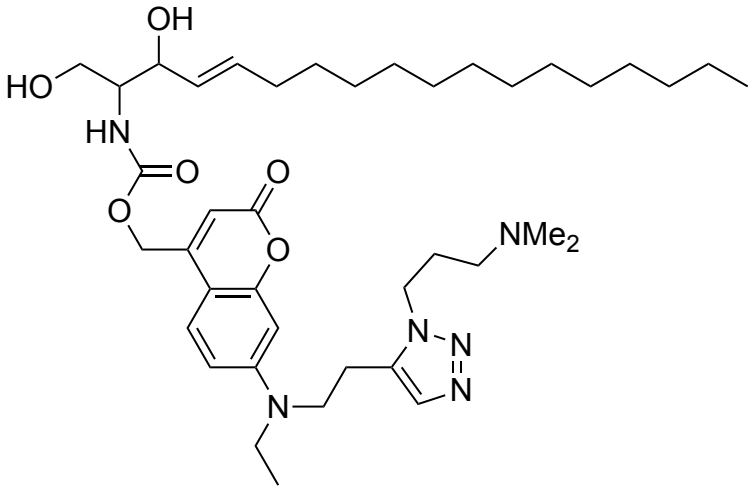

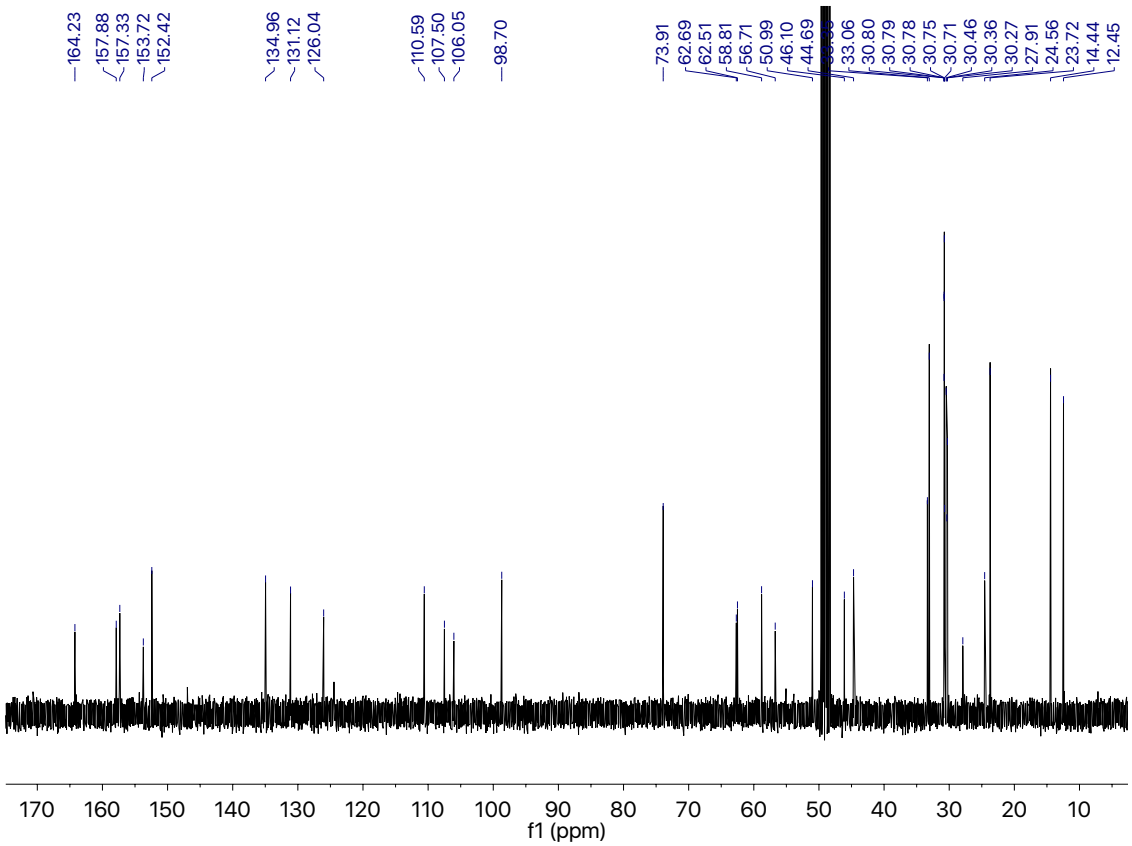

(E)-4-(4-(2-((4-((((1,3-dihydroxyoctadec-4-en-2-yl)carbamoyl)oxy)methyl)-2-oxo-2H-chromen-7-yl)(ethyl)amino)ethyl)-1H-1,2,3-triazol-1-yl)benzene-1,3-disulfonate (**20**) ^{1}H NMR:

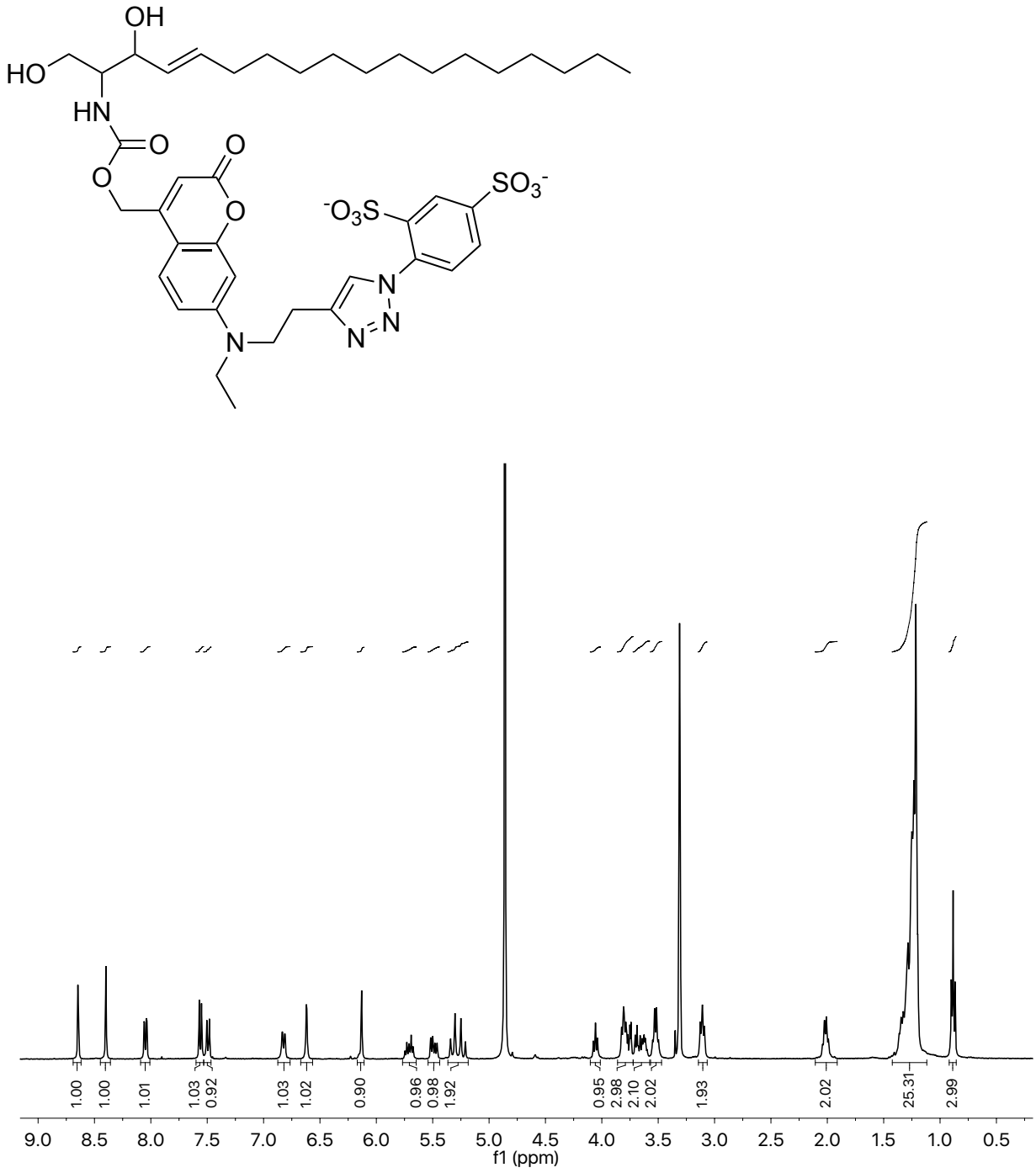

(E)-4-(4-(2-((4-((((1,3-dihydroxyoctadec-4-en-2-yl)carbamoyl)oxy)methyl)-2-oxo-2H-chromen-7-yl)(ethyl)amino)ethyl)-1H-1,2,3-triazol-1-yl)benzene-1,3-disulfonate (**20**) ^{13}C NMR:

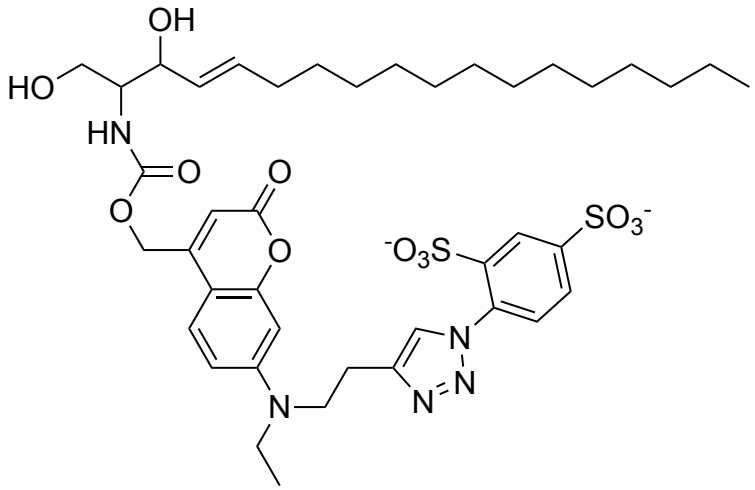

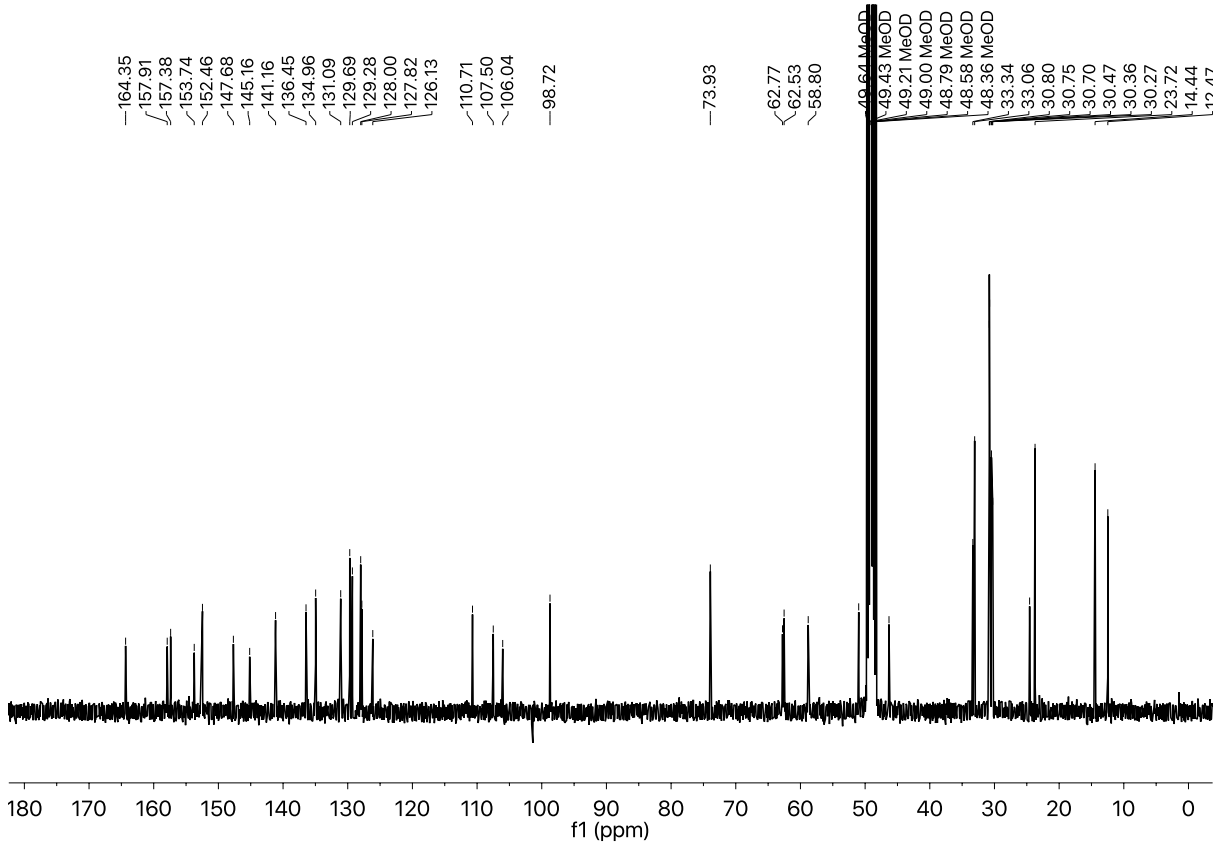

(7-(ethyl(2-(1-(3-(perfluorobenzamido)propyl)-1H-1,2,3-triazol-4-yl)ethyl)amino)-2-oxo-2H-chromen-4-yl)methyl (E)-(1,3-dihydroxyoctadec-4-en-2-yl)carbamate (**21**) ^{1}H NMR:

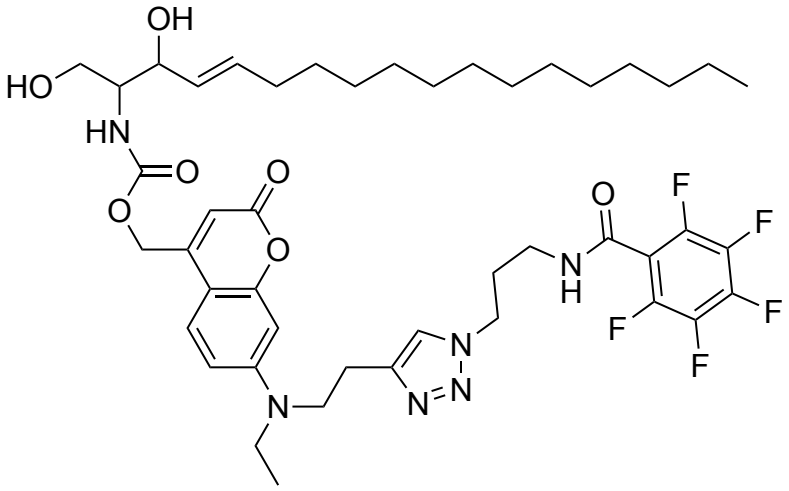

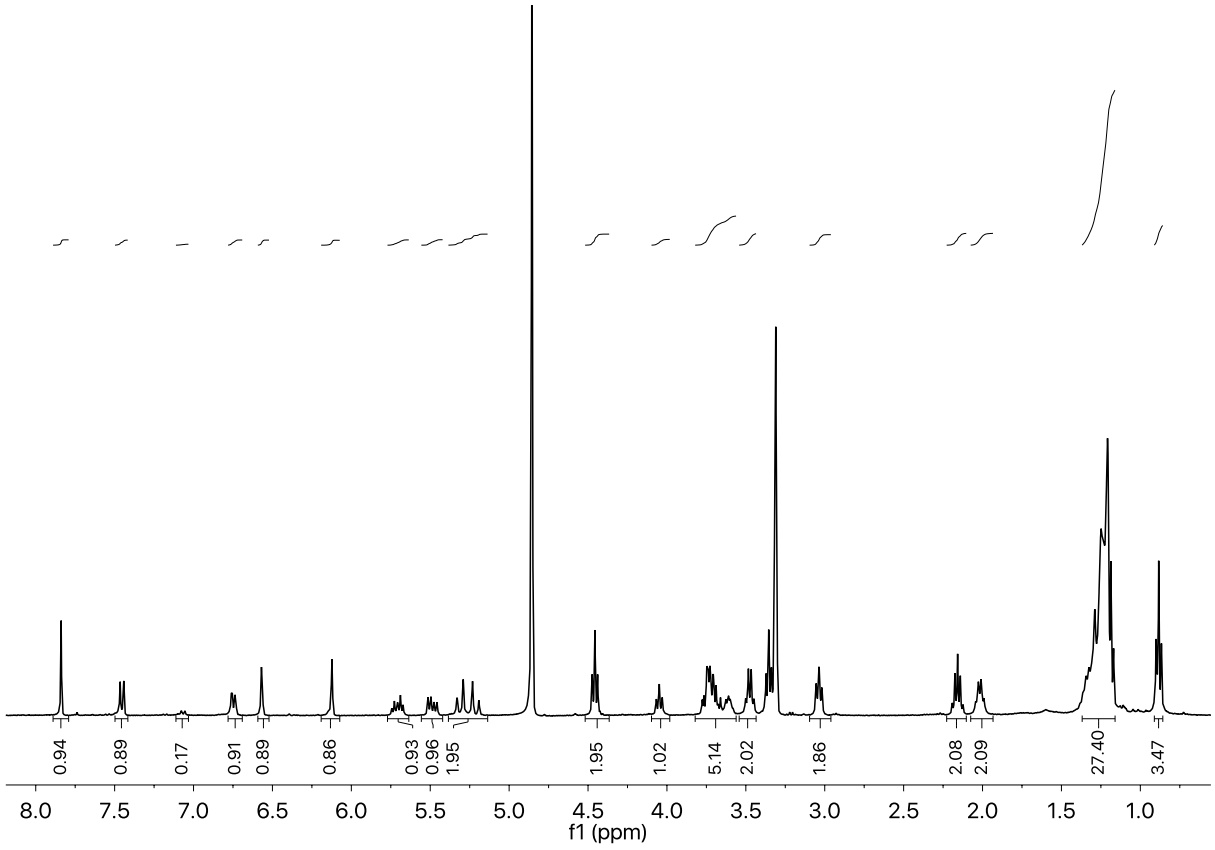

(7-(ethyl(2-(1-(3-(perfluorobenzamido)propyl)-1H-1,2,3-triazol-4-yl)ethyl)amino)-2-oxo-2H-chromen-4-yl)methyl (E)-(1,3-dihydroxyoctadec-4-en-2-yl)carbamate (**21**) ^{13}C NMR:

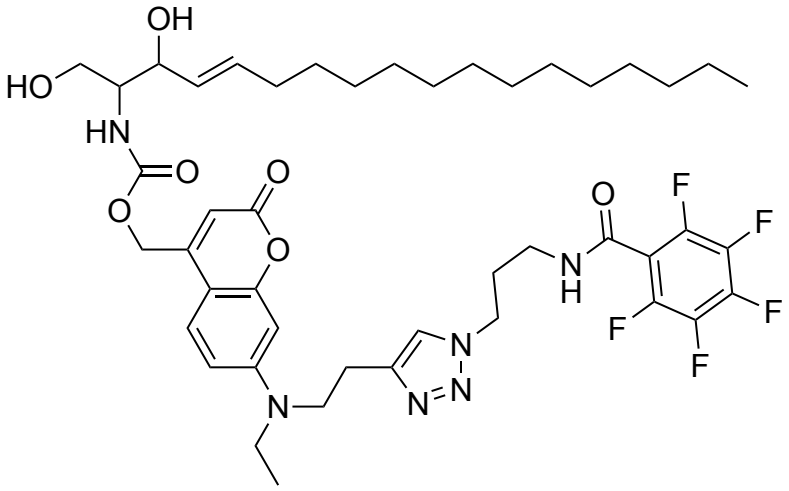

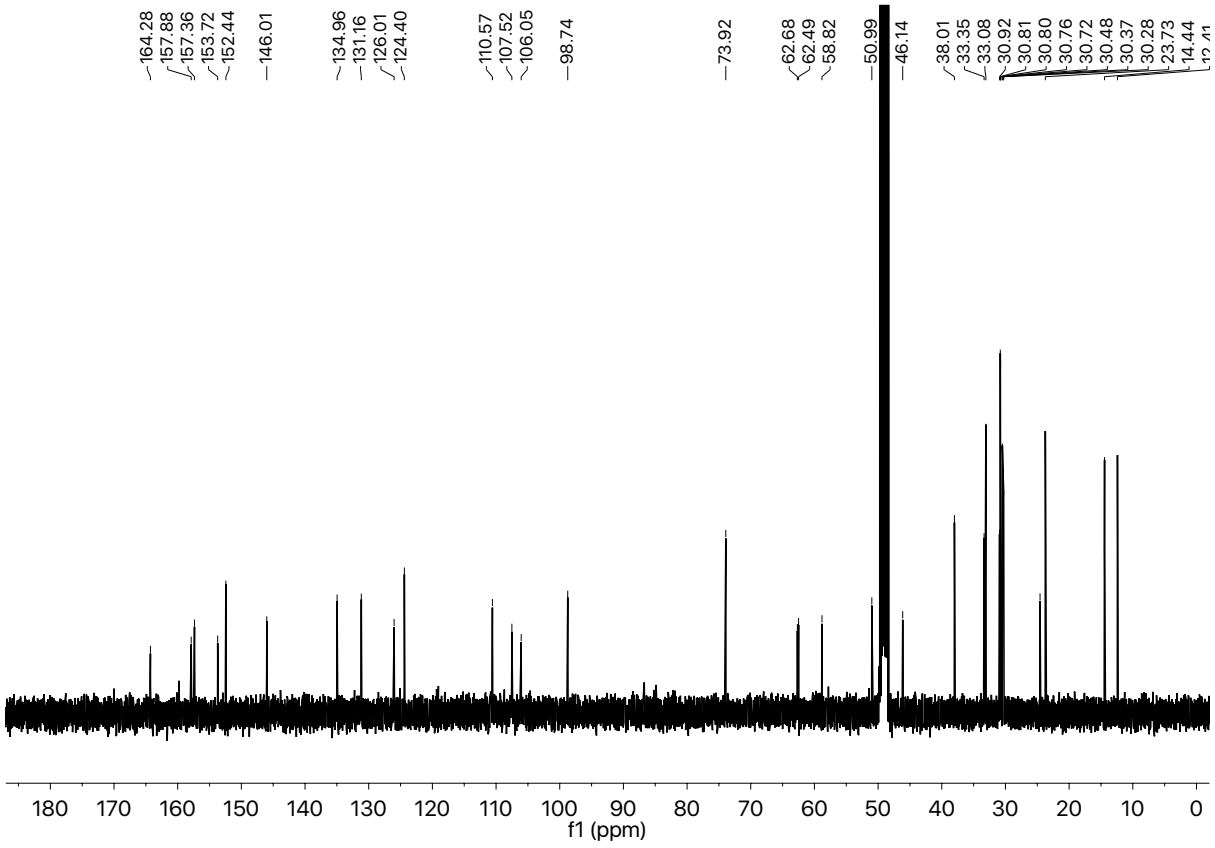

(7-(ethyl(2-(1-(3-(perfluorobenzamido)propyl)-1H-1,2,3-triazol-4-yl)ethyl)amino)-2-oxo-2H-chromen-4-yl)methyl (E)-(1,3-dihydroxyoctadec-4-en-2-yl)carbamate (**21**) ^{19}F NMR:

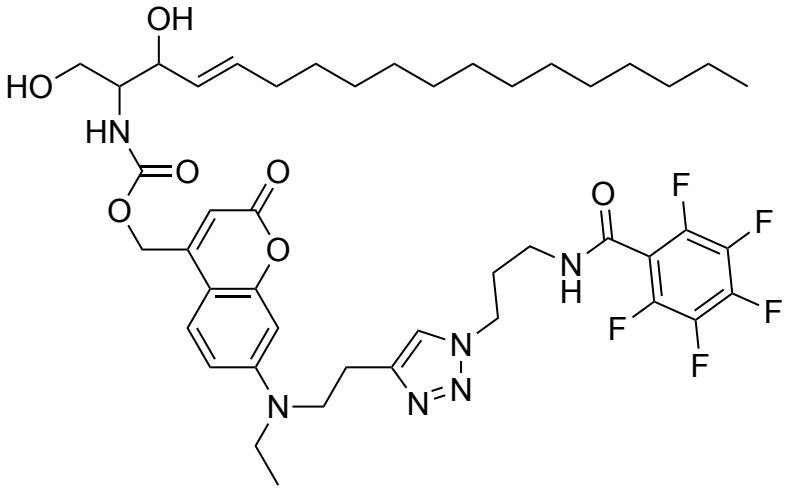

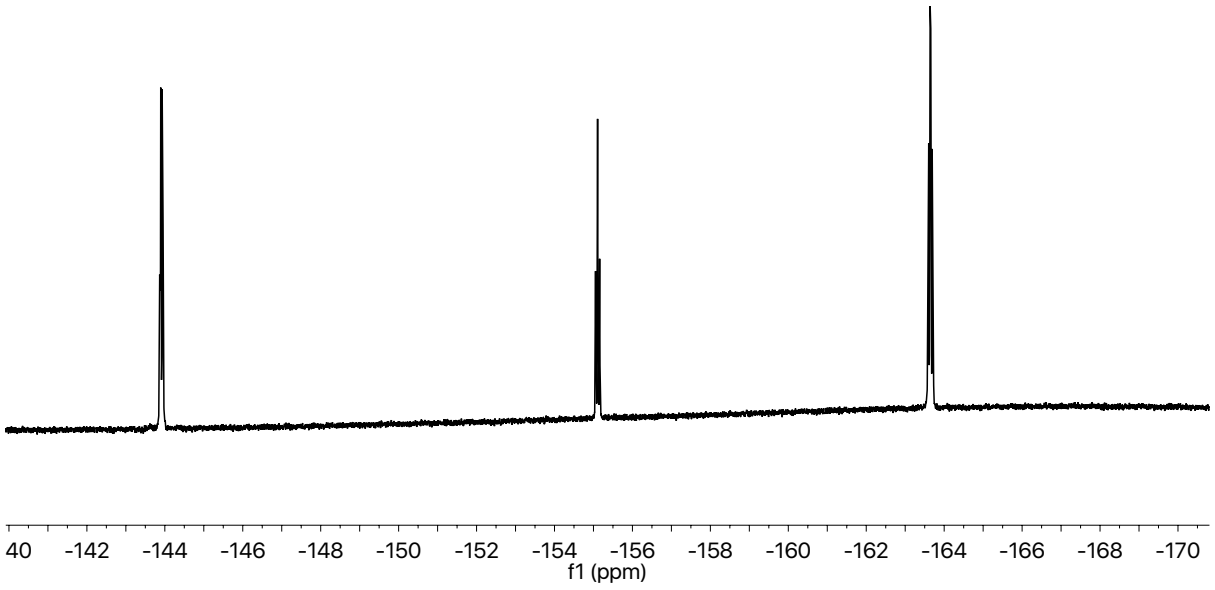

[1] G. Jones, W. R. Jackson, C. Y. Choi, W. R. Bergmark, *The Journal of Physical Chemistry* **1985**, *89*, 294-300.
[2] F. Stein, M. Kress, S. Reither, A. Piljic, C. Schultz, *ACS Chem Biol* **2013**, *8*, 1862-1868.
[3] H. Wickham, *ggplot2: Elegant Graphics for Data Analysis.*, Springer-Verlag New York, **2016**.
[4] a C. Beate, K. P. H. M., B. M. E., K. Karl, S. B. F., *Photochemistry and Photobiology* **2005**, *81*, 641-648; b A. C. Engler, D. K. Bonner, H. G. Buss, E. Y. Cheung, P. T. Hammond, *Soft Matter* **2011**, *7*, 5627-5637; c M. Carta, F. Lanore, N. Rebola, Z. Szabo, Silvia V. Da Silva, J. Lourenço, A. Verraes, A. Nadler, C. Schultz, C. Blanchet, C. Mulle, *Neuron* **2014**, *81*, 787-799; d D. Hoglinger, P. Haberkant, A. Aguilera-Romero, H. Riezman, F. D. Porter, F. M. Platt, A. Galione, C. Schultz, *Elife* **2015**, *4*.